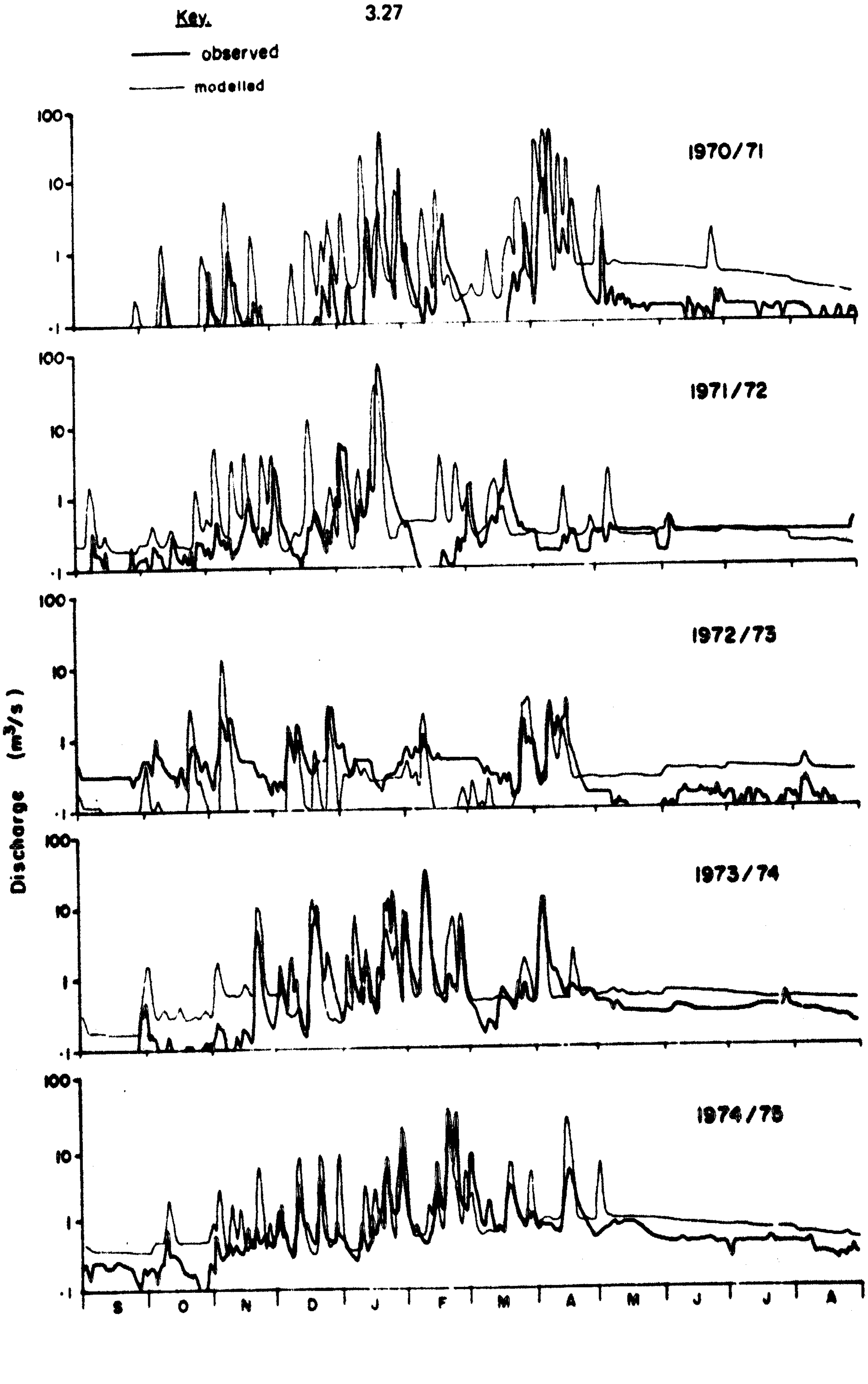

Fig. 3.22 : Modelled and observed daily discharges at station C2M05 for period 1970-09 – 1975-08

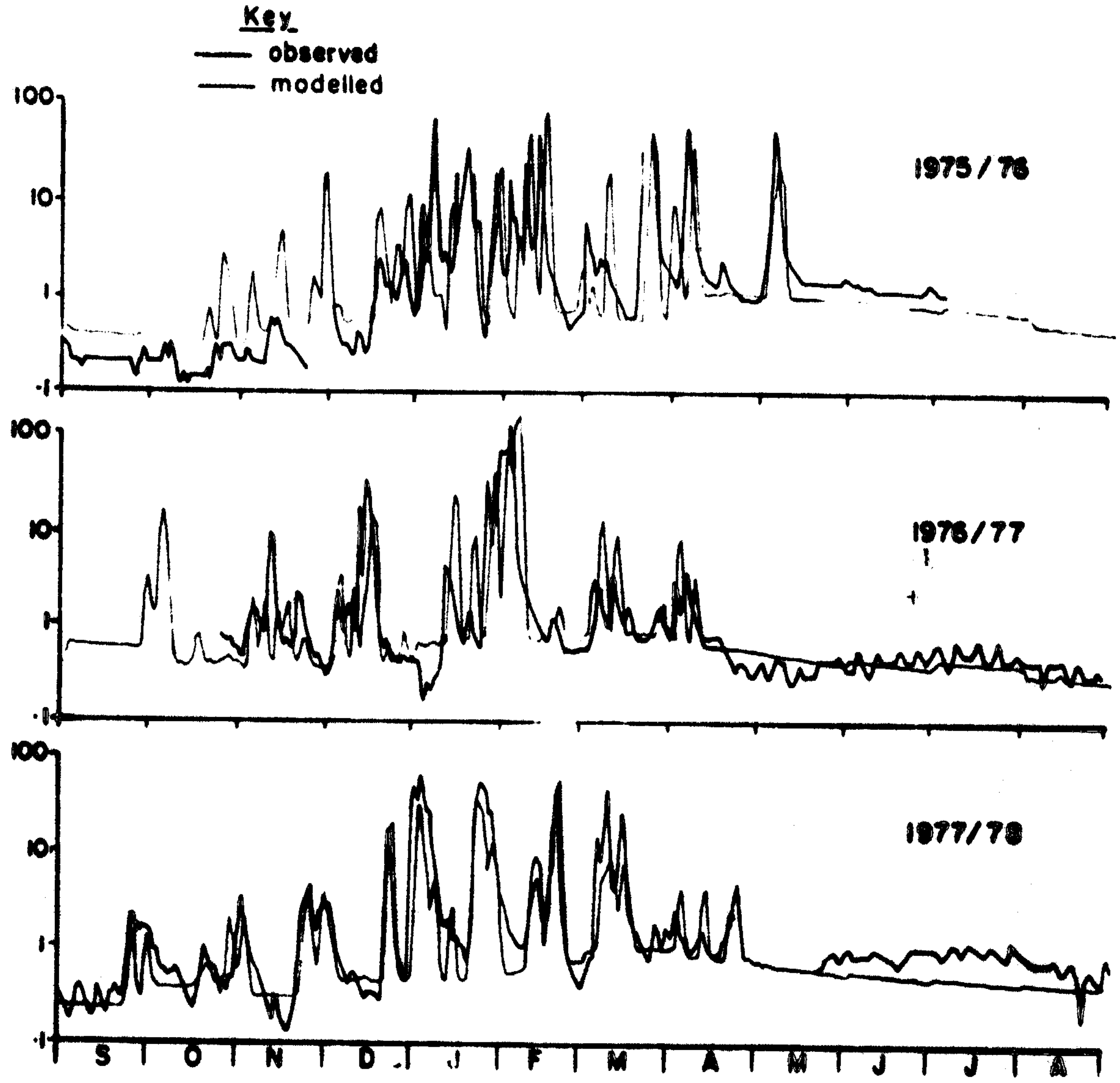

Fig. 3.22: Modelled and observed daily discharges at station C2M04 for period 1970-09 - 1978-08

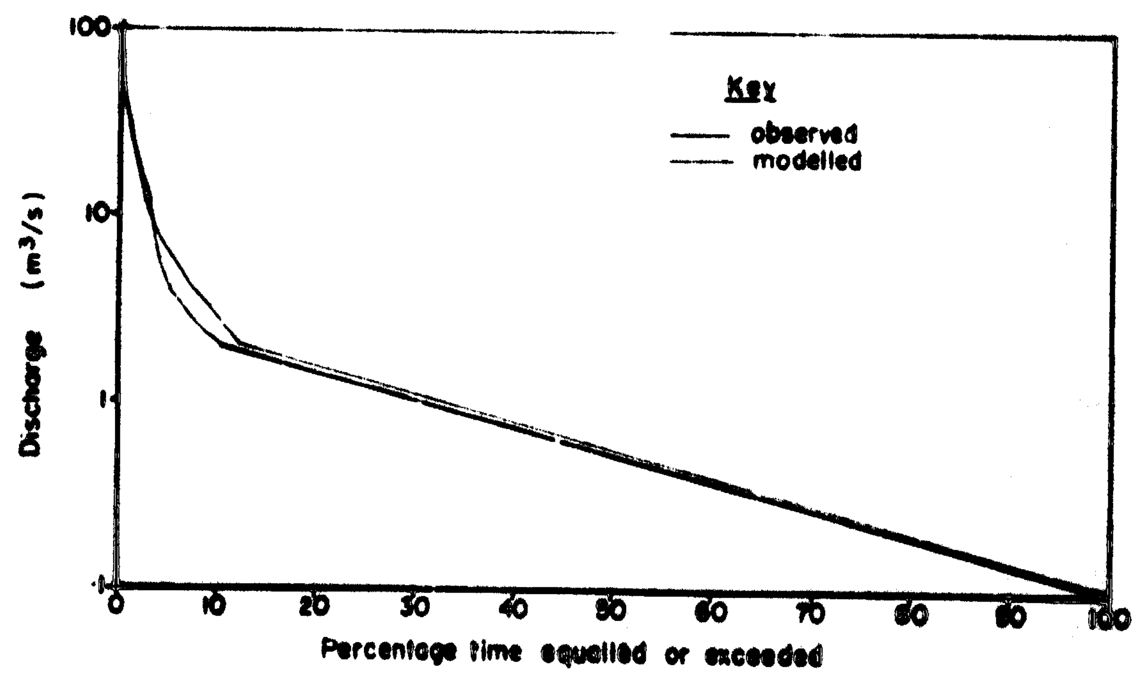

Fig. 3.23: Duration curve of modelled and observed daily discharges at station C2M05 for period 1970-09 - 1978-08

Station C2M14: C2M14 is a low level weir located in the Taaibos-spruit 12 km from its confluence with the Vaal river. The water level record is long and reliable, but the weir has been rated only for low flows. The Taaibosspruit catchment is extremely flat and contains 13 km^2 of vlei.

Fig. 3.24 is a plot of modelled and observed daily discharges for the period September 1970 to August 1978 and Fig. 3.25 shows the duration curves for the same period.

From Fig. 3.24 it can be seen that the observed base flows usually cease entirely soon after the end of the rainy season. Furthermore, it was found that even heavy rainfall events produce little or no runoff during the early part of the wet season. Although the weir is not rated for high flows it can be inferred from the water level record that severe floods do occur later in the wet season (for example, at the end of December 1977 a peak water level of 4,80m was recorded at C2M14 while the maximum rated discharge is 8,94 m^3/s at a level of 0,76m). Midgley (1978) estimates the 10-year recurrence interval flood peak at 174 m^3/s.

In order to model this catchment it was therefore necessary to assume high infiltration rates (in order to absorb the early rains) together with a relatively shallow soil moisture storage.* The result of this choice of model parameters is that most of the earlier storms are absorbed, yielding little runoff, but the model will generate large floods later in the wet season when the soil moisture storage nears capacity. These assumptions are reasonable for a very flat catchment such as that of the Taaibosspruit where much of the rainfall is likely to be caught in surface depressions from where it has ample time to infiltrate into the soil. The flat gradients will also increase the contact time of surface runoff and thus enhance infiltration. The assumption of small soil moisture storage is also compatible with a flat catchment, where poor drainage is likely to result in a water table near the surface.

---

* From Table 3.1 it can be seen that for catchment number 10 both SL (250 mm) and SE (300 mm) are large relative to ST (400 mm). This confines soil moisture fluctuations to within the rather shallow range of 150 mm. The high SL value also causes modelled base flows to diminish rapidly.

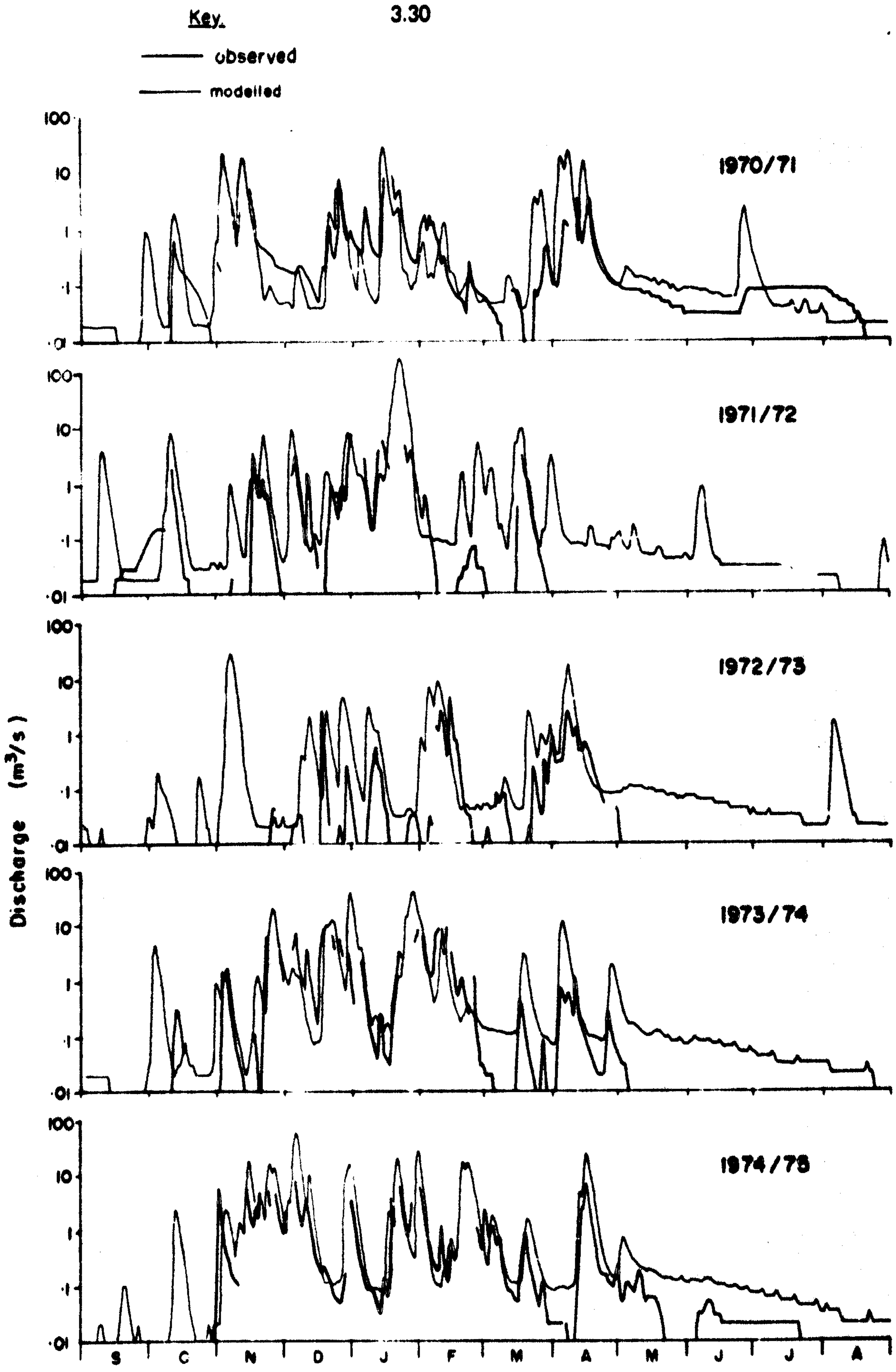

Fig. 3.24 : Modelled and observed daily discharges at station C2M14 for period 1970-09 – 1978-08

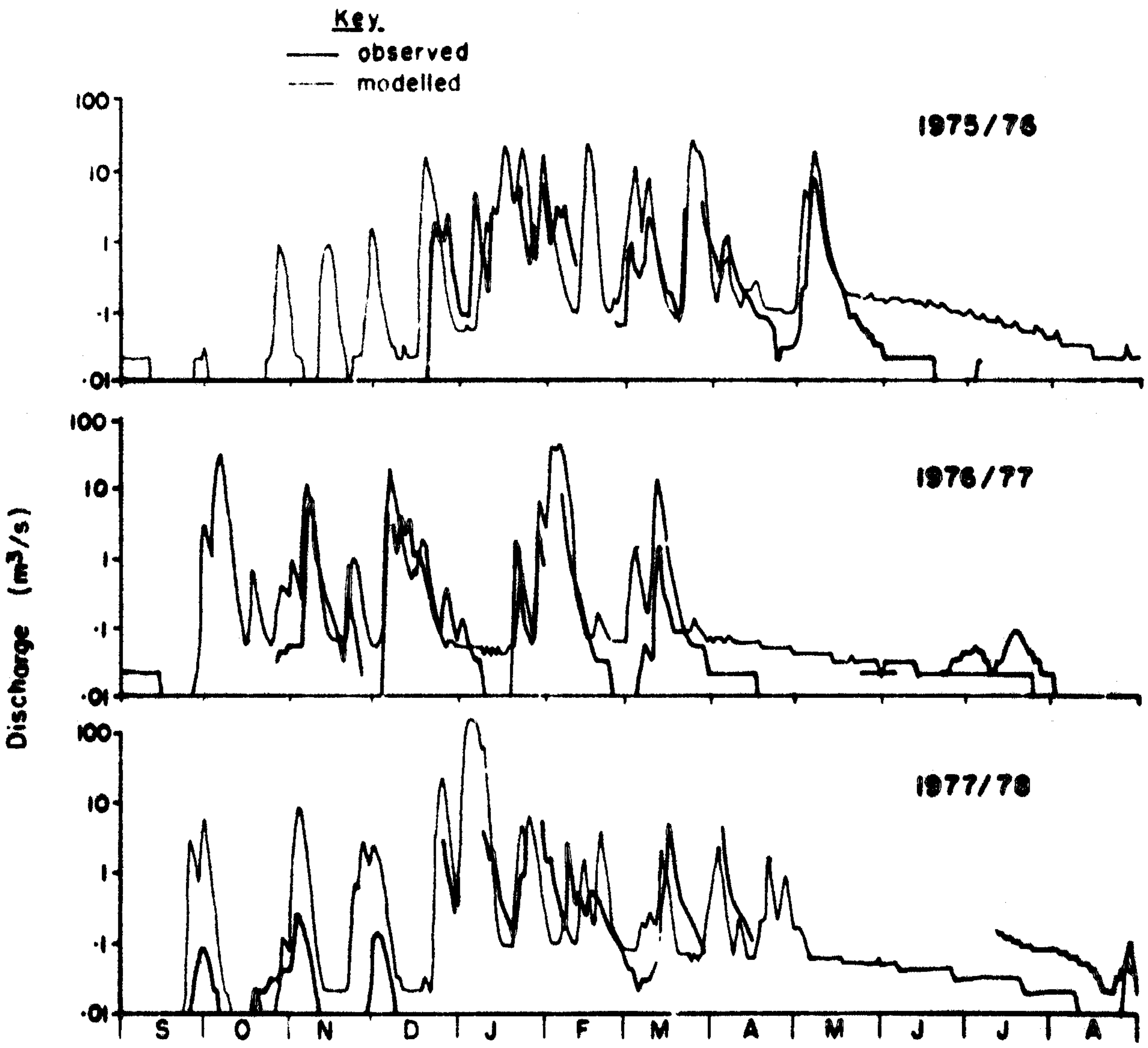

Fig. 3.24: Modelled and observed daily discharges at station C2M14 for period 1970-09 - 1978-08.

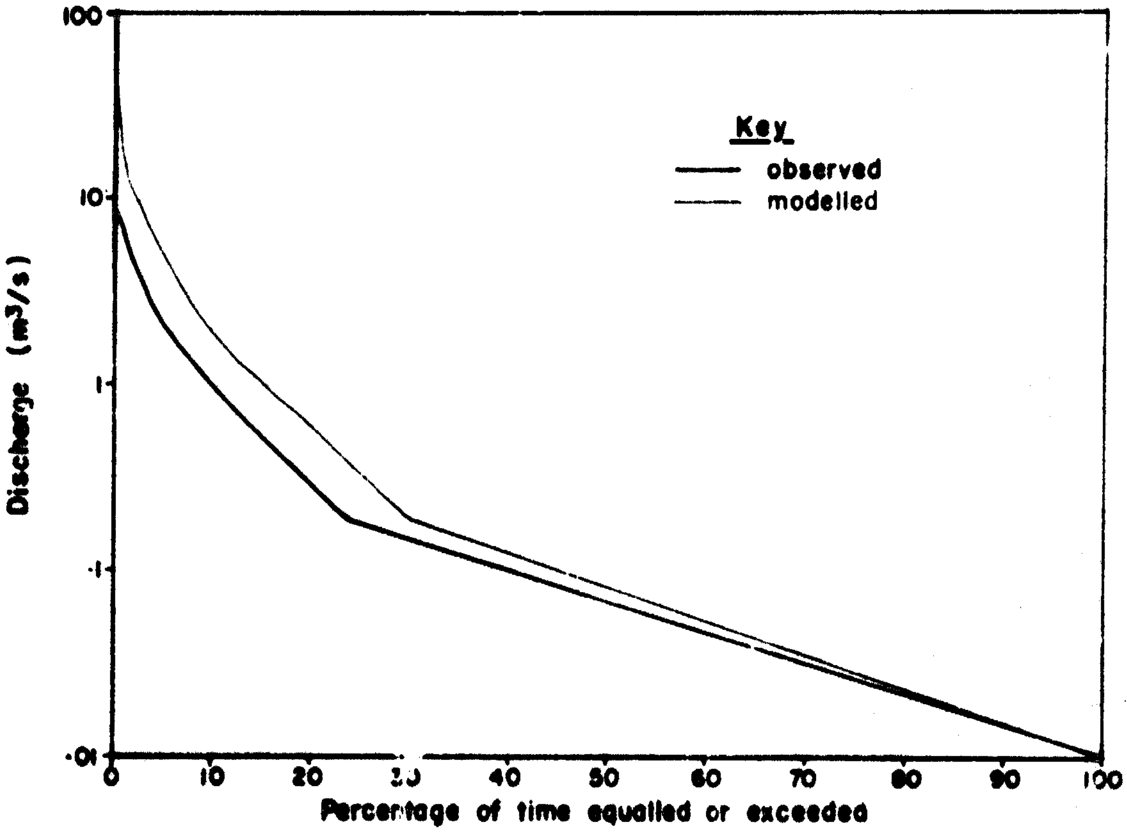

Fig. 3.25: Duration curve of modelled and observed daily discharges at station C2M14 for period 1970-09 - 1978-08

Inability to register even moderately high discharges at the gauges results, as is to be expected, in a low significance factor (see Table 3.3) and the modelled mean and standard deviation are consequently very much higher than the observed values. Little could be done to improve the calibration because of the truncated runoff record. It was deemed unwise to attempt to obtain a good fit for the range of flows which have been recorded as this would most likely result in under-estimation of the flood peaks due to the poor significance of the data sample (see section 3.1).

Barrage Wall: A long, reliable record of daily discharges from the Vaal Barrage is available. This record was used as a final check on the modelled discharges from the four tributaries draining the southern PWV region. The check was made by adding the modelled discharges to measured daily releases from Vaal Dam, subtracting known Barrage abstractions and comparing the resulting daily discharges with the observed Barrage releases. Storage attenuation effects in the Vaal Barrage were thus ignored. This assumption is not unreasonable when it is considered that the Barrage is normally operated in such a way as to maintain the water level as nearly constant as possible.

Fig. 3.26 is a plot of modelled and observed daily discharges for the period September 1970 to August 1978 while Fig. 3.27 shows the corresponding duration curves.

As can be seen from Table 3.3 and Figs. 3.26 and 3.27 an excellent fit has been obtained. The percentage error between the modelled and observed mean discharges given in Table 3.3 is 1,1 percent. It should be noted, however, that during the eight year period simulated the contribution of the modelled tributaries to the barrage was only 27,7 percent of the total inflow, the remainder being derived from Vaal Dam. Thus if the entire closing error is attributed to modelling deficiencies then the error in the modelled mean catchment runoff becomes 3,6 percent which is well within the accuracy with which the discharges can be measured. It might have been possible to improve the fit still further by adjusting the model parameters for subcatchment number 11 in such a way as to produce considerably more runoff. This course of action was rejected, however, on the basis that the required extreme catchment parameter values cannot reasonably be justified in terms of any known geological or other catchment feature. Furthermore, even small inaccuracies in the estimation of large flood discharges from Vaal Dam and Vaal Barrage could easily account for the entire 1,1 percent closing error.

3.2.2 Water quality modelling

Best-fit water quality parameter values used in programs NACLØ1 and NACLØ2 for each of the twelve subcatchments are given in Tables 3.4 and 3.2. Statistical properties of modelled and observed salt concentrations and salt loads are given in Tables 3.5 and 3.6. Figs. 3.28 to 3.38 are plots of modelled and observed daily salinities and salt loads at the water quality monitoring points shown in Fig. 3.2 for the period September, 1977 to August, 1978.

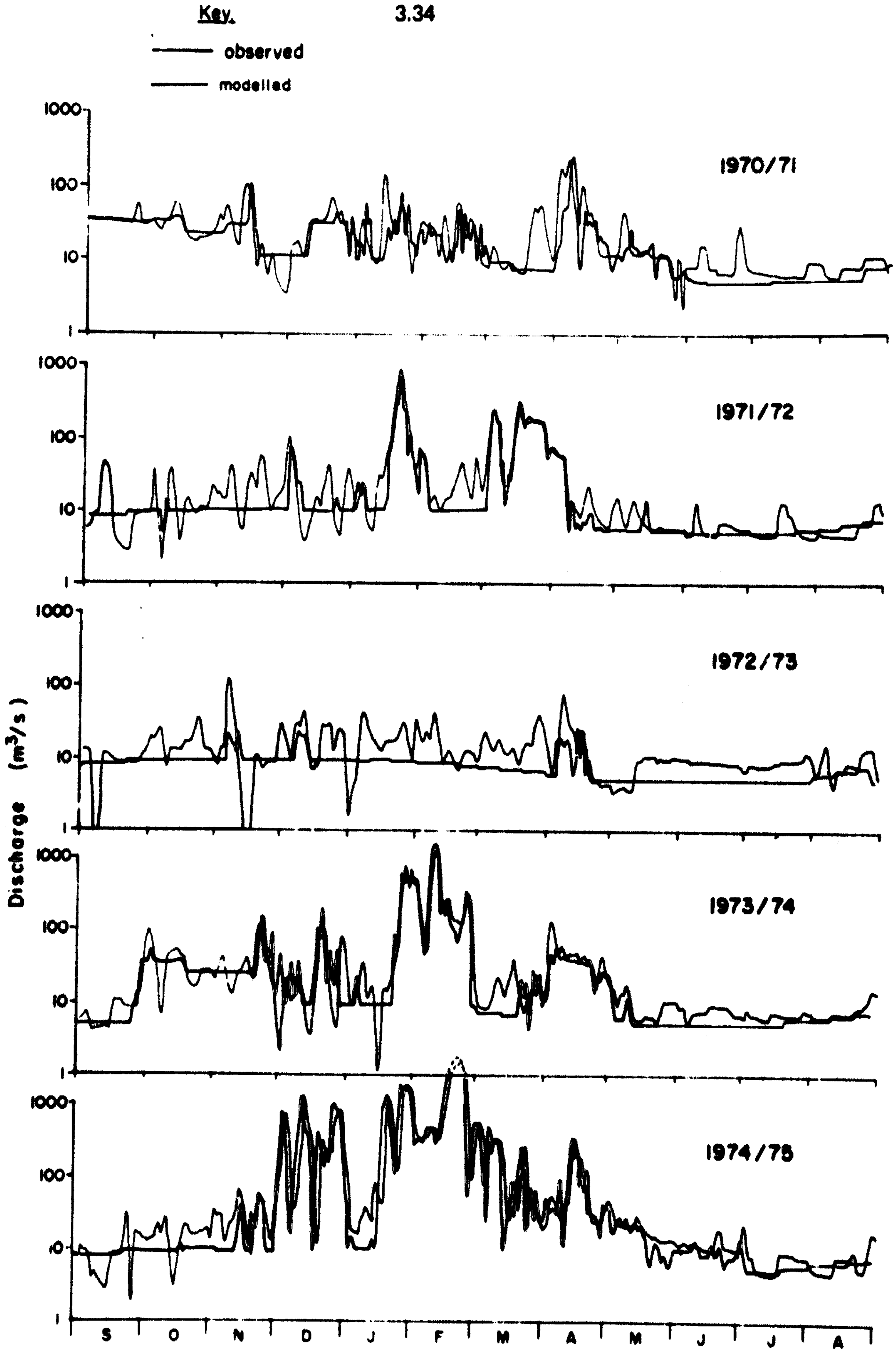

Fig. 3.26 : Modelled and observed daily discharges at Barrage wall for period 1970-09 - 1978-08

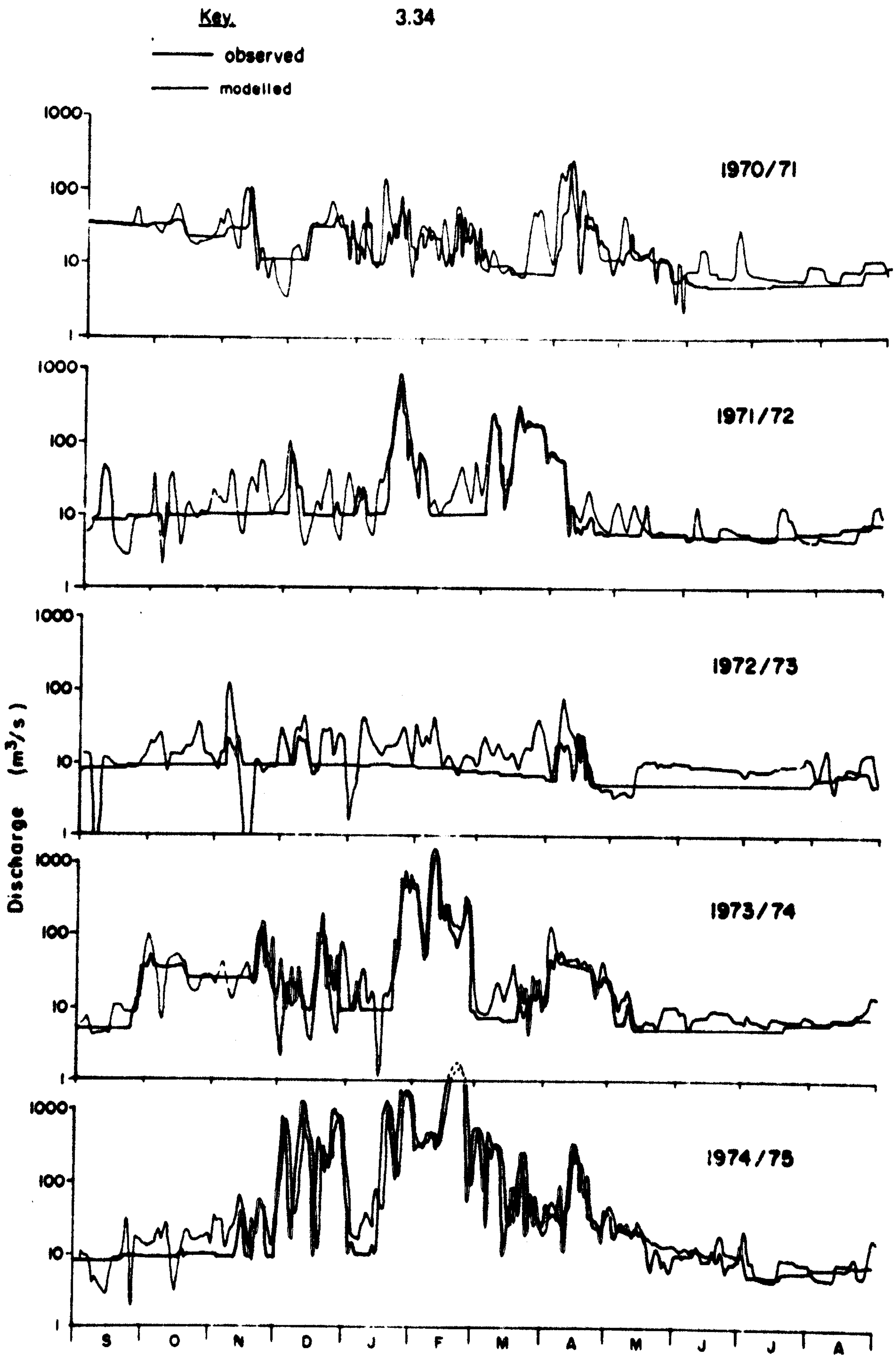

Fig. 3.26 : Modelled and observed daily discharges at Barrage wall for period 1970-09 – 1978-08

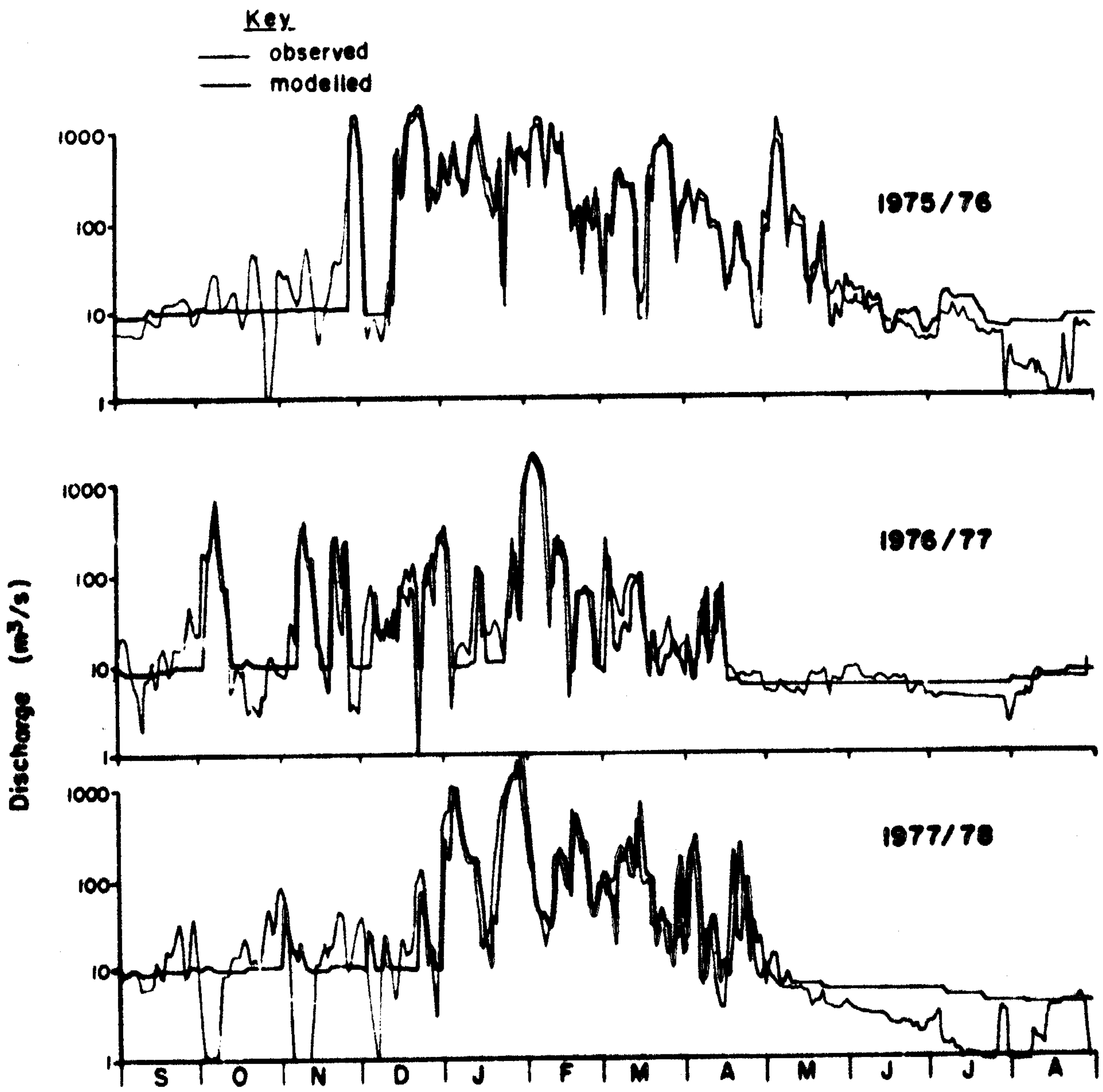

Fig. 3.26: Modelled and observed daily discharges at Barrage wall for for period 1970-09 - 1978-08.

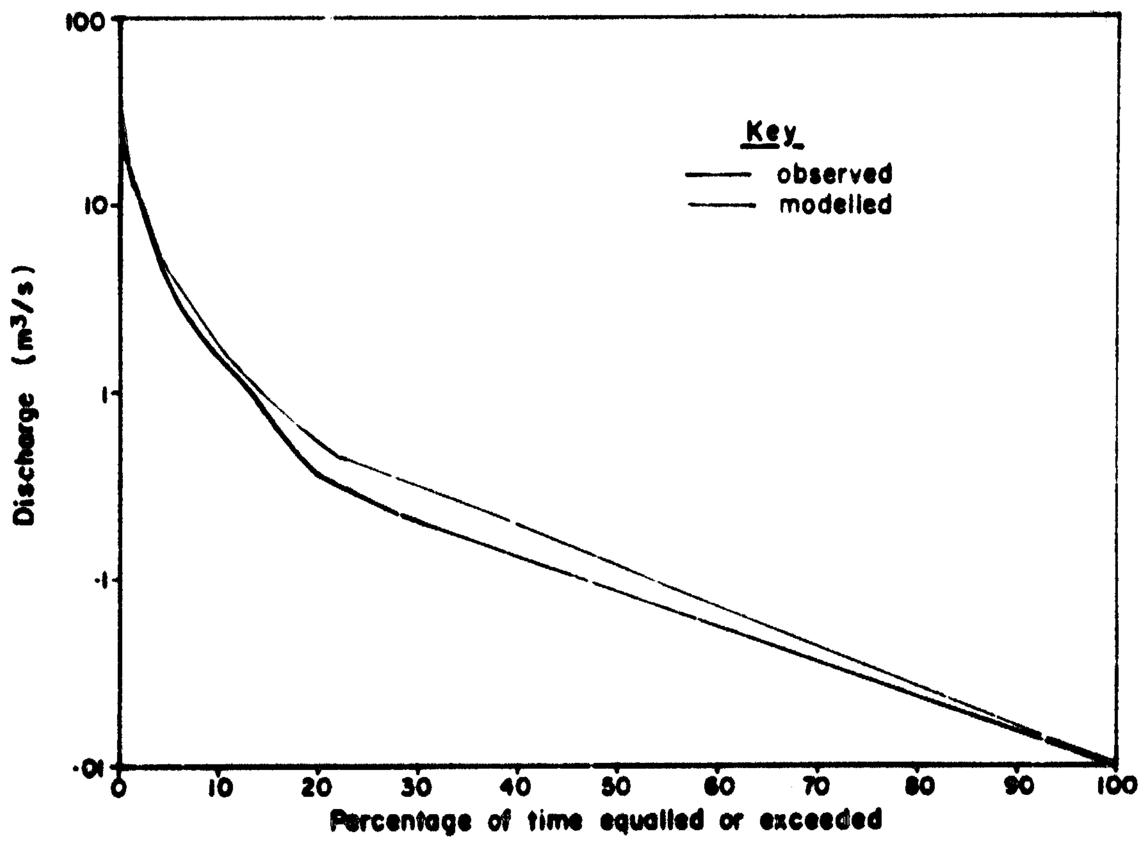

Fig. 3.27 : Duration curve of modelled and observed daily discharges at Barrage wall for period 1970-09 - 1978-08

Table 3.4: Water quality parameters used in program NACLØ1

Parameter	Subcatchment number											
	1	2	3	4a	4b	5	6	7	8	9	10	11
SALTR	57	97	133	52	30	53	12	11	11	15	42	164
APARR	-0,0007	-0,0008	-0,0007	-0,0007	-0,0007	-0,0007	-0,0010	-0,0010	-0,0010	-0,0020	-0,0007	-0,0007
BPARR	0,070	0,109	0,140	0,060	0,035	0,060	0,0187	0,0187	0,0187	0,040	0,040	0,170
SALTU	142	185	210	176	120	233	0	0	250	200	0	214
APARU	-0,0100	-0,0100	-0,0100	-0,0100	-0,0150	-0,0100	-0,0100	-0,0100	-0,0100	-0,0100	-0,0100	-0,0100
BPARU	0,800	1,000	1,200	1,000	0,800	1,200	0	0	0,400	1,200	0	1,200
PDEPS	0,90	0,90	0,90	0,85	0,85	0,90	0,90	0,90	0,90	0,90	0,80	0,90
CONCS	400	939	1059	730	453	526	167	251	156	770	440	694
CONCBG	10	10	10	10	10	10	4	4	4	10	10	10
PINTM	0,90	0,90	0,90	0,65	0,65	0,90	0,85	0,80	0,90	0,60	0,60	0,90
APARG	0	0	0	0	0	0	0	0	0	0	0	0

In calibrating the water quality parameters it is often possible to obtain a good fit between modelled and observed salt concentrations while that for salt loads is poor, or vice versa. Often, therefore, a compromise has to be reached. When the runoff record is suspect and the significance factor low (see Table 3.3), or where no record exists (such as at station S1), then the greater emphasis has to be placed upon the salt concentrations. In such cases the model parameters have been adjusted in such a way as to obtain a good fit between modelled and observed salt concentrations during the more significant modelled runoff events. This method of calibration should result in a reasonable estimate of the total salt load provided that the modelled discharges are sufficiently accurate.

Where the runoff record is good every effort has been made to optimise the load fit, particularly during flood events. For many of the catchments the base flows (and hence the base loads and salinities) are dominated by point flows over which the model parameters have little control.

Calibration results for each monitoring point are discussed in the following paragraphs.

Station K10: Successful calibration of the water quality model parameters is to a large extent dependent upon the accuracy with which the rainfall-runoff processes can be modelled. The poor runoff record at K10 therefore militated against good calibration of the water quality parameters. The same paucity of streamflow data made it impossible to optimise the fit between modelled and observed salt loads. An attempt was therefore made to achieve a good fit between modelled and observed salinities, particularly during the larger floods, such as those during January, February and March of 1978 (see Fig. 3.28). From Fig. 3.28 it can be seen that the modelled base flow TDS and the corresponding salt loads are considerably higher than those observed. It proved impossible to improve on this, however, because most of the base flow is composed of effluent discharges from the Johannesburg sewage works. Monthly effluent salt concentrations are used as input to the model (hence the monthly steps in the modelled salinities which may be seen in Fig. 3.28), but these values are based upon only three or four samples in each month and are therefore not true monthly averages. Part of the sewage effluent is also used for irrigation, but records of application rates and return seepages were not available and had to be estimated on the basis of the

Table 3.5: Statistical properties of modelled and observed daily TDS for the period 1977.09 - 1978.08 (units: mg/ℓ)

Tributary	Station number	Sample size	Observed		Modelled		Linear correlation coefficient	SF
			x̄	s	x̄	s		
Klip river	K10	354	571,9	85,3	717,4	186,9	0,594	0,994
	N8	301	1225,1	234,9	1211,8	256,8	0,782	0,974
	R6	345	1409,2	309,8	1296,5	281,1	0,826	0,988
	C2M15	355	847,9	148,9	898,8	222,9	0,840	0,993
Suikerbosrand	B9	51	1185,7	417,5	1137,9	492,1	0,893	0,989
	B10	354	895,2	376,3	799,6	329,8	0,750	0,943
	S1	350	154,7	6,8	146,3	14,5	0,171	0,998
	C2M04	355	597,3	264,4	510,6	223,6	0,438	0,919
Rietspruit	C2M05	355	871,9	286,3	937,8	281,2	0,788	0,995
Taaibosspruit	C2M14	40	645,4	390,6	387,7	109,9	0,536	0,842
Vaal river	ZB	365	205,0	98,5	211,3	90,0	0,882	1,000
	V1	365	511,9	195,0	587,8	267,8	0,870	1,000
	V2	365	469,1	174,4	546,4	242,4	0,852	1,000
	Barrage	364	475,2	173,3	444,9	162,7	0,964	1,000

Table 3.6: Statistical properties of modelled and observed daily salt loads for the year 1977.09 to 1978.08 (units: t/d)

Tributary	Station number	Sample size	Observed		Modelled		Linear correlation coefficient	SF
			x̄	s	x̄	s		
Klip river	K10	224	250,4	75,6	335,7	105,8	0,495	0,298
	N8	243	319,9	141,2	319,7	163,3	0,674	0,934
	R6	179	356,3	80,7	410,5	208,5	0,168	0,696
	C2M15	42	411,0	76,1	509,6	165,0	0,518	0,057
Suikerbosrand	B9	43	58,3	25,2	72,9	41,3	0,348	0,134
	B10	117	126,5	190,6	78,7	83,1	0,243	-0,091
	C2M04	338	306,7	667,2	363,8	899,8	0,801	0,979
Rietspruit	C2M05	326	134,1	195,6	105,0	180,5	0,645	0,944
Taaibosspruit	C2M14	76	2,7	7,3	13,4	58,0	0,637	-0,428
Vaal river	Barrage	364	1972,3	4728,6	1982,4	4615,5	0,914	1,000

area of land under irrigation. For the dry season of 1978 the observed TDS values for the point inputs to the stream were considerably higher than that at K10. This is most likely due to inaccuracies in the effluent salinity record. The model fit could have been improved by assuming substantial bed seepage losses between the sewage inputs and station K10 (of the order of 2 m^3/s within the space of 30 km) together with an equally large base flow input from the surrounding catchment in order to achieve the necessary dilution and flow volumes. Such highly inconsistent assumptions are obviously untenable and therefore no further attempt was made to improve the fit.

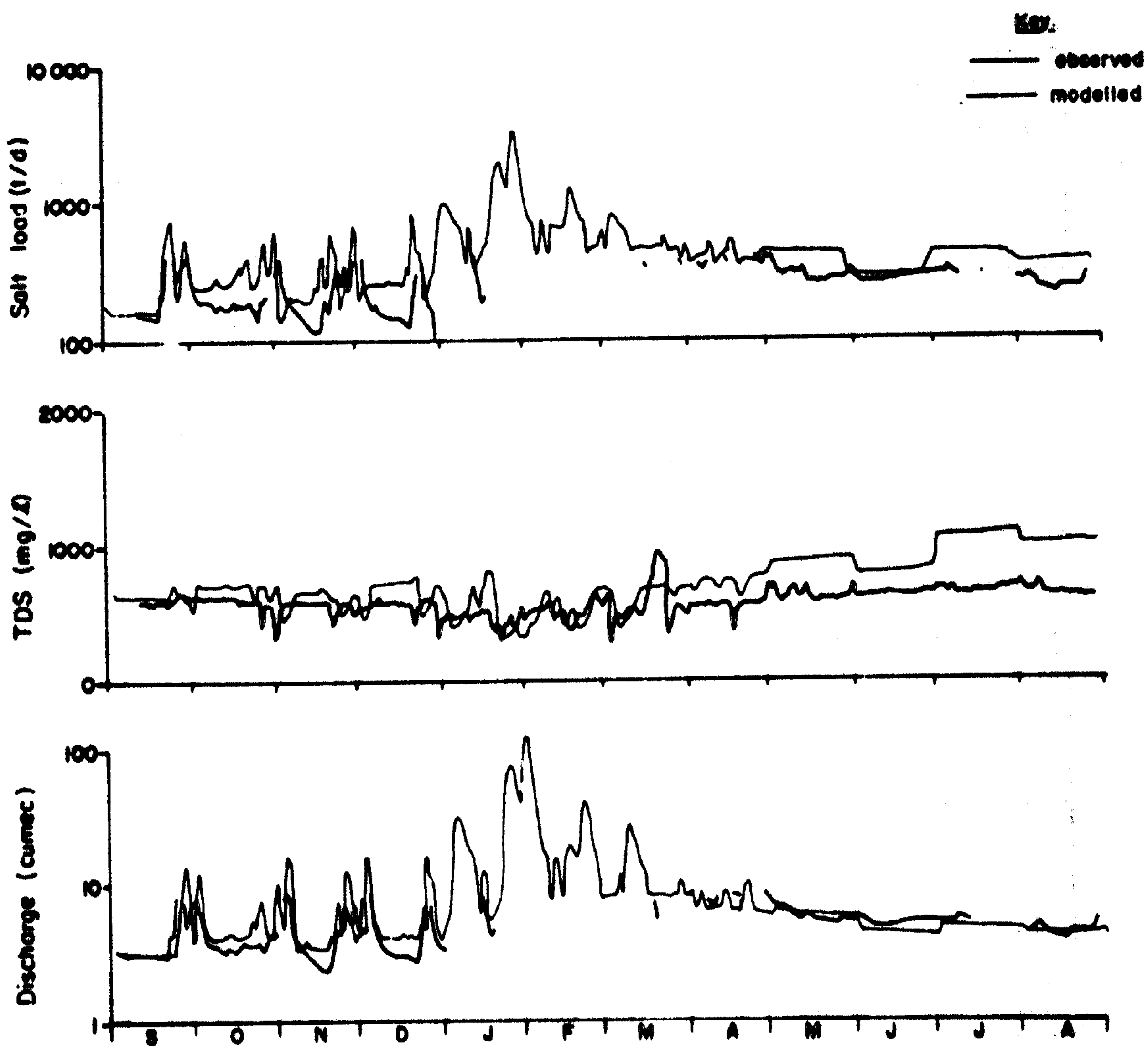

Fig. 3.28 Modelled and observed daily discharges, TDS and salt loads at station K10 for period 1977-09 – 1978-08

Station N8: Base flows at N8 are dominated by saline shaft water pumped from the ERPM gold mine, together with municipal effluents. It was found that the effluent discharges exceeded the measured base flows at N8. An earlier attempt to reduce base flows by increasing the vlei evaporation parameters failed because this led to unacceptably high modelled salinities. It was therefore necessary to specify a small bed seepage loss (10 Ml/d) from the upper reach (reach number 2 of Fig. 3.3) of the Natalspruit. As can be seen from Tables 3.5 and 3.6 and Fig. 3.29 a good fit has been attained between modelled and observed salt loads and concentrations.

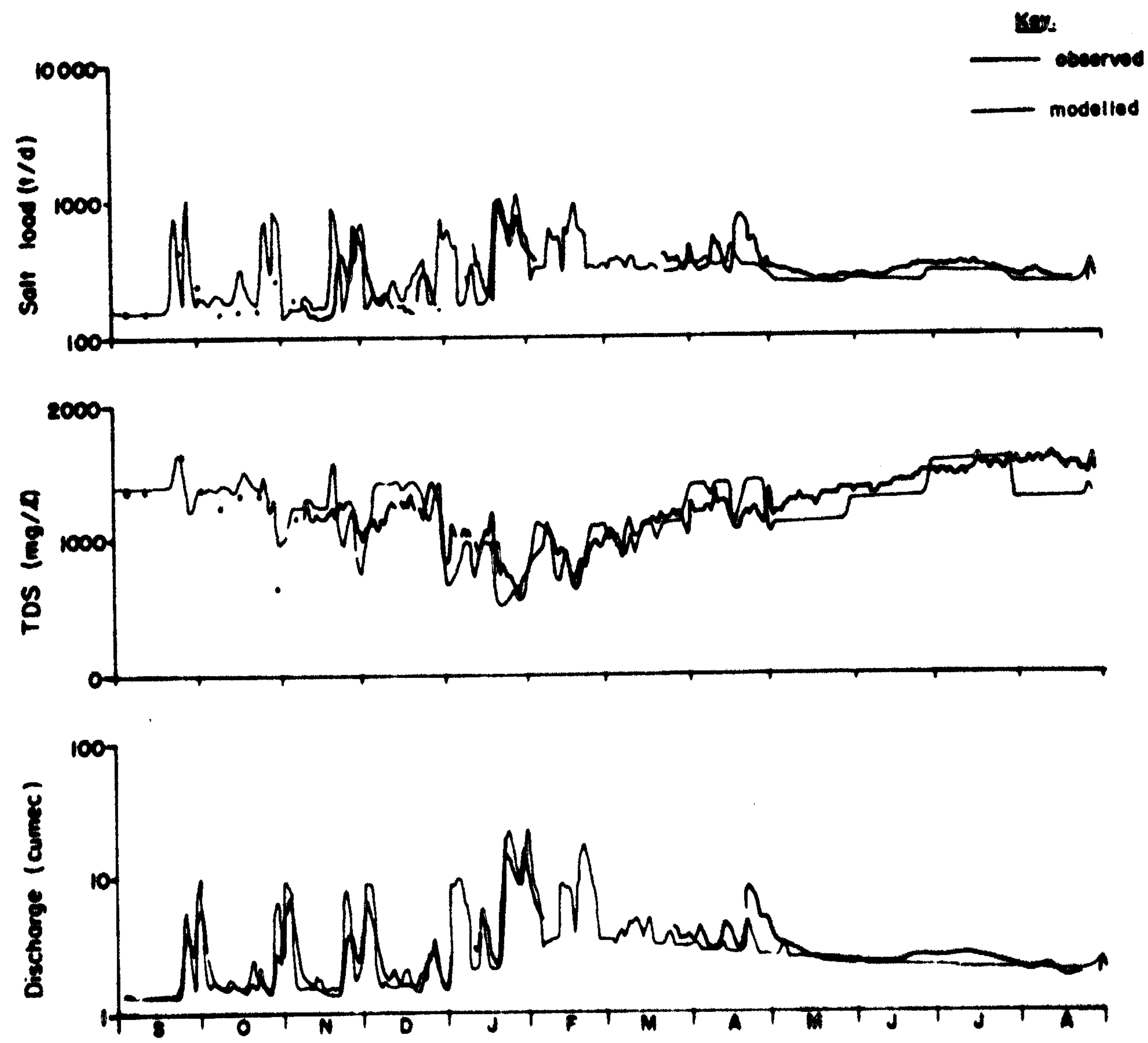

Fig. 3.29 · Modelled and observed daily discharges, TDS and salt loads at station N8 for period 1977-09 — 1978-08

Station R6: As with station N8 the base flows at R6 are largely derived from mine pumpage. The poor discharge record, however, precludes accurate modelling of salt loads. The calibration was therefore based on the fit between modelled and observed daily salt concentrations, especially during flood events (see Fig. 3.30). Modelled salt concentrations during the dry season of 1978 are lower than those observed. This could not be improved upon, however, as the base flows are composed mostly of point source effluents which are poorly monitored. Fig. 3.30 and Table 3.5 display a reasonably good fit between modelled and observed TDS.

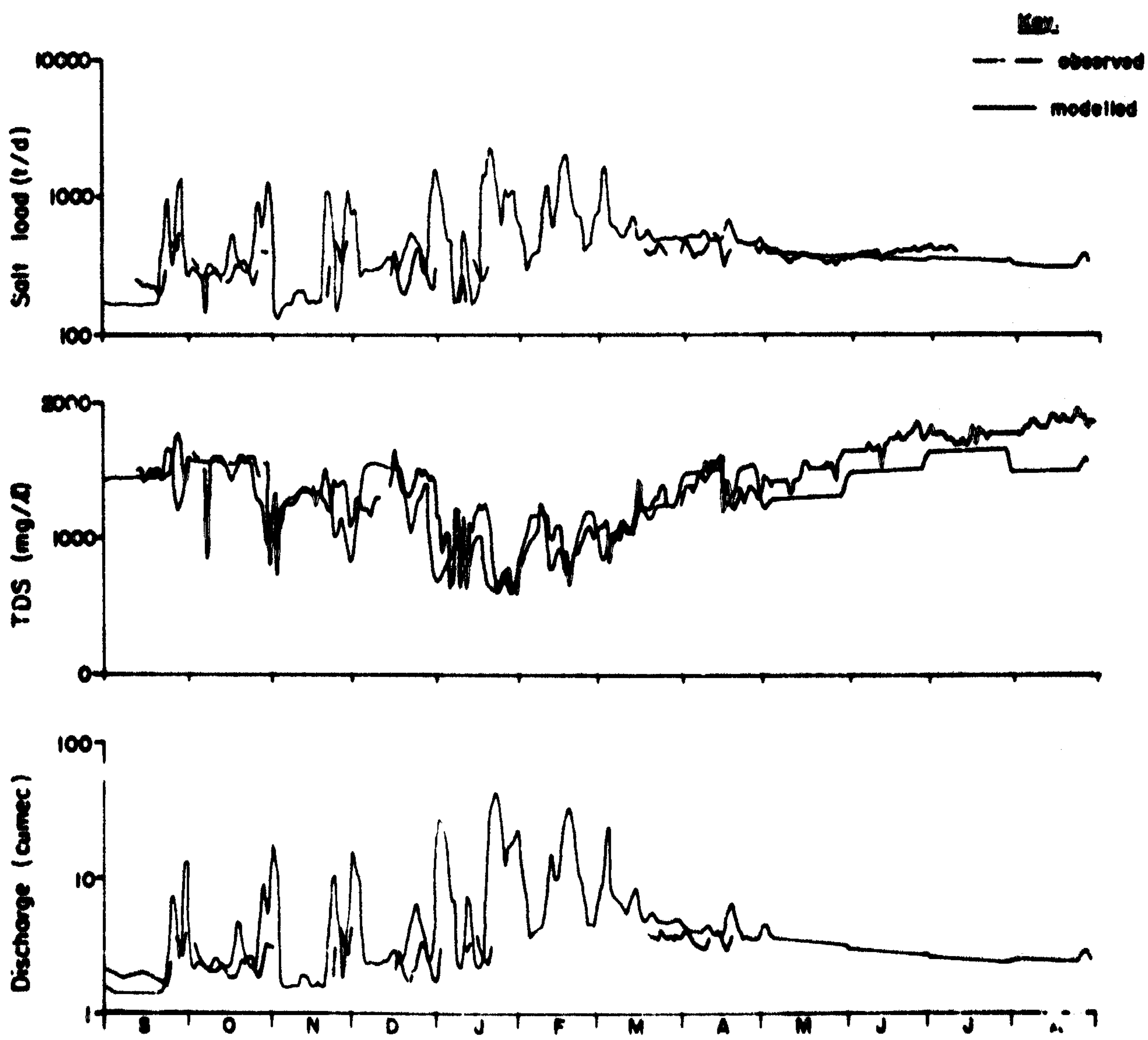

Fig. 3.30. Modelled and observed daily discharges, TDS and salt loads at station R6 for period 1977-09 — 1978-08

Station C2M15: The virtual absence of streamflow records makes a direct comparison between modelled and observed salt loads impossible. From Fig. 3.31 it can be seen that reasonable agreement has been achieved between modelled and observed salt concentration during the wet season, but the modelled salinities tend to be too high during the dry season of 1978. This latter effect is due to the previously discussed shortcomings in the record of sewage effluent entering the Klip river upstream of monitoring point K10.

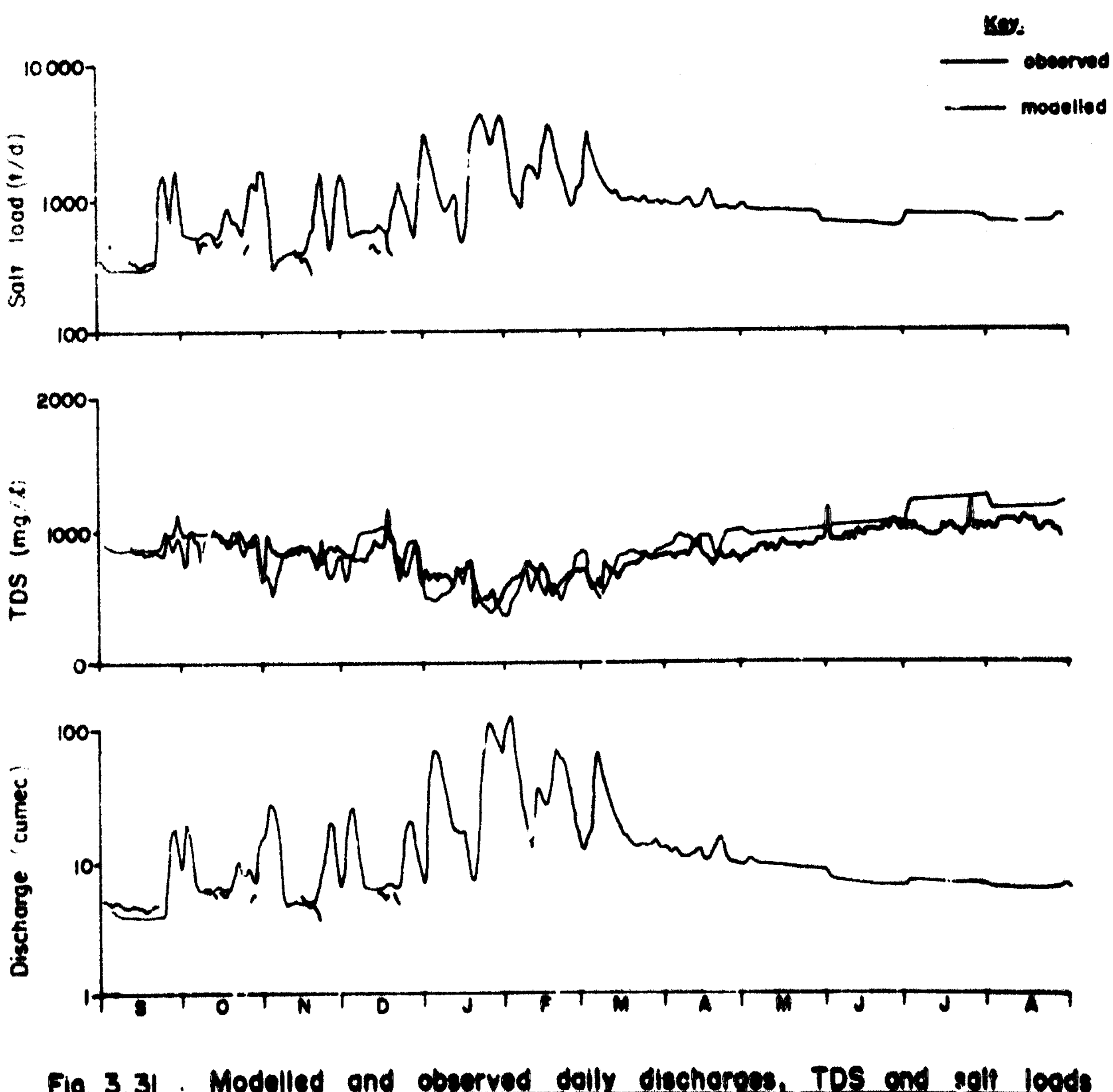

Fig. 3.31 Modelled and observed daily discharges, TDS and salt loads at station C2M15 for period 1977-09 — 1978-08

Station B9: Although the daily TDS sample size is small, it can be seen from Table 3.5 that the significance factor is high. This is due to the attenuating effect of the lakes which obviates the necessity for more frequent water quality sampling. The significance factor for salt loads is low, however, because of the break in the flow record during the most significant flow event of the year (see Fig. 3.32). A reasonably good fit was achieved between modelled and observed salt concentrations, although the modelled concentrations failed to rebound rapidly enough after the floods of early 1978.

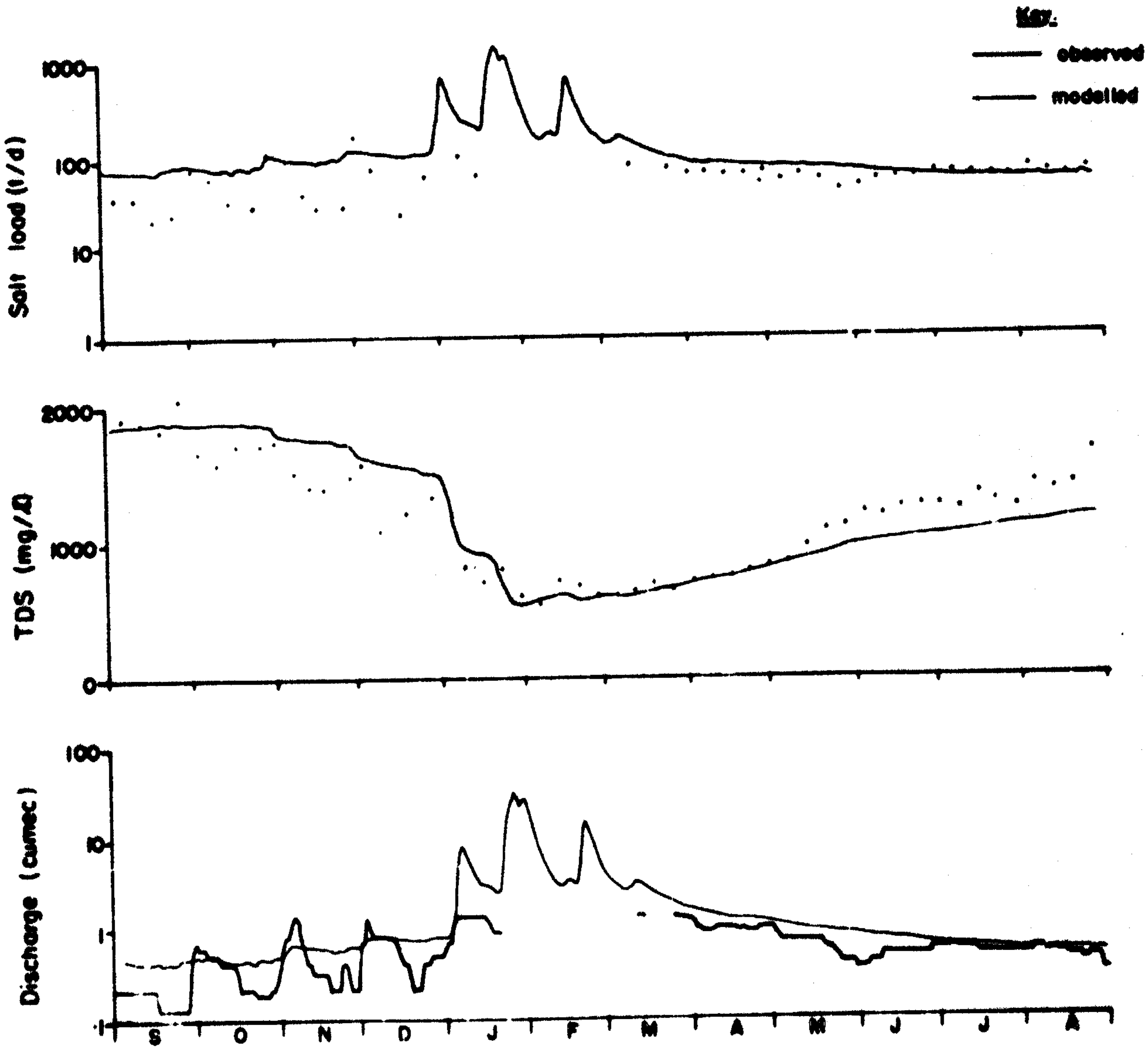

Fig. 3.32 . Modelled and observed daily discharges, TDS and salt loads at station B9 for period 1977-09 — 1978-08

Station B10: Comparison of modelled and observed salt loads is rendered meaningless by the defective flow record. Although the salt concentrations of Fig. 3.33 are in close agreement during the major flood events, there is no guarantee that a good estimate of the total salt load has been made because of the uncertainty of the modelled discharges. The nearest reliable streamflow recorder is at station C2M70, but the record there cannot be used to verify the modelled discharges at B10 because the greater portion of the Suikerbosrand catchment lies between the two stations.

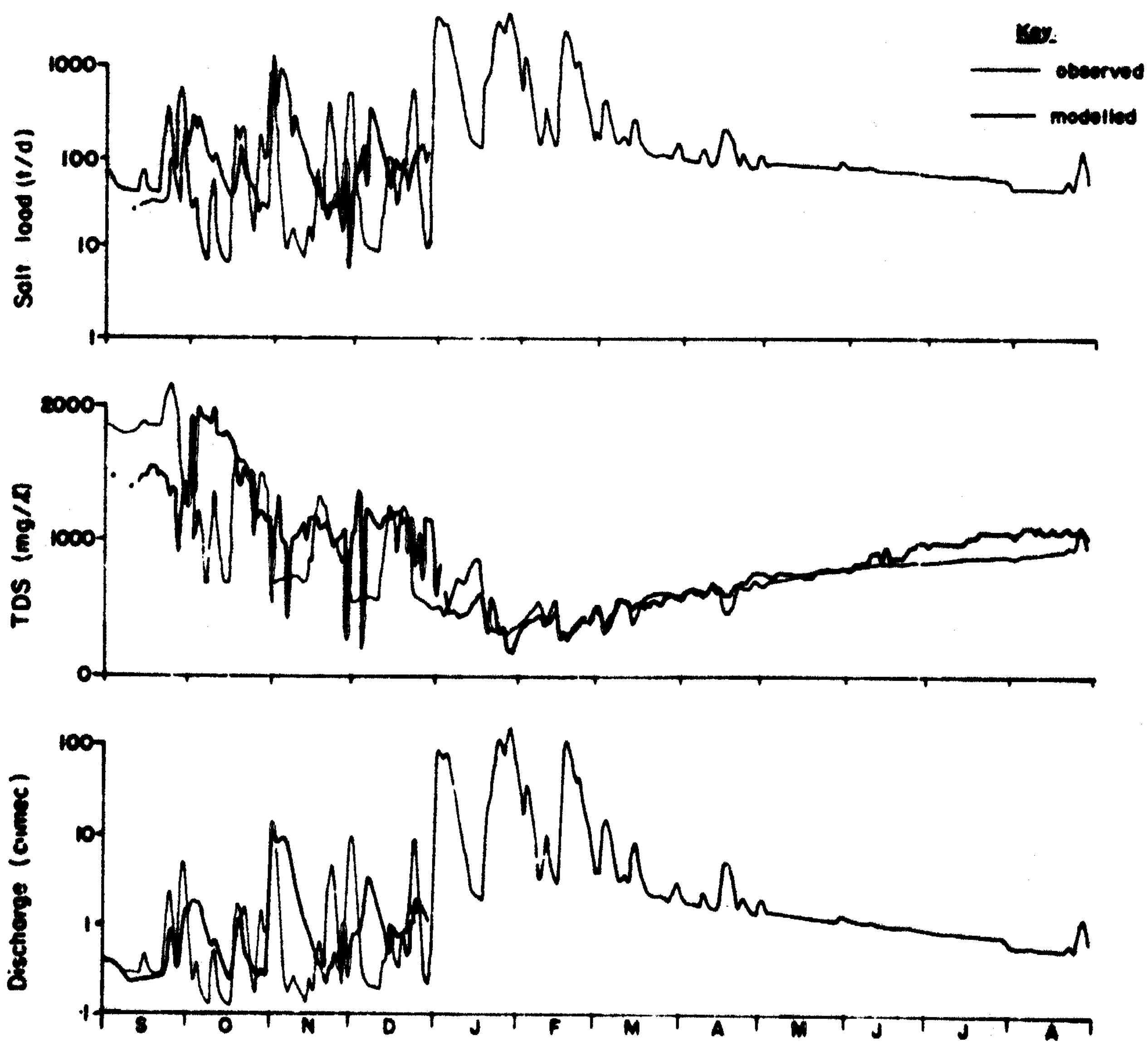

Fig. 3.33 . Modelled and observed daily discharges, TDS and salt loads at station B10 for period 1977-09 — 1978-08

The poor fit between modelled and observed salinities during the first four months of the simulation is attributable to uncertainties in the geometry of the vleis upstream of B10. During low flow conditions evaporation has a crucial effect on salinities. It was found during calibration that even a small change in the assumptions as to the vlei cross-sectional properties, such as a slightly deeper channel, had a profound effect upon salt concentrations.

The water quality parameters for subcatchment 4b were therefore adjusted in such a way as to produce a reasonable fit between modelled and observed salt loads at station C2M04 where the record of observed daily salt loads is nearly complete.

<u>Station S1</u>: Subcatchment number 8 is virtually undeveloped and as a result the salinities are exceptionally low. It is evident from Table 3.5 and Fig. 3.34 that the standard deviation of the modelled daily salt concentrations is considerably higher than that of the observed values. This is due to a number of factors. In the first instance the assumptions made in the washoff model

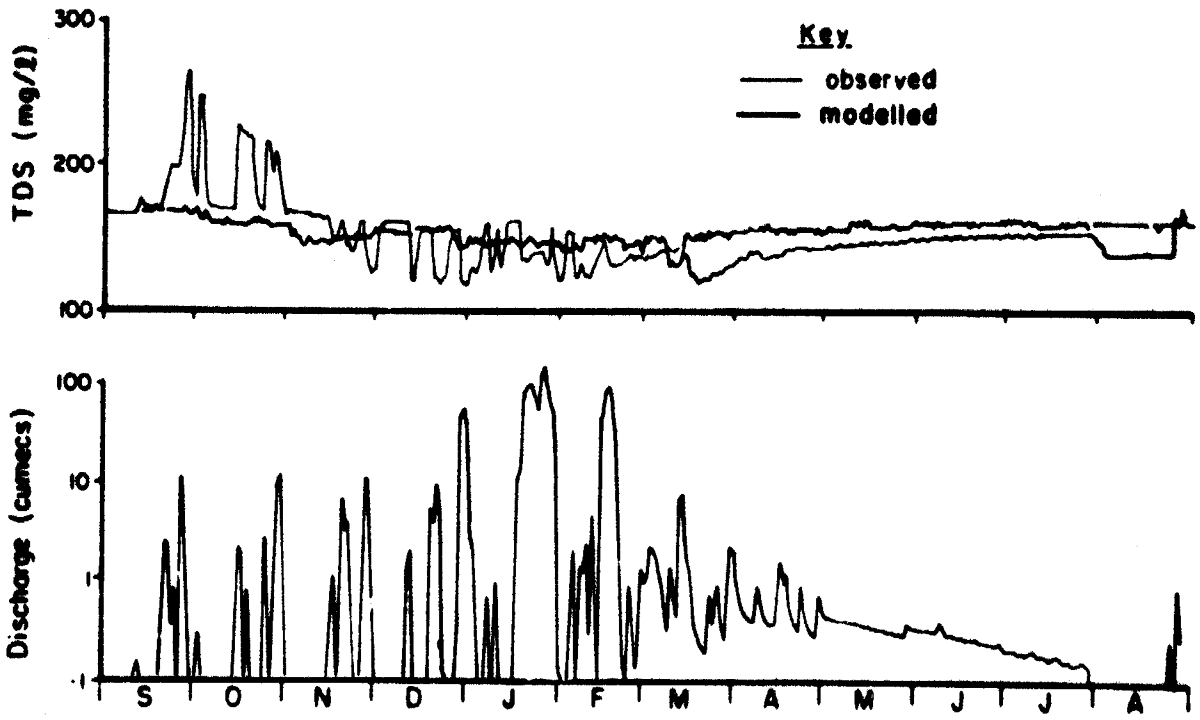

Fig. 3.34: Modelled and observed daily TDS at station S1 for period 1977-09 - 1978-08

make a certain amount of dilution during high discharges inevitable. The observed salinities, however, are remarkably constant, even during the highest discharges. Modelling is further complicated by uncertainties in the geometry of the large vleis upstream of S1.

Parameter adjustment was concentrated on achieving as close a fit between modelled and observed salt concentrations during the larger floods as possible.

The poor fit should not adversely affect the overall modelling of the Suikerbosrand because of the relatively low salt concentrations involved.

Station C2M04: The salt recharge rates for subcatchments 6 and 7 were set equal to those calibrated for subcatchment 8 because all three catchments are sparsely populated and undeveloped. Water quality parameters for subcatchment 4b were then adjusted to obtain a reasonable fit between modelled and observed daily salt loads at station C2M04. From Fig. 3.35 it can be seen that a good fit was achieved between modelled and observed daily salt loads. The exceptionally high modelled salt concentrations in September 1977 are due to concentration through evaporation of very small modelled discharges, which as can be seen are less than 0,1 m^3/s. The salt loads involved, however, are insignificant. The modelled mean daily salt load given in Table 3.6 is 18,6 percent lower than that observed. This error was not removed by adjusting the water quality parameters because for the year simulated the modelled discharges are also 17,8 percent higher than those observed. (The purpose of the model calibration was not merely to obtain the best fit possible for a single year, but to arrive at model parameter values which would also be applicable to other hydrological sequences. Had the observed discharges for the year 1977/78 been 18 percent higher then the salt load washed off the catchment would also have been higher, although not by as much as 18 percent).

Station C2M05: From Fig. 3.36 and Table 3.5 it can be seen that a reasonably good fit has been obtained between modelled and observed salt loads and salt concentrations. Table 3.6, however, shows that the modelled mean daily salt load is 21 percent less than that observed. This is brought into perspective, however, by

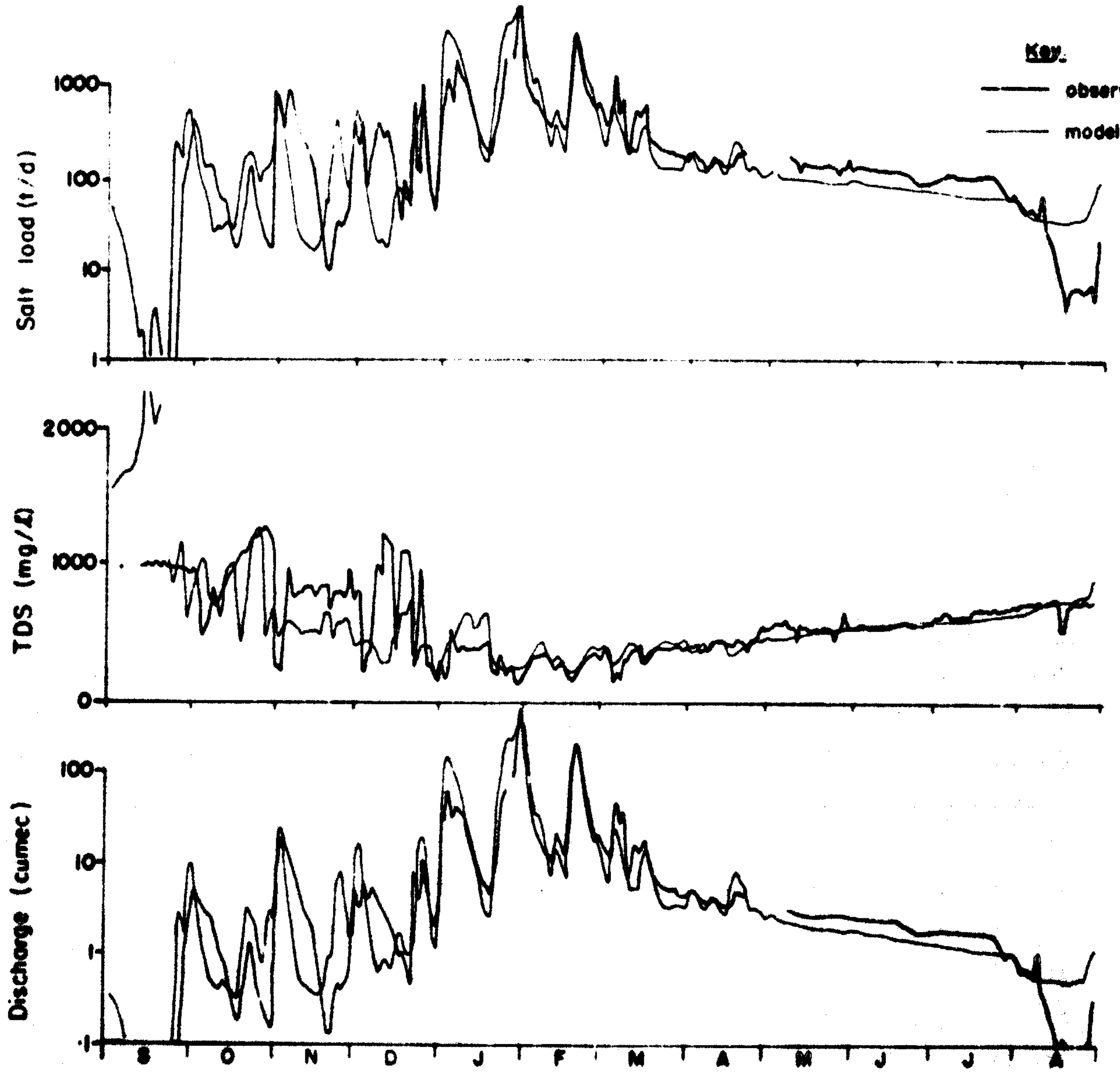

Fig. 3.35 . Modelled and observed daily discharges, TDS and salt loads at station C2M04 for period 1977-09 — 1978-08

the fact that the modelled discharge during the year 1977/78 was 35 percent lower than that observed (the error for the period 1970.09 - 1978.08, calculated from Table 3.3, is less than one percent). To compensate for the error in the modelled discharges for this one year by introducing a compensating error in the salt storage recharge rates would lead to unrealistic values which would not be applicable to other hydrological sequences. If, for example, the salt recharge rates were increased by 21 percent in order to improve the fit for the period 1977.09 to 1978.08, then a simulation of the period 1970.09 to 1978.08 would yield excessive salt loads. In circumstances such as these, where the modelled discharges differ markedly from those observed, it is difficult to calibrate the water quality parameters which control the salt recharge rate because the salt load washed off is a function of both the discharge and the salt storage. The salt storage is in turn dependent on the antecedent conditions. Depending, therefore, upon the relative magnitudes of the salt storages and the recharge rates, the water quality parameters should be adjusted so that the modelled salt load at C2M05 for the period 1977.09 to 1978.08 is somewhere between 0 and 35 percent less than that observed. The choice of the salt recharge rate parameters for subcatchment number 9 is therefore somewhat subjective and has a rather wide margin of error associated with it.

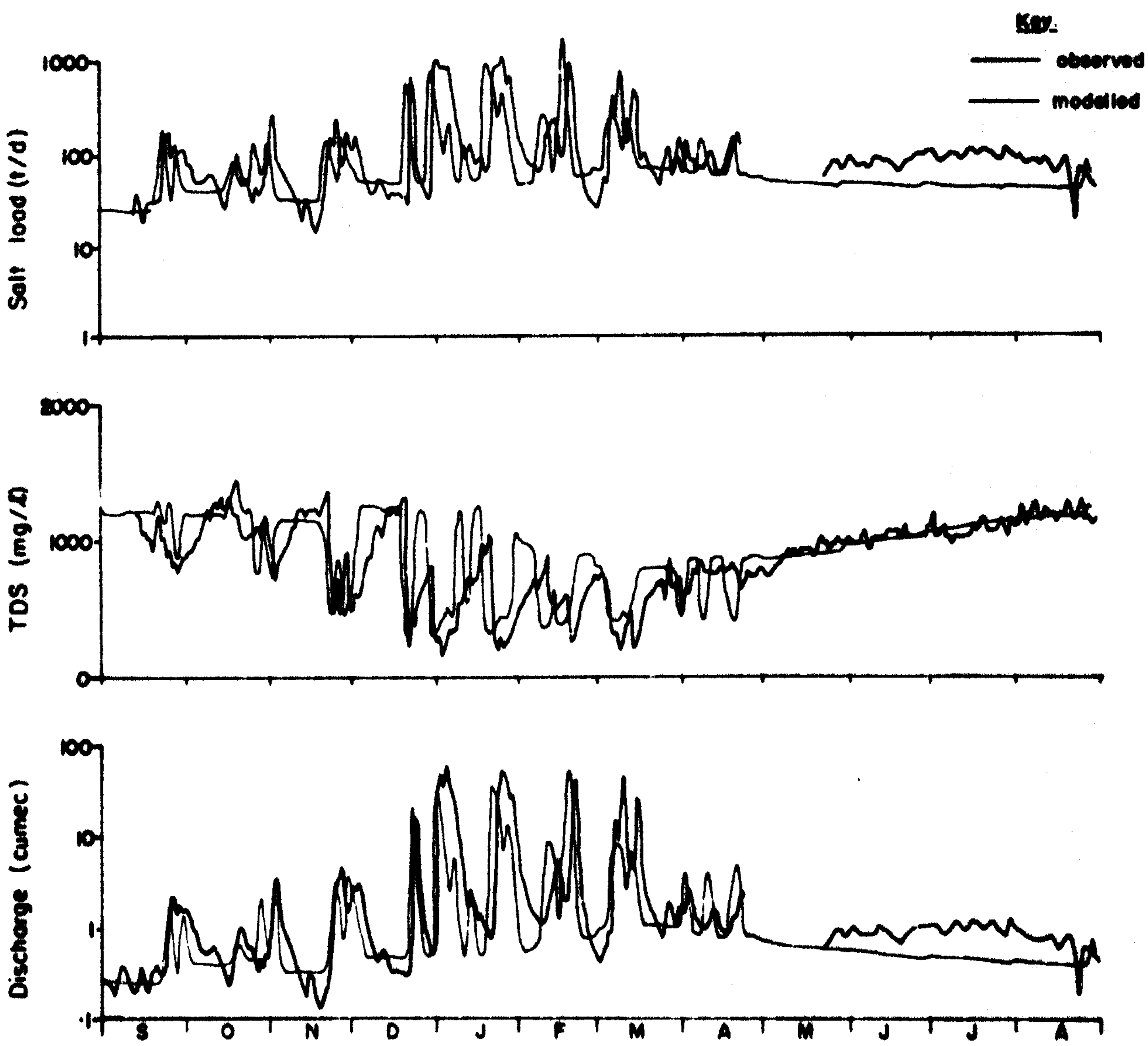

Fig. 3.36 . **Modelled and observed daily discharges, TDS and salt loads at station C2M05 for period 1977-09 — 1978-08**

Station C2M14: Both streamflow and water quality data are extremely sparse as is reflected by very poor significance factor for observed salt loads in Table 3.6. The choice of water quality parameters for subcatchment number 10 was therefore rather arbitrary. Although the catchment is undeveloped and sparsely populated, it was thought likely that atmospheric pollution from the nearby petrochemical industries and power stations situated in subcatchment number 11 could enhance the salt generation rates. The pervious surface recharge rate BPARR was therefore set somewhat higher than that used for the other undeveloped catchments (subcatchments 6, 7 and 8).

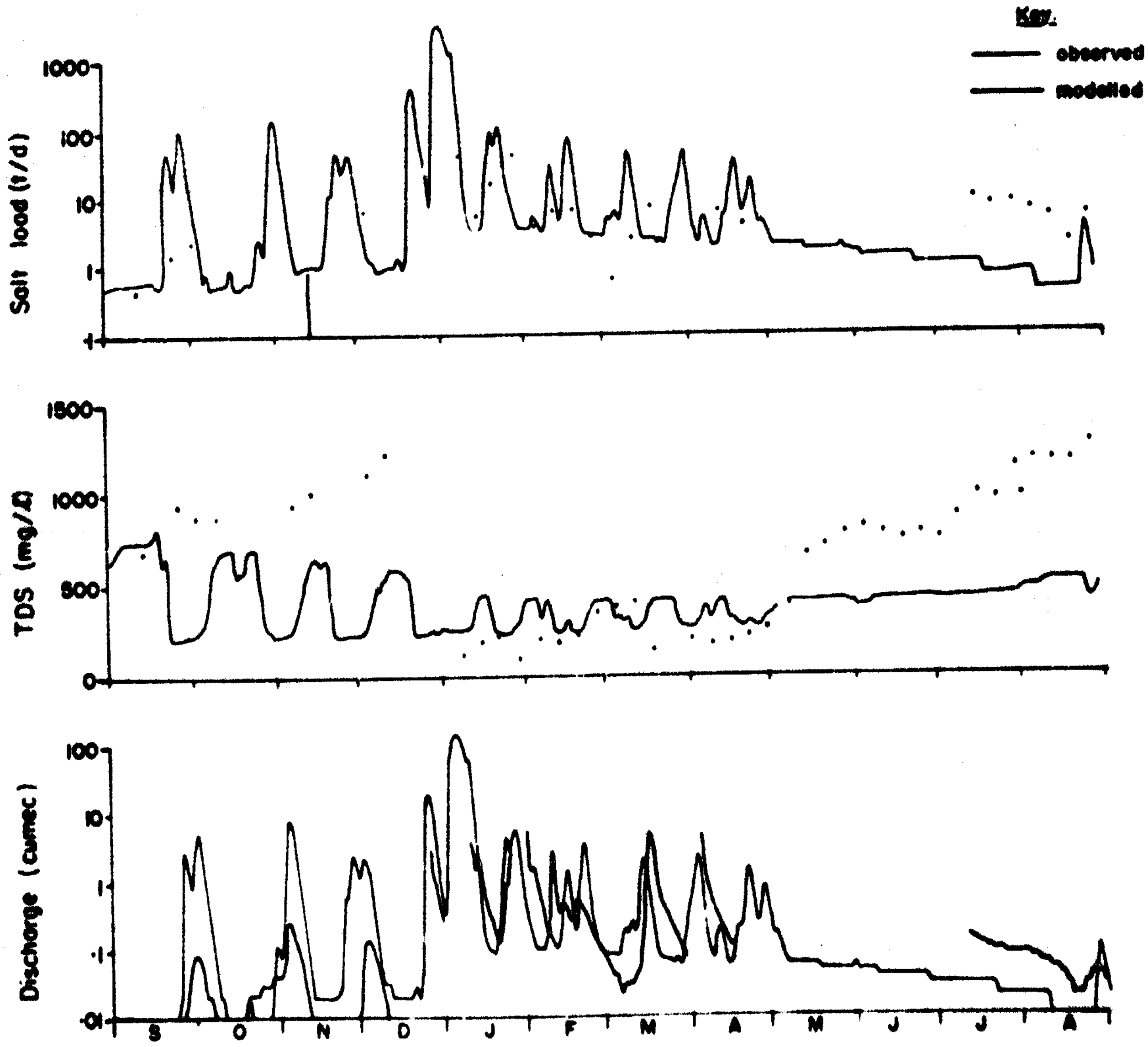

Fig. 3.37 Modelled and observed daily discharges, TDS and salt loads at station C2M14 for period 1977-09 — 1978-08

<u>Barrage wall</u>: Subcatchment number 11 was calibrated using the record at the Vaal Barrage wall. Obviously the model parameters for this catchment contain implicitly the accumulated errors in the modelling of all the other subcatchments. The comparison between modelled and observed values was made by means of a one-dimensional cell-type level-pool model of the Vaal Barrage described by Mileikowsky (1980). Input to the Barrage model comprises daily discharges from Vaal Dam (in this case observed values) and in the four major tributaries of the Vaal Barrage (in this case modelled values) along with the associated daily salt concentrations. Monthly abstractions from each of the nine Vaal Barrage intakes are also specified. Washoff from subcatchment number 11 was assumed to enter the Vaal Barrage at the mouth of the Taaibosspruit. Model parameters for subcatchment number 11 were adjusted until a good fit was obtained between modelled and observed daily salt loads passing downstream at the Barrage. From Fig. 3.38 and Tables 3.5 and 3.6 it can be seen that an exceptionally good fit was achieved.

Details of modelled and observed salt concentrations at the Rand Water Board intakes are also given in Fig. 3.38 and Table 3.5. Generally the fit is good, except for the dry season of 1978 when the modelled salinities at the Zuikerbosch intakes are too low while those at the two Vereeniging intakes are too high. This can be partly explained by the very pronounced stratification of the Vaal Barrage between the Zuikerbosch intakes and the Suikerbosrand mouth (Mileikowsky, 1980). Whenever the Vaal Dam discharges are small relative to the inflow from the tributaries, water is drawn upstream from the tributaries to the Zuikerbosch intakes resulting in a sharp rise in salt concentrations (Vaal Dam salinities are low, of the order of 120 mg/ℓ). This upstream advection is enhanced due to the effect of the stratification which allows the less saline water from Vaal Dam to move over the denser saline water which is moving upstream. The Barrage model, however, assumes complete mixing within each of its 57 cells and thus cannot duplicate the stratification effects and consequently models less salt being drawn into the Zuikerbosch intakes. The intakes upstream of the Klip and Suikerbosrand draw sixty percent of the water pumped from the Vaal. As the modelled salt load drawn off upstream of the major tributaries is too little, it is inevitable that the modelled salt load passed to the downstream

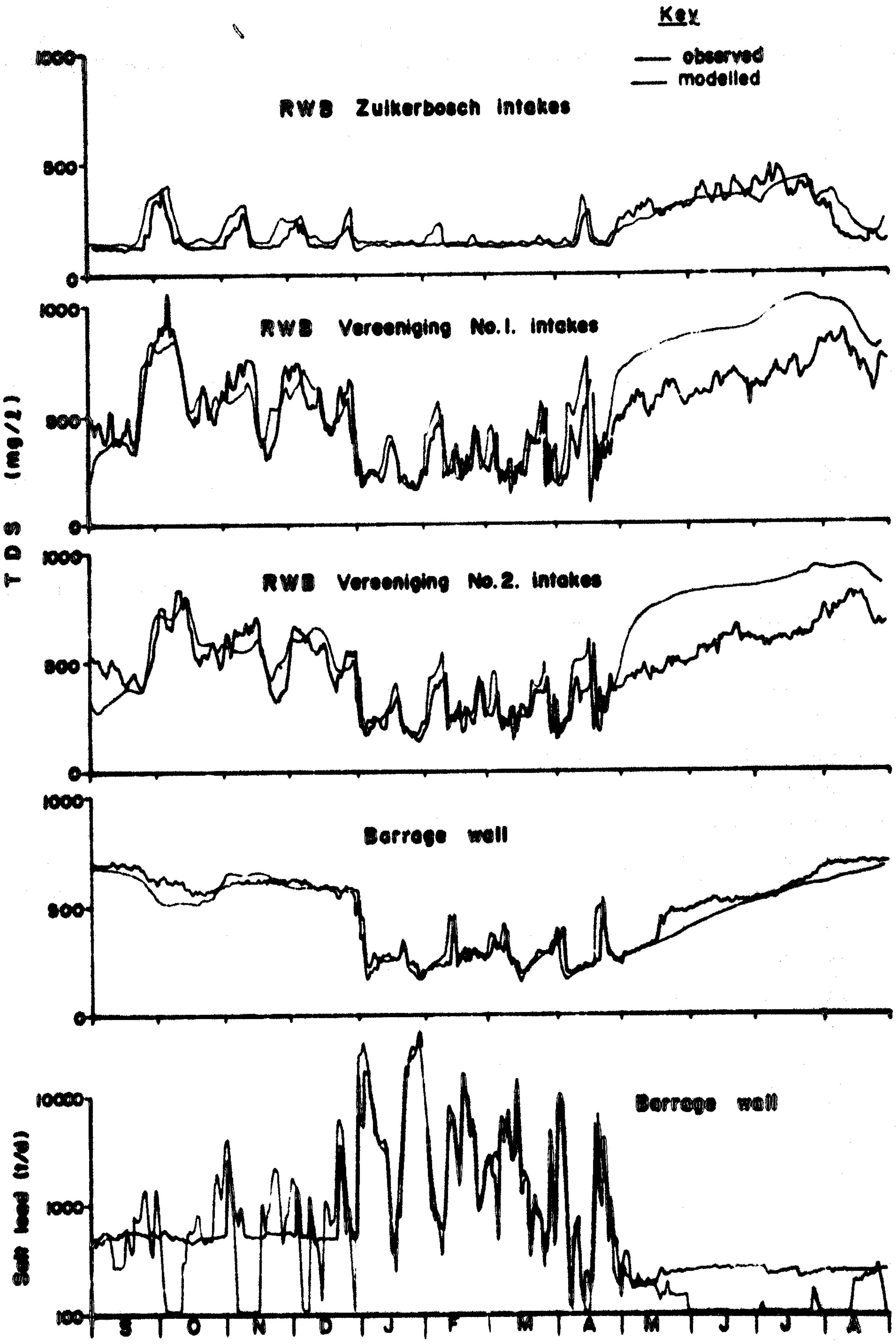

Fig. 3.38: Modelled and observed daily salinities at monitoring points in the Vaal Barrage for the period 1977-09 - 1978-09

Vereeniging intakes will be too high.

The high modelled Klip river base flow salinities (Fig. 3.31) will also result in modelled salinities at the Vereeniging intakes being too high. What is not clear, however, is the contradiction between the salinities at the Vereeniging intakes and those at the Barrage wall during the dry season where the modelled salt concentrations for the former are too high and those of the latter slightly too low. It is possible that the error in the modelled Klip river base flow salinities (which are too high) are compensated for by a similar underestimation of the base flow salt loads entering from the Rietspruit, Taaibosspruit and catchment number 11 (all of these inputs enter the Vaal Barrage downstream of the Vereeniging intakes).

Apart from the winter season, the fit between modelled and observed salinities is highly satisfactory. The two major tributaries of the Vaal Barrage, the Klip and Suikerbosrand, have their confluence between the Rand Water Board Zuikerbosch and Vereeniging No. 1 intakes. The salinities occurring at these two points are therefore indicative of the accuracy with which the two tributaries have been modelled. The good agreement between modelled and observed salt concentrations in the wet season, during which the greater part of the salt load enters the Barrage, therefore serves as a confirmation of the adequacy with which the model parameters have been evaluated.

Fig. 3.39 is a duration curve of modelled and observed daily salt loads released at the Barrage wall during the year 1977/78. It should be noted that 40 percent of the water and 72 percent of the salt load entering the Barrage during this period was derived from the modelled catchments, the remainder coming from Vaal Dam. Only 44 percent of the salt load derived from the catchments comes from point inputs, the remaining 56 percent being derived from diffuse sources. The diffuse-source contribution of the southern PWV catchment to the total salt load entering the Barrage is therefore 40 percent, nearly all of which is washed off in the wet summer season. The modelled washoff salt loads therefore tend to dominate the peak salt loads of Fig. 3.38 and the left hand side of the

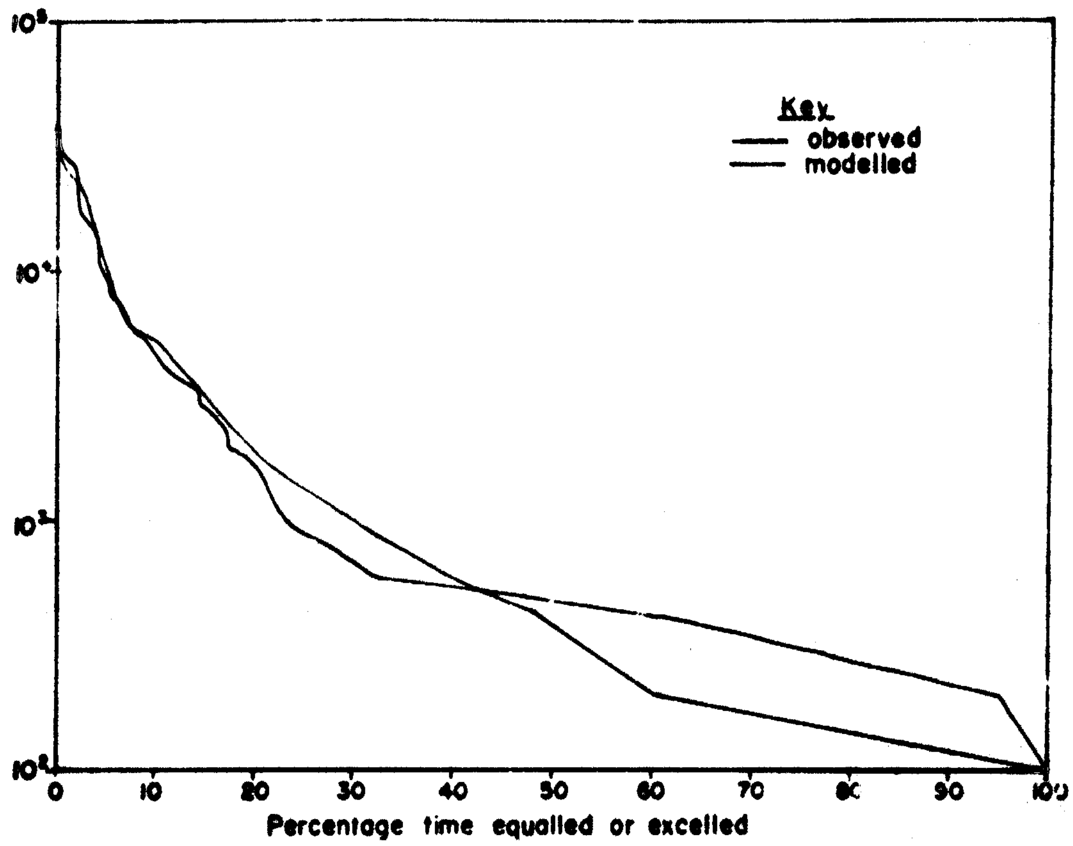

Fig.3.39: Duration curve of modelled and observed daily salt loads at the Barrage wall for period 1977-09 - 1978-08

duration curve given in Fig. 3.39 (where the fit is also best). The duration curve of modelled daily salt loads is too low on the right hand side of Fig. 3.39 due to the fact that during the winter of 1978 the modelled discharges were lower than those observed (see Fig. 3.26. The fit for the previous seven winter seasons is, however, much better). The winter flows are dominated by observed point discharges and releases from Vaal Dam.

It is therefore clear that the washoff of diffuse source salts has been successfully modelled for the southern PWV catchment as a whole, although less favourable results have been achieved for some of the poorly gauged individual subcatchments. The calibration results are considered adequate for the purpose for which the model was developed, viz. to create a planning tool which can be used to compare the merits of various management strategies which have been proposed to improve the mineral quality of water supply to the PWV region.

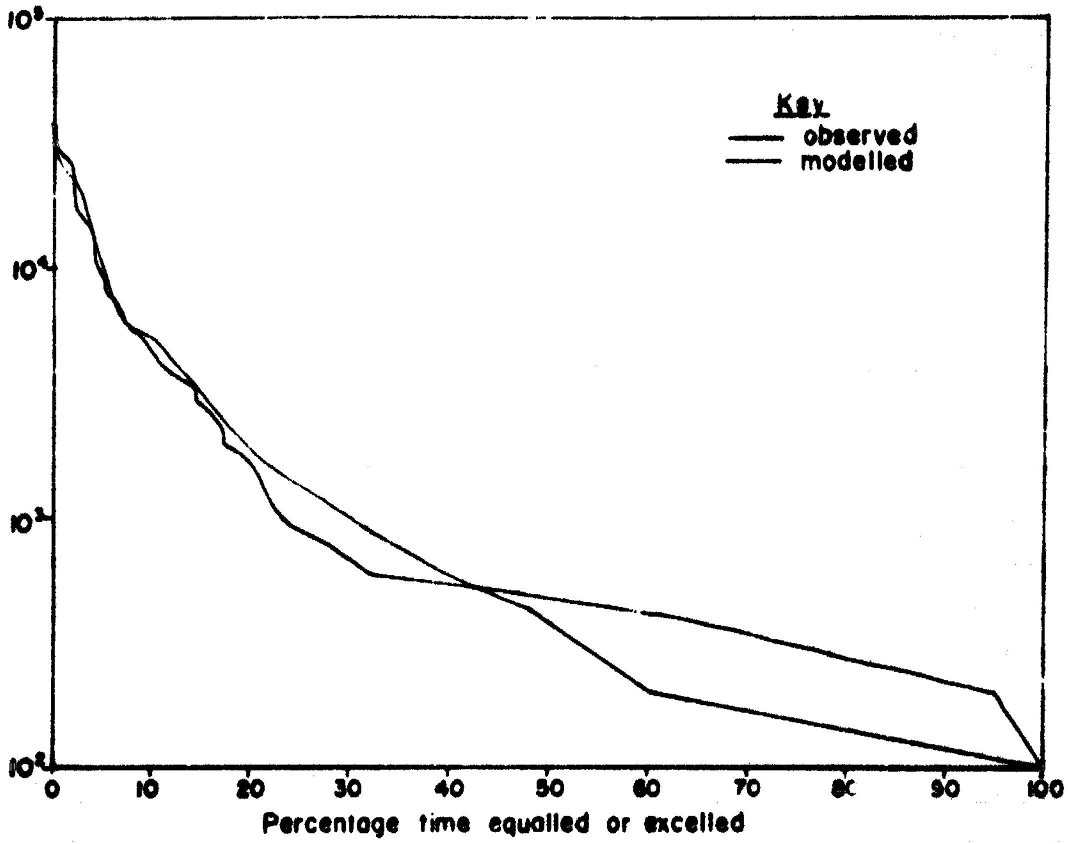

Fig. 3.39: Duration curve of modelled and observed daily salt loads at the Barrage wall for period 1977-09 - 1978-08

duration curve given in Fig. 3.39 (where the fit is also best). The duration curve of modelled daily salt loads is too low on the right hand side of Fig. 3.39 due to the fact that during the winter of 1978 the modelled discharges were lower than those observed (see Fig. 3.26. The fit for the previous seven winter seasons is, however, much better). The winter flows are dominated by observed point discharges and releases from Vaal Dam.

It is therefore clear that the washoff of diffuse source salts has been successfully modelled for the southern PWV catchment as a whole, although less favourable results have been achieved for some of the poorly gauged individual subcatchments. The calibration results are considered adequate for the purpose for which the model was developed, viz. to create a planning tool which can be used to compare the merits of various management strategies which have been proposed to improve the mineral quality of water supply to the PWV region.

3.3 Correlation between salt generation rates and catchment characteristics

In order to make valid comparisons among the effects of different management options on the mineral quality of supply water at various points in a dynamic system such as the PWV complex, it becomes necessary to simulate each option for more than one sequence of hydrology and for more than one demand condition. For example, an option that requires the diversion of saline mine pumpage out of the catchment might prove an attractive solution in the short term for present-day conditions of demand when the effect of mine pumpage on water quality is very pronounced. Ten or twenty years from now, however, at present growth rates, the water demand (and hence the effluent return flows from sewage works) will have doubled or quadrupled while mine pumpage will probably remain constant, or even decrease. Moreover, it is almost certain that the diffuse source salt load generated will also be much greater than at present. The relative effect of saline mine pumpage would therefore be less significant than at present and the option of diverting these discharges might then become less attractive than other options. The same is true of most of the other options.

Planning, by its very nature, is future-orientated and any scheme that is implemented will almost certainly not be called upon to cope with present-day conditions. It would therefore be shortsighted to compare options solely on the basis of present-day conditions.

The Secretary for Water Affairs (1977), Hall (1980) and others have made estimates of the future demand conditions likely to arise within the PWV region. Water demands can readily be related to effluent return flows and reasonable assumptions can be made regarding the relationship between salinities of the water supplied and of the effluents returned. More difficult to estimate, however, are the changes that are likely to occur in the rate at which diffuse source salts are generated.

An attempt was therefore made to derive a relationship between the salt generation rates calibrated in section 3.2.2 and the physical characteristics of the twelve subcatchments, in order to establish a basis for making reasonable estimates of future salt generation rates. It must be stated at the outset that there is a wide margin of error in the salt recharge rates calibrated for many of the subcatchments due to the shortness of the period during which concurrent streamflow and water quality data are available and to defects in the records at some of the monitoring points. The split between salts derived from catchments 10 and 11, for example, is rather arbitrary because of the all but useless record at station C2M14. The good results obtained for the catchment as a whole in section 3.2, however, are encouraging. The good fit between modelled and observed salinities in the Barrage serves as an indirect confirmation of the parameter values adopted for the individual catchments, although of course there may be compensating errors. The large difference between the salt generation rate for the undeveloped catchments (numbers 6,7 and 8) and that for say subcatchment 2 cannot be disputed. There are no natural geological features that could account for the vast differences in the salt loads generated in these catchments and it is therefore reasonable to assume that the difference is due to human activities. Indeed, at the time when the Witwatersrand ("white waters ridge") was so named the region was renowned for its clear waters.

Catchment characteristics related to human developments that might conceivably influence the generation of diffuse source salts were therefore identified and quantified for each subcatchment. These, along with salt generation rates as calibrated in section 3.2.2, are summarised in Table 3.7 and linear cross-correlations among the variables are shown in Table 3.8.

From Table 3.8 it is clear that there is good cross-correlation among many of the X-variables. Furthermore it may be seen that X10, supply of industrial water, is strongly correlated with salt generation rate. All other X-variables that correlate well with the salt generation rate also correlate strongly with X10. Subsequent multiple linear correlation analysis showed that a simple linear regression between X10 and Y produces the most reliable fit. Inclusion of other parameters either leads to spurious correlations (due to the strong cross-correlations among the X-variables) or else produces illogical results (such as regression coefficients which suggest that salt generation rates decrease with increasing industrialised area). The best-fit linear regression equation was found to be:

$$Y = 2{,}5788\ (X10) + 24{,}112 \qquad (3.4)$$

Table 3.7 : Catchment characteristics and salt generation rates

Parameter code	Catchment characteristic	Units	Subcatchment number											
			1	2	3	4a	4b	5	6	7	8	9	10	11
X1	Impervious area	$km^2 x10^{-3}/km^2$	37	89	20	59	14	7	0	0	3	6	0	29
X2	Residential area	"	159	373	48	291	58	34	0	1	17	25	0	75
X3	Industrial area	"	14	96	8	26	6	3	0	0	0	6	0	44
X4	CBD area	"	11	7	0	13	1	0	0	0	0	0	0	0
X5	Mine dump area	"	16	35	7	64	16	0	0	0	0	4	0	0
X6	Irrigated area	"	27	8	45	1	6	24	19	6	0	4	0	0
X7	Vlei area	"	15	20	0	0	40	0	0	0	39	0	15	0
X8	Manufacturing industry working population	$head/km^2$	222	359	26	98	35	10	0	0	0	17	1	55
X9	Residential population	"	1403	1218	232	564	245	84	0	21	9	118	10	287
X10	Industrial water supply	$Ml/year/km^2$	20	70	32	81	10	18	0	0	0	28	0	71
X11	Other water supply	"	169	144	5	83	8	2	0	0	0	8	0	15
Y	Salt generation rate	$kg/km^2/d$	100	198	164	119	46	68	19	19	20	47	35	228

Table 3.8 : Cross correlations among catchment variables

Variable	X1	X2	X3	X4	X5	X6	X7	X8	X9	X10	X11	Y
X1 Impervious area	1,000	0,984	0,895	0,753	0,793	-0,031	0,037	0,899	0,812	0,807	0,787	0,726
X2 Residential area		1,000	0,832	0,820	0,864	-0,084	0,058	0,877	0,800	0,727	0,790	0,607
X3 Industrial area			1,000	0,422	0,498	-0,160	0,040	0,844	0,630	0,844	0,627	0,774
X4 CBD area				1,000	0,859	-0,002	0,001	0,690	0,808	0,417	0,818	0,320
X5 Mine dump area					1,000	-0,149	0,016	0,561	0,560	0,524	0,549	0,356
X6 Irrigated area						1,000	-0,293	0,060	0,188	-0,074	0,139	0,170
X7 Vlei area							1,000	0,184	0,134	-0,283	0,127	-0,228
X8 Manufacturing pop								1,000	0,936	0,609	0,932	0,577
X9 Residential pop.									1,000	0,513	0,990	0,520
X10 Ind.water supply										1,000	0,484	0,927
X11 Other water supp											1,000	0,442
Y Salt generation rate												1,000

Fig. 3.40 shows the relationship between salt generation rates and industrial water supply for each catchment.

Obviously it would be a gross oversimplification to assume that equation 3.4 can now be used to predict salt generation rates. A cursory examination of Fig. 3.40 shows that use of equation 3.4 would lead to an error of over 100% in the case of subcatchment 9.

It must be borne in mind that not all industries can be expected to produce the same quantity of pollution per unit of water consumed. The high correlation coefficient (0,927) nevertheless suggests that there is a strong relationship between industrial water supply and salt generation rate. This is not unexpected, as industrial water consumption is a good measure of human pollution-producing activity in the catchment.

Fig. 3.40: Diffuse source salt generation rate plotted against industrial water supply for 8 PWVS catchments.

Although industrial water consumption cannot be used directly to predict salt generation rates, it does provide an indicator of the *growth* of salt generation rates in a catchment (provided that the industries located within the catchment or pollution control measures do not change too radically).

Table 3.9 shows the annual industrial water consumption in each subcatchment from September 1970 to August 1979. Linear and power regressions were then used to smooth the values in Table 3.9. The regression equations used are given in Table 3.10. Smoothed values are given in Table 3.11.

Table 3.9 : Annual industrial water consumption within each subcatchment (Mℓ)

Sub-catchment	Year								
	1970/71	71/72	72/73	73/74	74/75	75/76	76/77	77/78	78/79
1	102008	12813	13524	14302	14410	15458	16590	17713	17644
2	16195	17506	18031	20128	23000	25455	26889	26696	28944
3	3266	3266	2860	3360	4021	3777	3564	13986	24599
4a	8604	8623	9363	9790	10348	10890	11598	11823	12082
4b	9482	9443	9853	10275	10700	11038	10913	10889	10996
5	10290	9973	9422	9164	9337	10123	10303	8640	11307
6	0	0	0	0	0	0	0	0	0
7	0	0	0	0	0	0	0	0	0
8	0	0	0	0	0	0	0	0	0
9	18215	22264	23618	26213	30354	33083	29659	28884	33153
10	0	0	0	0	0	0	0	0	0
11	59311	55880	59486	60022	59477	61820	60761	68103	73503
Total	137371	139768	146159	153254	161647	171644	170277	186734	209228

Table 3.10 : Regression equations used to smooth annual industrial water consumption values

Sub-catchment	Regression equation	R^2	RMS error
1	$S = 11164+538{,}78.(YEAR-1968{,}44)^{1{,}1247}$	0,989	284
2	$S = -3318785+1692{,}67.(YEAR)$	0,967	787
3	$S = -213374+109{,}89.(YEAR)$ 1970< YEAR<1976	0,389	276
	$S = -20771136+10513{,}50.(YEAR)$ 1976<YEAR<1978	0,999	45
4a	$S = 1366+833{,}42.(YEAR-1958{,}31)^{0{,}8430}$	0,981	163
4b	$S = 1868+6354{,}90.(YEAR-1967{,}31)^{0{,}1609}$	0,904	194
5	$S = -79319+45{,}17.(YEAR)$	0,025	735
9	$S = 2704+18320{,}18.(YEAR-1969{,}56)^{0{,}2258}$	0,906	1759
11	$S = 55867+0{,}000010.(YEAR-1958{,}37)^{7{,}1390}$	0,364	1859

Table 3.11 : Smoothed values of annual industrial water consumption - Mℓ

Sub-catchment	Year								
	1970/71	71/72	72/73	73/74	74/75	75/76	76/77	77/78	78/79
1	12054	12717	13413	14134	14876	15635	16408	17194	17991
2	15768	17460	19153	20846	22538	24231	25924	27616	29309
3	3115	3225	3335	3445	3555	3665	3775	14048	24560
4a	8385	8888	9384	9875	10361	10842	11319	11791	12260
4b	9319	9708	10016	10274	10496	10692	10867	11026	11172
5	9659	9704	9750	9795	9840	9885	9930	9975	10021
9	17904	22589	25107	26916	28353	29557	30601	31526	32359
11	56257	56570	57078	57874	59085	60878	63471	67142	72245

Smoothed annual industrial water supply values from Table 3.11 were then divided by the corresponding catchment areas and substituted into equation 3.4 to yield annual growth factors to be associated with the salt generation rate for each subcatchment. The growth factors thus derived are listed in Table 3.12. No details of industrial water supply were available prior to 1970. The values reflected in Table 3.12 before this date are extrapolations.

Table 3.12 : Annual growth factors for diffuse-source salt generation rate

Year	Sub-catchment							
	1	2	3	4a	4b	5	9	11
1964/65	49,4	61,0	38,4	83,2	35,4	68,9	33,2	176,5
1965/66	51,1	72,1	39,1	89,1	37,8	69,1	38,6	176,5
1966/67	52,8	83,3	39,7	94,9	39,9	69,3	44,0	176,5
1967/68	54,6	94,4	40,4	100,7	41,7	69,5	49,4	176,5
1968/69	56,4	105,6	41,0	106,4	43,2	69,7	54,7	176,5
1969/70	58,3	116,7	41,6	112,1	44,5	69,9	60,1	176,6
1970/71	60,2	127,8	42,3	117,7	45,6	70,1	65,5	177,1
1971/72	62,2	139,0	42,9	123,3	46,5	70,4	76,3	178,0
1972/73	64,3	150,1	43,6	128,9	47,2	70,6	82,1	179,4
1973/74	66,4	161,2	44,2	134,3	47,8	70,8	86,3	181,5
1974/75	68,7	172,4	44,8	139,8	48,3	71,0	89,6	184,8
1975/76	70,9	183,5	45,5	145,1	48,7	71,2	92,4	189,7
1976/77	73,2	194,6	46,1	150,5	49,1	71,4	94,8	196,8
1977/78	75,6	205,8	106,1	155,7	49,5	71,6	96,9	206,7
1978/79	78,0	216,9	167,4	161,0	49,8	71,9	98,9	220,6

The values in Table 3.12 now provide the annual growth factors, GROW, in program NACLØ1, the catchment washoff model (see equations 2.28 and 2.33). Estimates of future industrial demands can be used to compute diffuse-source salt generation growth factors which in turn can be used to simulate the washoff from each subcatchment. The following limitations should, however, be borne in mind:

a) Shortcomings in the streamflow and water quality records impose fairly wide margins of error on the salt recharge parameters for some of the individual subcatchments

b) The strong correlation between salt recharge rates and industrial water supply may be merely coincidental

c) Changes within the catchments, such as introduction of new industries and air pollution controls, may radically alter the relationship between diffuse source salt generation rates and industrial water demands.

The relationship established nevertheless serves as the best available basis for estimating future diffuse source salt loads.

3.4 Verification of model parameters

3.4.1 Streamflow modelling

The calibration parameters controlling the synthesisation of daily discharges were verified using recorded discharges for the period 1978.09 to 1979.08. Table 3.13 gives statistical details for each station. The fit obtained for individual subcatchments is [illegible]rally not as good as for the calibration period (compare the r[illegible] Table 3.13 with those of Table 3.3). This could be a co[illegible]e of the exceptionally dry conditions experienced in the 1[illegible] season. The fit obtained at the Barrage wall is nevertheless still good. Fig. 3.41 is a plot of modelled and observed daily discharges at the Barrage wall while Fig. 3.42 shows the corresponding duration curves (for the sake of brevity, plots at the other stations have been omitted). From Fig. 3.41 it can be seen that the base flows are not well reproduced by the model. Use of the logarithmic scale makes the fit appear poorer than it actually is and furthermore Fig. 2.58 does not reflect the Barrage abstractions, which averaged 16,5 m^3/s during the 1978/79 season. Another detracting factor is that the Barrage model was operated with the assumption that the supply level was constant, whereas in fact significant fluctuations of level do occur. The modelled mean and standard deviation are, however, in good agreement with those observed and the correlation coefficient is high (see Table 3.13). Moreover the long calibration period (eight years) is in itself a partial verification of the calibration parameters.

Table 3.13 : Statistical properties of modelled and observed daily discharges for the period 1978.09 - 1979.08

Tributary	Station number	Sample size	Observed (m^3/s)		Modelled (m^3/s)		Linear correlation coefficient	SF
			$\bar{x}$	s	$\bar{x}$	s		
Klip river	K10	289	5,235	1,596	3,923	0,640	0,143	0,610
	N8	362	2,000	0,801	2,158	1,102	0,496	0,980
	R6	346	2,148	0,519	2,318	1,291	0,392	0,922
	C2M21	341	6,633	1,968	6,398	2,499	0,563	0,922
	C2M15	121	5,532	0,654	5,763	1,458	0,106	0,604
Suikerbosrand	B9	365	0,341	0,111	0,381	0,067	0,193	1,000
	B10	310	0,313	0,204	0,642	0,730	0,385	0,897
	C2M70	326	1,495	6,929	1,019	2,307	0,715	0,987
	C2M04	326	1,685	9,733	1,182	2,630	0,808	0,942
Rietspruit	C2M05	365	0,959	2,118	0,595	1,258	0,682	1,000
Taaibosspruit	C2M14	357	0,192	0,524	0,523	2,707	0,748	0,697
Vaal river	Barrage	364	5,496	14,744	5,593	15,707	0,827	0,998

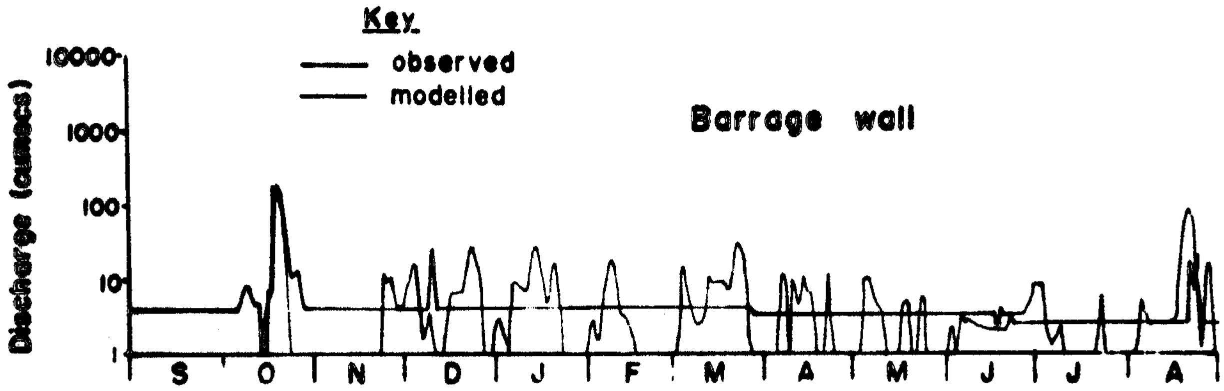

Fig. 3.41: Modelled and observed daily discharges at Barrage wall for period 1978·09 - 1979·08

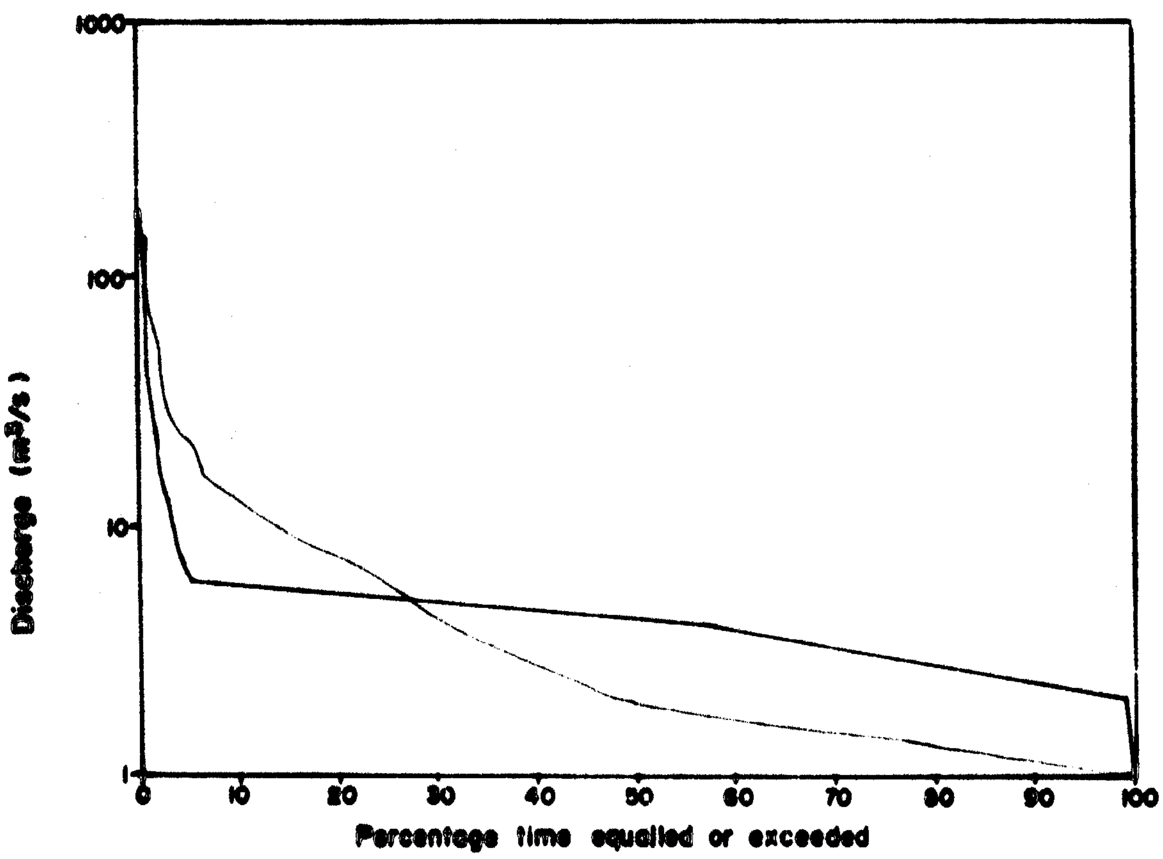

Fig. 3.42: Duration curve of modelled and observed discharges at Barrage wall for period 1978·09 - 1979·08

3.4.2 Water quality modelling

Using the growth factors given in Table 3.12 it was possible to verify the calibrated water quality parameters for two periods, viz. 1978.09 - 1979.08 and 1973.09 - 1977.08. Because of the paucity of water quality data at other points in the system for the latter period, however, modelled and observed salinities could be compared only at the monitoring stations in the Vaal Barrage.

Verification proceeded as follows:
Using the specified dynamic growth factors the water quality parameters were first re-calibrated for each subcatchment in Table 3.12. (There was no need to re-calibrate the remaining undeveloped subcatchments; these were assumed to be stationary). Changes were made only to parameters SALTR, BPARR, SALTU, BPARU and CONCS and these were adjusted so as to yield modelled salt loads at each station similar to those modelled in section 3.2 for the period 1977.09 to 1978.08. The new parameter values thus obtained are given in Table 3.14. These parameter values are applicable to the year 1965, the starting date of the simulation. For each subsequent year the values of BPARR and BPARRU are adjusted according to the growth factors (see equations 2.28 and 2.33).

Table 3.14 : Calibrated starting values (1965) of water quality parameters for dynamic conditions

Subcatchment	Parameter				
	SALTR	BPARR	SALTU	BPARU	CONCS
1	46,0	0,0605	92,0	0,5227	272
2	48,8	0,0621	55,0	0,2964	295
3	82,0	0,1540	76,0	0,4343	412
4a	46,0	0,0580	94,0	0,5344	400
4b	26,0	0,0312	87,0	0,5721	290
5	55,0	0,0624	213,0	1,1550	528
9	10,0	0,0287	68,0	0,4111	295
11	137,0	0,1530	193,0	1,0800	548

The newly calibrated dynamic parameters were then used to simulate catchment washoffs for the two verification periods. Output from the washoff model was fed into the Barrage model so that modelled and observed daily salinities at the Barrage monitoring points could be compared. Results for the two verification periods are discussed below:

a) <u>1978.09-1979.08</u>: The statistical properties of modelled and observed daily salt concentrations at all monitoring points for the period 1978.09 to 1979.08 are given in Table 3.15 while those for daily salt loads are given in Table 3.16. Fig. 3.43 shows plots of modelled and observed daily salt concentrations at the four Barrage water quality monitoring stations, as also the daily salt loads leaving the Barrage wall. Fig. 3.44 shows the duration curves of modelled and observed daily salt loads passing the Barrage wall for the same period. Comparison of Tables 3.15 and 3.16 with Tables 3.5 and 3.6 reveals that the fit for the period 1978.09 - 1979.08 is not as good as that obtained for the calibration period. The fit is, however, acceptable at the key Rand Water Board abstraction points. Of particular interest during the 1978/79 season is the frequent occurrence of reverse flow conditions upstream of the infalls of the Klip and the Suikerbosrand, resulting in high salinities at the Rand Water Board Zuikerbosch intakes. This was the consequence of the DWA's deliberate policy of reducing releases from Vaal Dam. The ability of the model to duplicate the exceptionally high TDS peak occurring under these conditions at the end of August 1979 is most encouraging. The modelled flood of October 1978, however, failed to dilute the Barrage water sufficiently at the Vereeniging intakes and as a result the salt stored in the Barrage was not flushed out to the required extent. The fit between modelled and observed daily salt loads leaving the Barrage is good in the region of the higher peaks, but poor for the smaller events. This latter effect is attributable to the factors discussed in section 3.4.1; the result was a poor fit at the lower discharges. The modelled and observed mean and standard deviation for daily salt loads leaving the Barrage are, however, close (see Table 3.16).

Table 3.15 : Statistical properties of modelled and observed daily TDS for the period 1978.09 - 1979.08

Tributary	Station number	Sample size	Observed (mg/ℓ)		Modelled (mg/ℓ)		Linear correlation coefficient	SF
			$\bar{x}$	s	$\bar{x}$	s		
Klip river	K10	338	545,7	55,6	658,2	111,2	0,474	0,998
	N8	361	1220,8	140,7	1303,6	109,7	0,228	0,997
	R6	324	1507,4	237,3	1395,9	167,5	0,341	0,998
	C2M15	365	879,3	113,1	931,4	111,0	0,476	1,000
Suikerbosrand	B9	51	1568,7	94,4	1379,1	89,5	0,616	0,998
	B10	359	1322,1	575,8	995,7	179,6	0,525	0,992
	S1	365	156,0	9,8	142,3	13,3	0,156	1,000
	C2M04	340	760,8	464,0	643,2	218,5	0,604	0,986
Rietspruit	C2M05	364	1100,7	204,0	1143,5	208,9	0,606	0,999
Taaibosspruit	C2M14	47	901,2	268,1	429,6	110,7	0,505	0,980
Vaal river	ZB	365	223,3	81,4	230,5	84,8	0,828	1,000
	V1	350	617,9	123,0	660,7	123,8	0,767	0,988
	V2	347	600,4	105,2	634,7	103,5	0,779	0,995
	Barrage	363	595,9	109,4	643,6	53,7	0,872	0,989

Table 3.16 : Statistical properties of modelled and observed daily salt loads for the period 1978.09 - 1979.08

Tributary	Station number	Sample size	Observed t/d		Modelled t/d		Linear correlation coefficient	SF
			$\bar{x}$	s	$\bar{x}$	s		
Klip river	K10	263	249,6	93,0	223,7	51,6	0,366	0,708
	N8	358	208,3	79,9	240,3	113,0	0,498	0,968
	R6	305	281,4	76,6	282,7	142,4	0,277	0,938
	C2M15	121	404,4	82,6	439,1	119,1	-0,052	0,611
Suikerbosrand	B9	51	46,6	15,6	45,0	6,1	0,267	0,996
	B10	308	38,3	27,0	57,6	58,6	0,288	0,889
	C2M04	303	58,2	207,2	52,3	72,2	0,701	0,944
Rietspruit	C2M05	364	76,2	73,0	45,7	53,8	0,713	0,999
Taaibosspruit	C2M14	66	6,5	13,5	6,8	25,4	0,463	0,121
Vaal river	Barrage	362	299,8	969,0	315,3	935,9	0,813	0,999

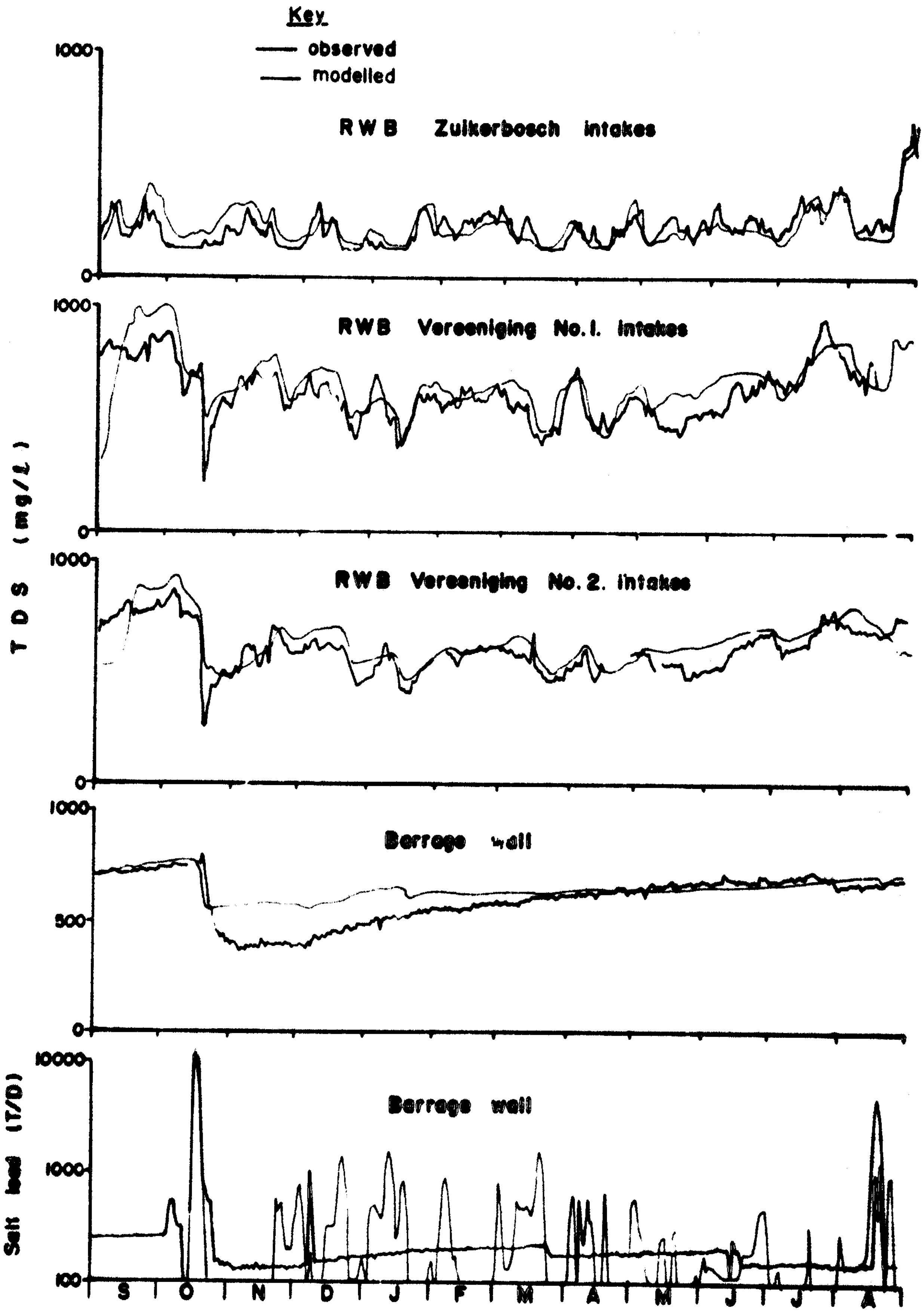

Fig 3.43: Modelled and observed daily salinities at monitoring points in the Vaal Barrage for period 1978-09 – 1979-08

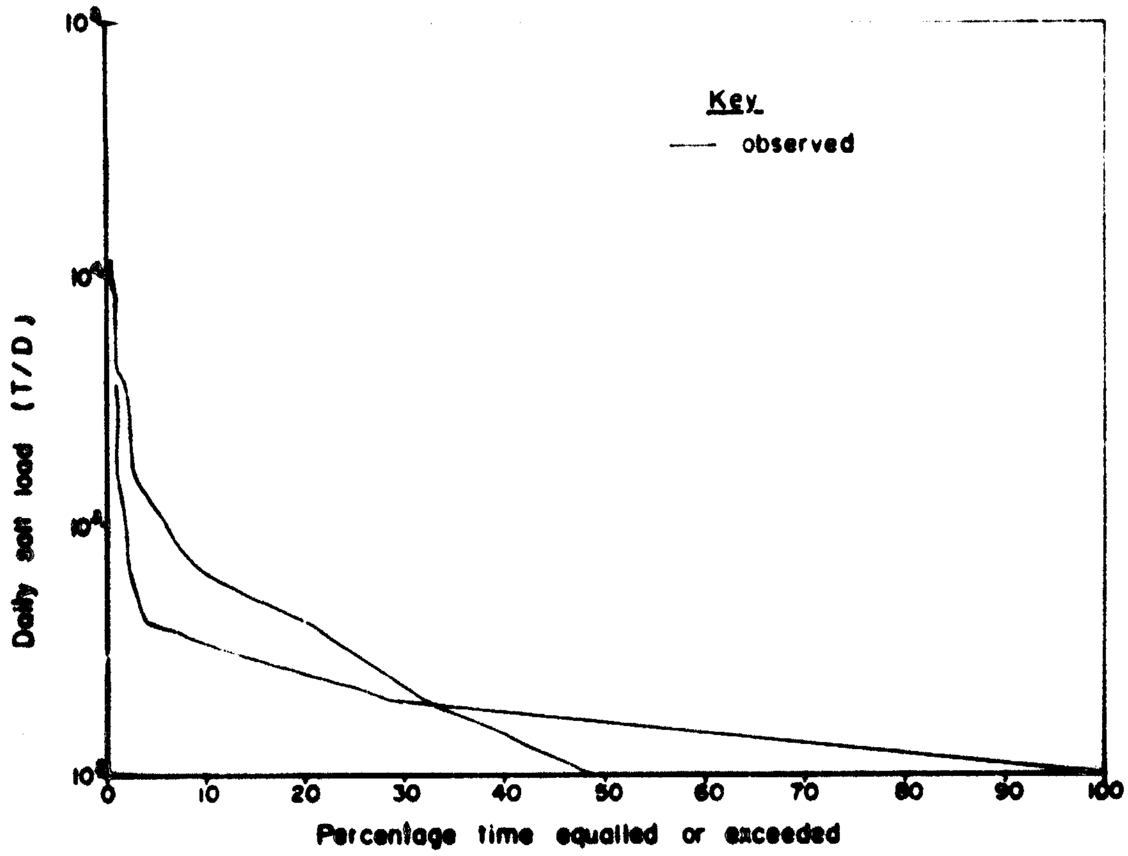

Fig.3.44: Duration curve of modelled and observed daily salt loads at Barrage wall for period 1978-09 - 1979-08.

b) 1973.09-1977.08: Tables 3.17 and 3.18 give statistical properties of modelled and observed daily salt concentrations and salt loads for monitoring points in the Vaal barrage. Figs. 3.45 to 3.48 show modelled and observed daily salt concentrations at the four Barrage monitoring points.

Table 3.17 : Statistical properties of modelled and observed daily TDS in the Vaal Barrage for the period 1973.09 - 1977.08

Station	Sample size	Observed (mg/ℓ)		Modelled (mg/ℓ)		Linear correlation coefficient	SF
		$\bar{x}$	S	$\bar{x}$	S		
ZB	1249	137,4	43,3	157,7	46,0	0,604	0,978
V1	1447	366,4	156,9	429,2	196,7	0,808	0,998
V2	1423	347,2	155,4	405,3	190,0	0,831	0,982
Barrage	1461	350,9	151,0	392,2	179,4	0,929	1,000

Table 3.18 : Statistical properties of modelled and observed daily salt loads leaving Vaal Barrage for the period 1973.09 - 1977.08

Station	Sample size	Observed (t/d)		Modelled (t/d)		Linear correlation coefficient	SF
		$\bar{x}$	S	$\bar{x}$	S		
Barrage	1461	2110,3	5279,6	1948,1	4201,0	0,954	1,000

Fig. 3.49 shows daily salt loads leaving the Barrage while Fig. 3.50 gives the corresponding duration curves. From Table 3.17 and Fig. 3.45 it can be seen that the fit between modelled and observed daily salt concentrations at the Zuikerbosch intakes is not as good

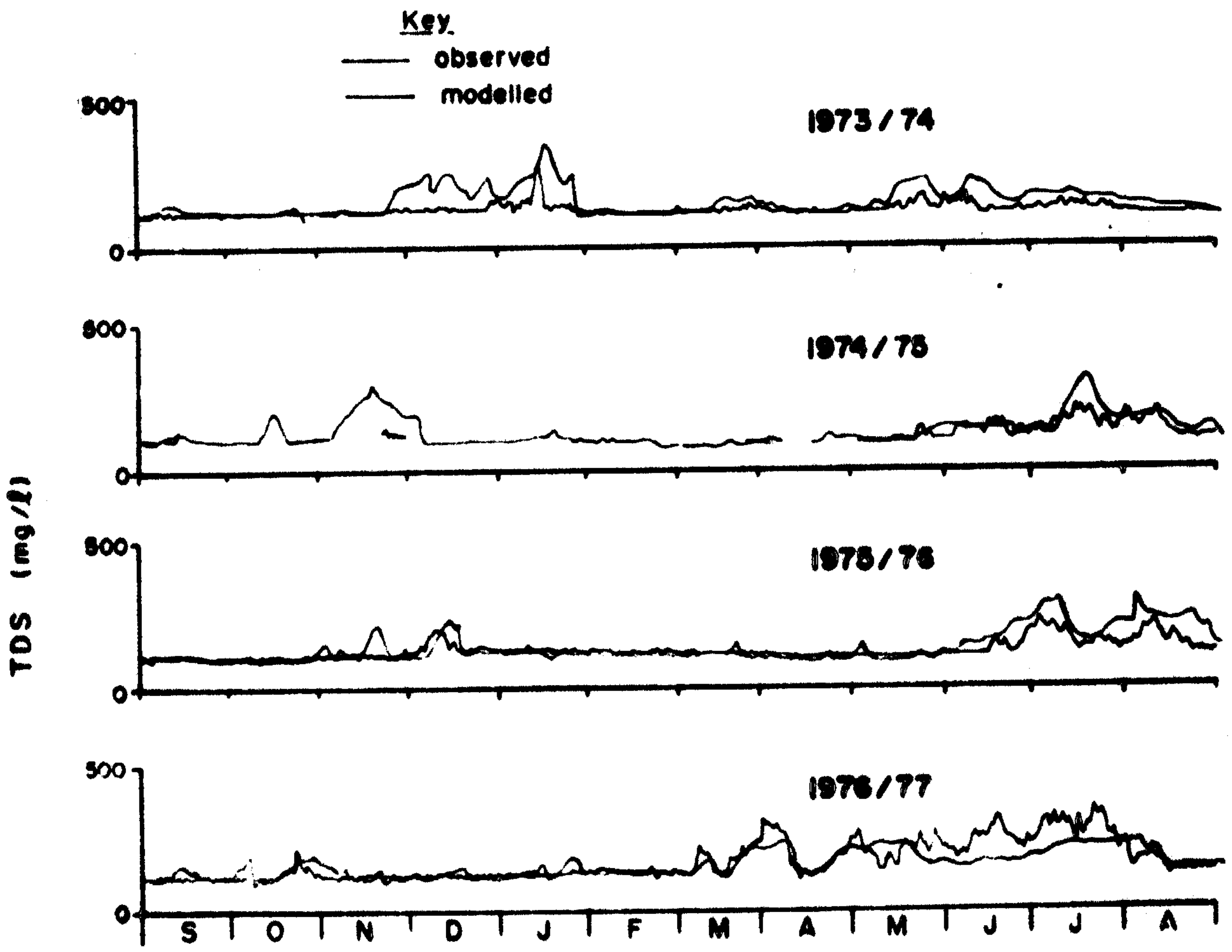

Fig.3.45: Modelled and observed daily TDS at RWB Zuikerbosch intakes for period 1973-09 - 1977-08

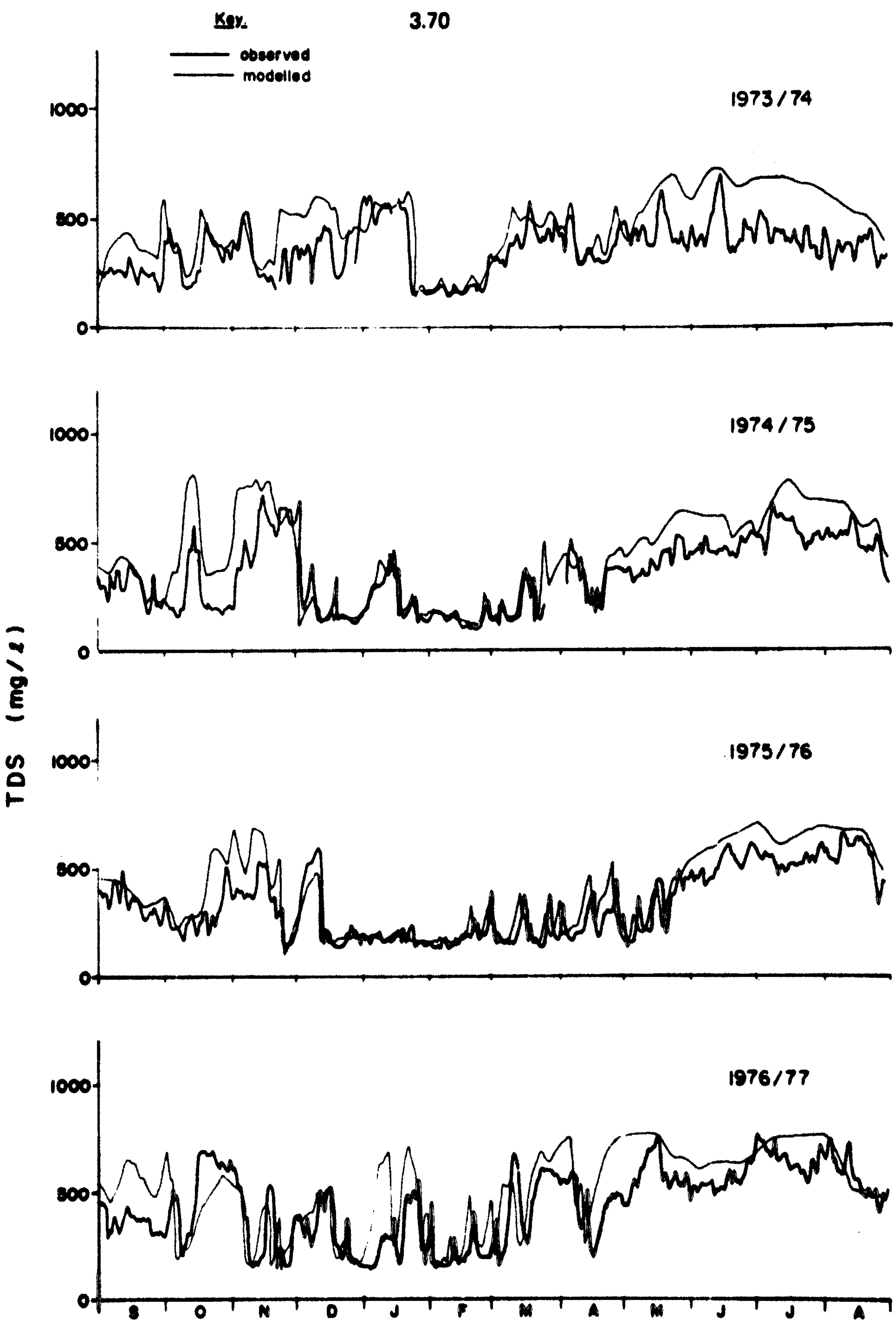

Fig. 3.46 : Modelled and observed daily TDS at RWB Vereeniging No. 1 intakes for period 1973-09 - 1977-08

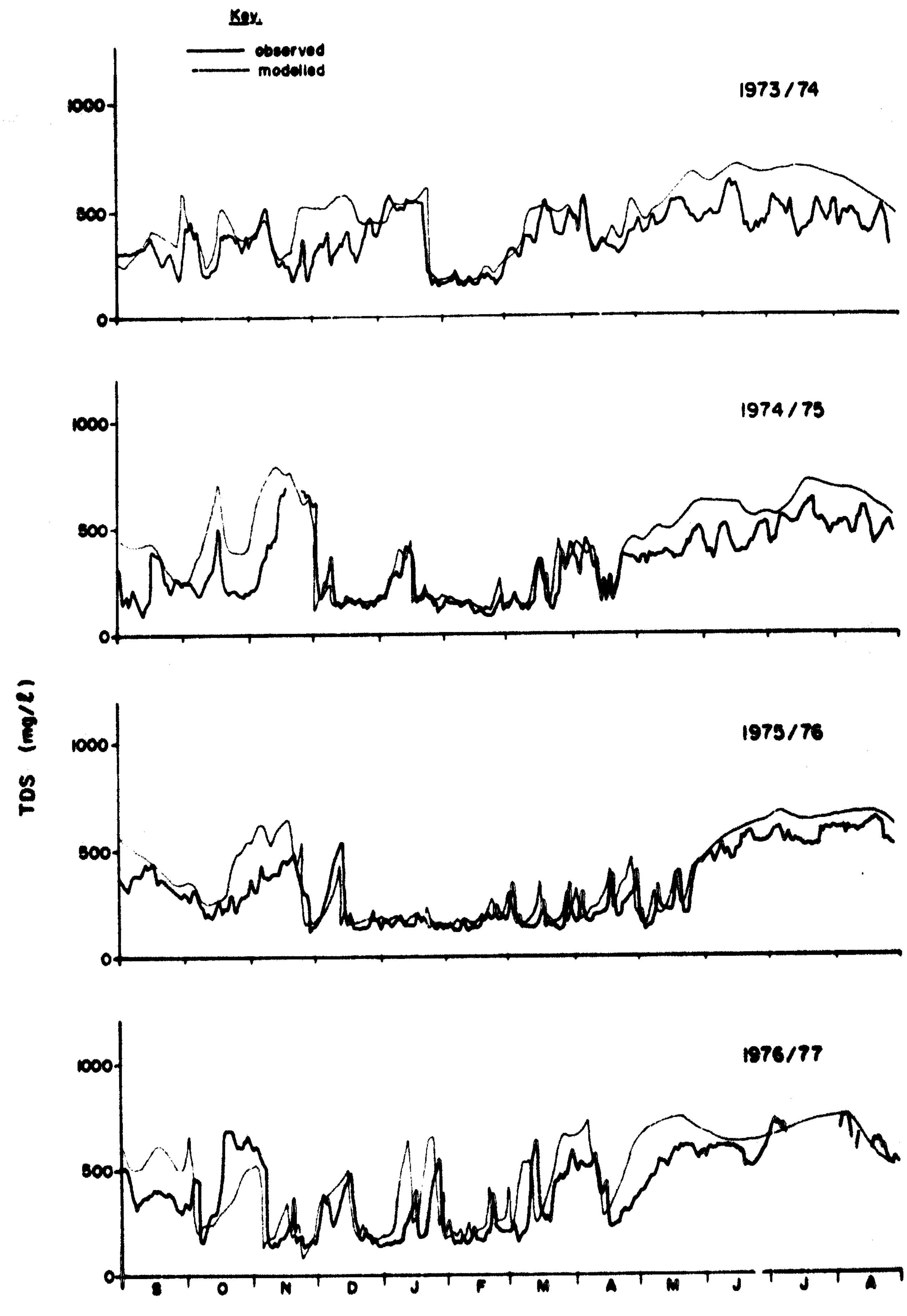

Fig. 3.47 : Modelled and observed daily TDS at RWB Vereeniging No. 2 intakes for the period 1973-09 -- 1977-08

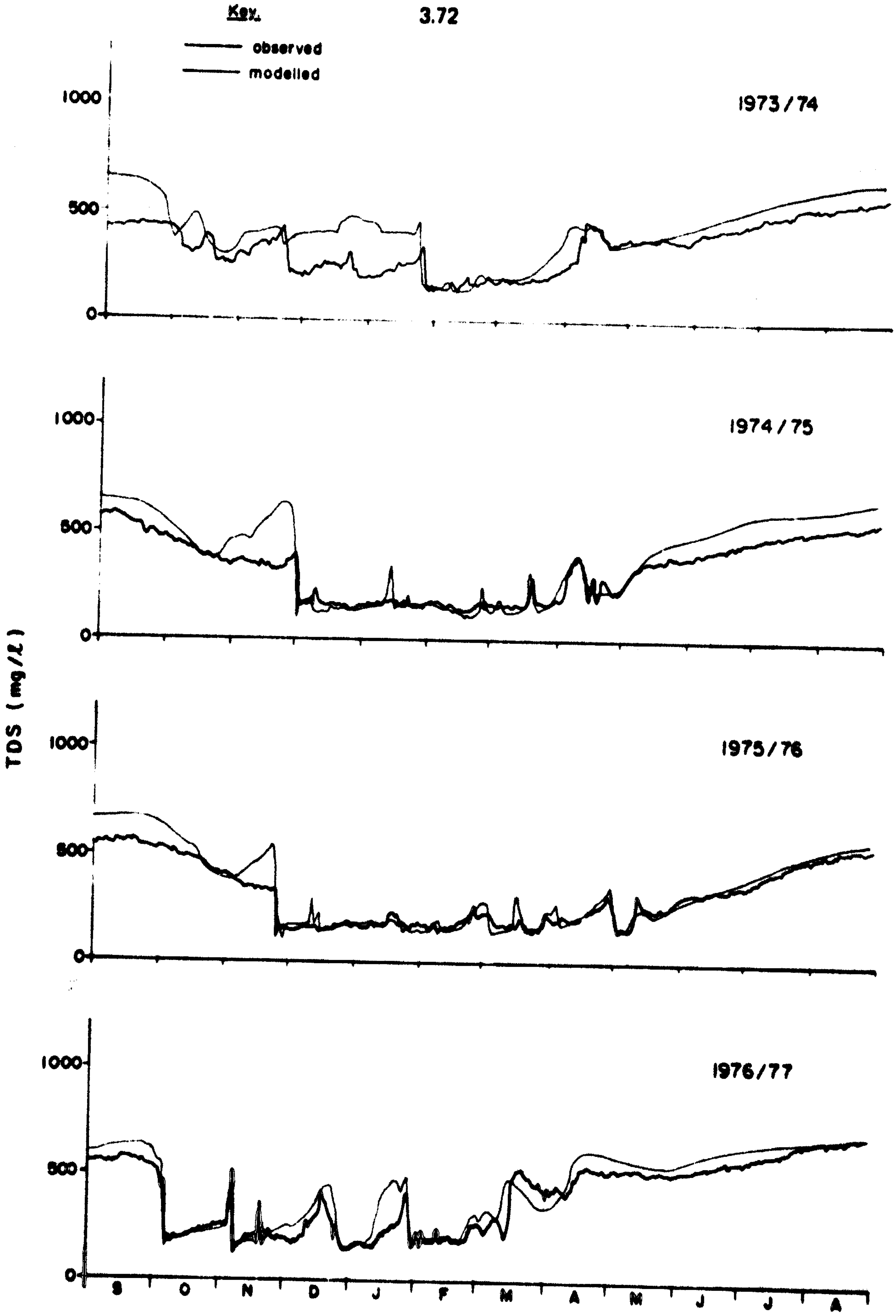

Fig. 3.48 : Modelled and observed daily TDS at Barrage wall for the period 1973-09 — 1977-08

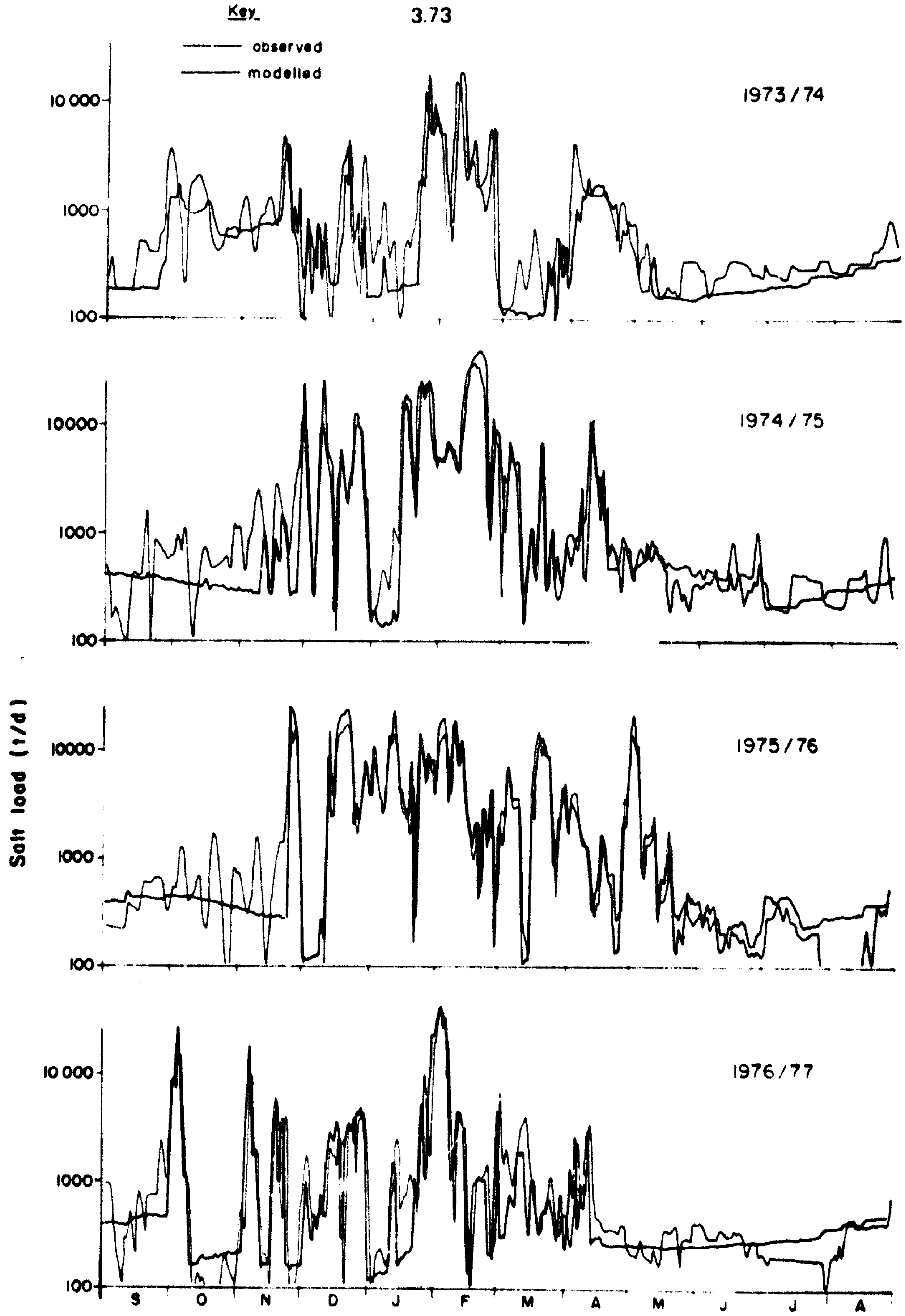

Fig 3.49 : Modelled and observed daily salt loads at Barrage wall for the period 1973-09 — 1977-08

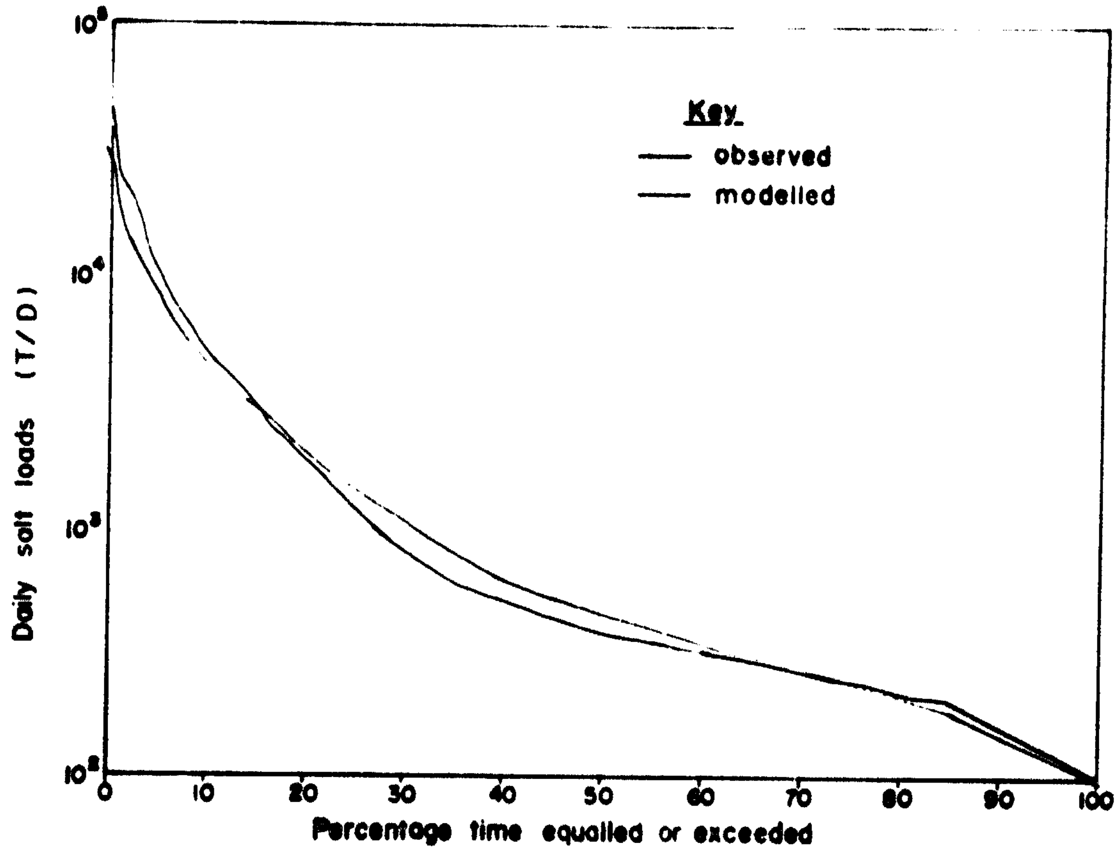

Fig. 3.50: Duration curve of modelled and observed daily salt loads leaving Barrage for period 1973-09 - 1977-08.

as was obtained for the calibration year. The poor fit, particularly in the earlier years, is most likely attributable to poor point flow data. Data pertaining to mine pumpage are especially scarce. Estimates of quantities of shaft water discharged to stream for most of the mines of the southern PWV catchment were based on values provided by Clausen (1976). His estimates, however, are based largely upon records of electrical power consumed by the pumps and therefore do not differentiate between water discharged as effluent and that used consumptively (such as slurry pumped to slimes dams). It was possible to make a direct comparison between Clausen's figures and those obtained from two of the gold mines (Durban Deep and Grootvlei Proprietary, situated in subcatchments 1 and 4b respectively). Estimates from the two sources are given in Table 3.19.

<u>Table 3.19 : Estimates of annual volumes of mine shaft water pumped to stream</u> (Mℓ)

Mine	Year	Source of estimate		Percentage difference
		Clausen	Mines	
Durban Deep	1973	2690	1153	133
	1974	2650	1352	96
	1976	6923	5255	32
Grootvlei Prop.	1975	5821	4460	31
	1976	6611	5129	29

In 1973 there were eight gold mines still operative. This number had diminished to six by the end of 1976. All mine pumpage values used as input to the model prior to 1977, other than those given in Table 3.19, were based on Clausen's figures. (Since 1977 monthly effluent data have been submitted to the Water Research Commission by the mines still in production). It is clear from Table 3.19, therefore, that the margin of error associated with the mine pumpage values is wide. This is particularly serious in view of the high salt concentrations involved. (Salt concentrations in excess of 10 000 mg/ℓ have been recorded). Water quality data prior to 1977 are also not available for the mines, but Clausen (1977) maintains that the salt concentrations of the shaft water have been declining. Salinities of shaft water in these earlier years are also less predictable because the salt concentrations vary according to the level from which the water is pumped, and previous history of water levels in the workings (when the water level is reduced, for example, iron pyrites is oxidised and if the water level subsequently rises sulphates are leached out). Estimates of salt loads pumped from mine workings before 1977 are therefore highly inaccurate.

From Table 3.17 and Figs. 3.45 to 3.48 it can be seen that the modelled salt concentrations tend to be higher than those observed, especially during the drier months. Modelled salt loads, however, tend to be lower than those observed. This is probably due to the fact that for this period the modelled discharges are lower than those observed (see Table 3.20). As a consequence the total modelled salt load must also be lower and the salt concentrations should be higher. As can be seen from Table 3.18 and Figs. 3.49 and 3.50 the fit between modelled and observed daily salt loads passing through the Barrage sluices is good.

Table 3.20 gives modelled and observed annual runoffs and salt loads derived from the southern PWV catchment, together with weighted average salt concentrations for each year simulated. Weighted growth factors for the entire catchment are also included in Table 3.20. Values contained in Table 3.20 are plotted in Fig. 3.51.

Table 3.2 : Modelled and observed annual catchment runoffs, salt loads and weighted salt concentrations

Year	Catchment runoff ($m^3 x 10^6$)		Salt load ($t x 10^3$)		Salt concentration (mg/ℓ)		Growth factor
	Observed	Modelled	Observed	Modelled	Observed	Modelled	
1973/74	520	549	274	318	526	579	99,6
1974/75	1739	1192	671	532	386	447	101,9
1975/76	1440	951	595	472	413	497	104,8
1976/77	895	693	444	413	497	595	108,3
1977/78	1236	1308	643	654	520	500	115,8
1978/79	322	325	249	254	774	781	124,7

Fig. 3.51 demonstrates the profound effect that the hydrology has upon the quantity of salt washed off in any given year. During the period 1974.09 to 1977.08 the observed annual runoffs are greater than those modelled, and as a result the modelled salt loads are low. The surfeit of salt stored on the catchment, however, results in modelled average salt concentrations that are too high. During the period 1977.0? to 1979.08, however, the modelled and observed annual runoffs are very close, and as a result the salt loads and concentrations are also in good agreement. From Fig. 3.51 it can be seen that the relationship between the annual salt loads derived from the catchment and the corresponding growth factors for salt

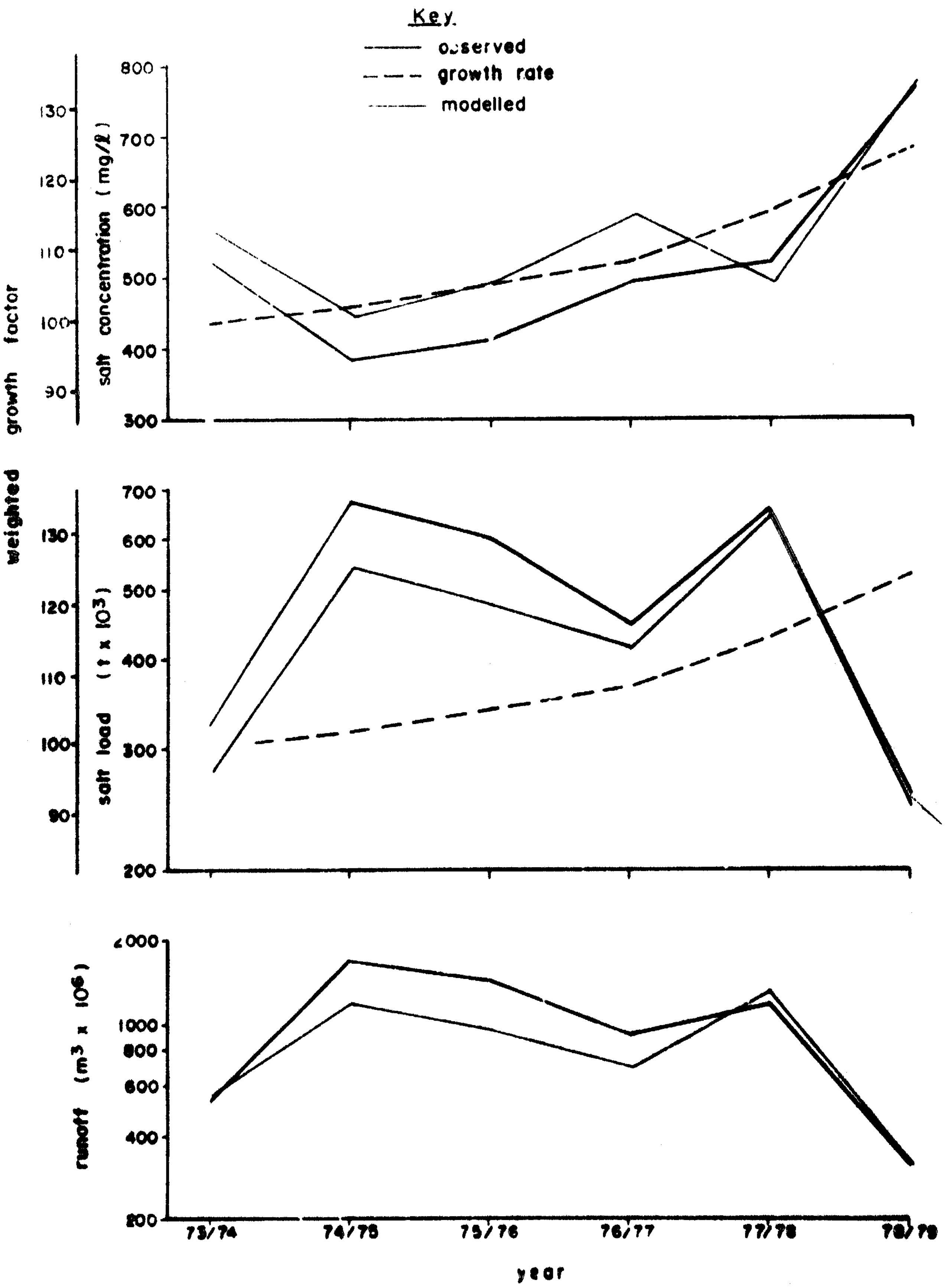

Fig. 3.51: Modelled and observed annual catchment runoffs, salt loads and weighted salt concentrations.

generation rate is completely obscured by variations in the hydrology, although there does seem to be some correlation between the weighted average salt concentrations and the growth factors.

The correlation between salt generation rate and industrial water supply cannot, therefore, be conclusively verified as the simulation period is too short. The good fit between modelled and observed values at the Vaal barrage monitoring points for the 6 years simulated with parameters based on only a one-year calibration period does, however, serve to confirm the adequacy of the model and indirectly gives credibility to the adopted growth factors (if the growth factors had been unreasonable, then the model fit could be expected to be very poor). Definite verification of the growth factors will not be possible until a few more years of data become available. The chosen growth factors are, however, quite plausible and should provide a sound basis for comparing the effects of various management strategies on water qualities within the system under various demand conditions.

CHAPTER 4 : PARAMETER SENSITIVITY

A series of model runs was made to test the sensitivity of the modelled output from programs NACLØ1 and NACLØ2 to changes in calibration model parameters.

The sensitivity of the modelled output from a 600 km² catchment for the period 1977.09 to 1978.08 to changes in each calibration parameter was judged by varying each parameter in turn (while keeping the remaining parameters constant), and noting changes in the modelled means and standard deviations.

Parameter sensitivity analyses for programs NACLØ1 and NACLØ2 are discussed in sections 4.1 and 4.2.

4.1 Program NACLØ1

Average daily rainfall and evaporation data for subcatchment 2 were used as input to the model with a running-in period from 1965.09 to 1977.08. The direct modelled catchment response was used to test the sensitivity of the washoff model to changes in each parameter (i.e. the channel routing model, NACLØ2, was not used).

The sensitivity of the modelled output to changes in the parameters controlling runoff and water quality are described in sections 4.1.1 and 4.1.2.

4.1.1 Runoff parameters

Base line parameter values (about which each in turn was varied) are given in Table 4.1. The model response to changes in each parameter is discussed below.

Table 4.1 : Base line parameter values used in sensitivity analyses of runoff parameters for program NACLØ1

Parameter	Value	Parameter	Value	Parameter	Value
POW	3	AI	0,8	LAG	0
SL	0	ZMINN	0	GL	4
SE	140	ZMAXN	15	QOBS	0,05
ST	400	PI	1,5	DGL	0
FT	0,4	TL	1,5		

a) <u>POW</u> : The response of modelled daily discharges and salt concentrations to changes in POW is shown in Fig. 4.1 while Fig. 4.2 shows the effect on modelled means and standard deviations. This parameter controls the rate at which percolation of soil moisture to the groundwater diminishes as soil moisture storage decreases (see Fig. 2.7 of section 2.2.1). It follows, therefore, that an increase in POW leads to a more rapid reduction of base flow discharges after flood events. From Fig. 4.1 it can be seen that the effect of POW is most pronounced towards the end of the dry season when the soil moisture storage is small. The greater persistence of the base flows for lower values of POW increases the ratio of percolation to evaporative losses from the soil moisture. The increased flushing effect leads to a reduction of salt concentrations during both the dry and the wet seasons. Flood peaks at the onset of the rainy season, however, are little affected by changes in POW because an increase in base flows is accompanied by a decrease in evaporation from the soil moisture and as a result the soil moisture storage at the end of the dry season (which in turn controls infiltration rates) is not greatly altered.

Fig. 4.2 shows that increasing the value of POW leads to a reduction in total discharge (the difference being lost due to increased evaporation from the soil moisture), while the reduction in base flows together with insignificant changes to the flood peaks causes an increase in the standard deviation. Reduced flushing of the soil moisture also leads to increased average salt concentrations. The standard deviation of daily salt concentrations does not rise as rapidly as the mean because the increase in concentrations applies to both base flows and flood peaks (although the latter to a lesser extent).

Changes in POW in the range 3-∞ have little effect upon modelled discharges because they result only in small changes to base flows which are already approaching zero. The influence upon salt concentrations, however, continues to be significant.

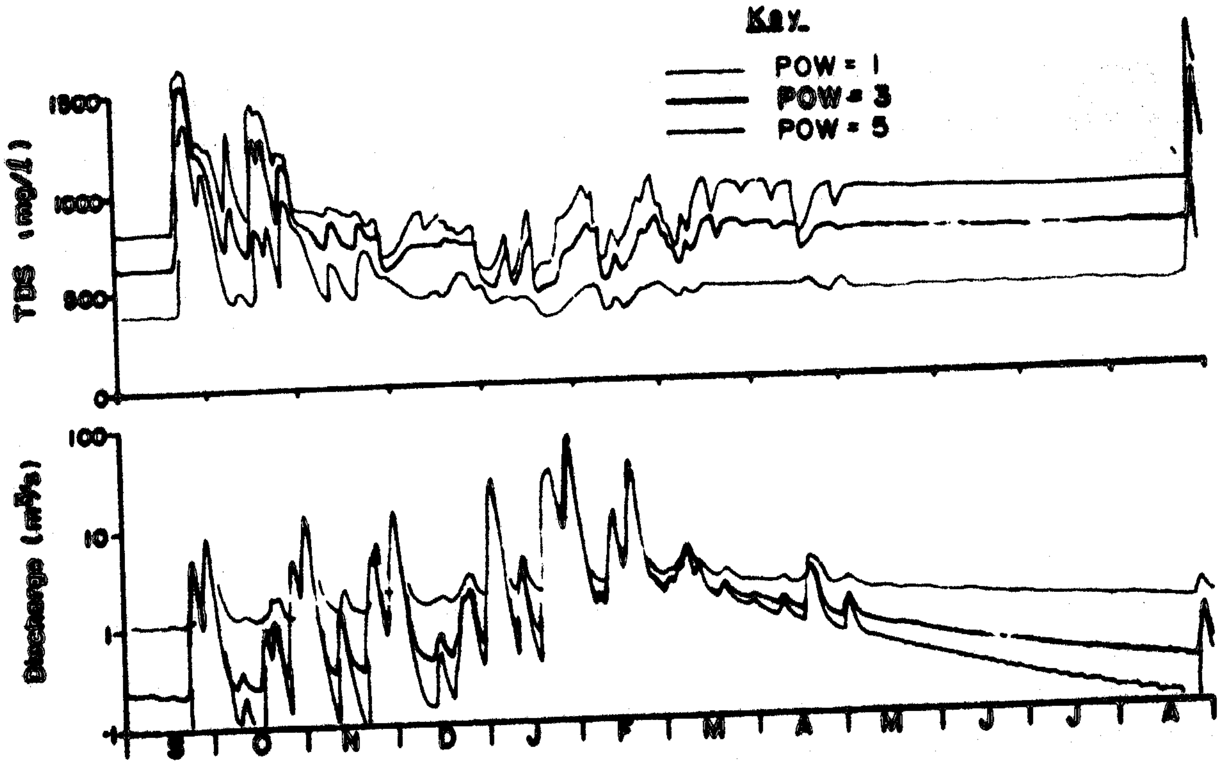

Fig. 4.1: Sensitivity of modelled daily discharges and soil concentrations to changes in POW

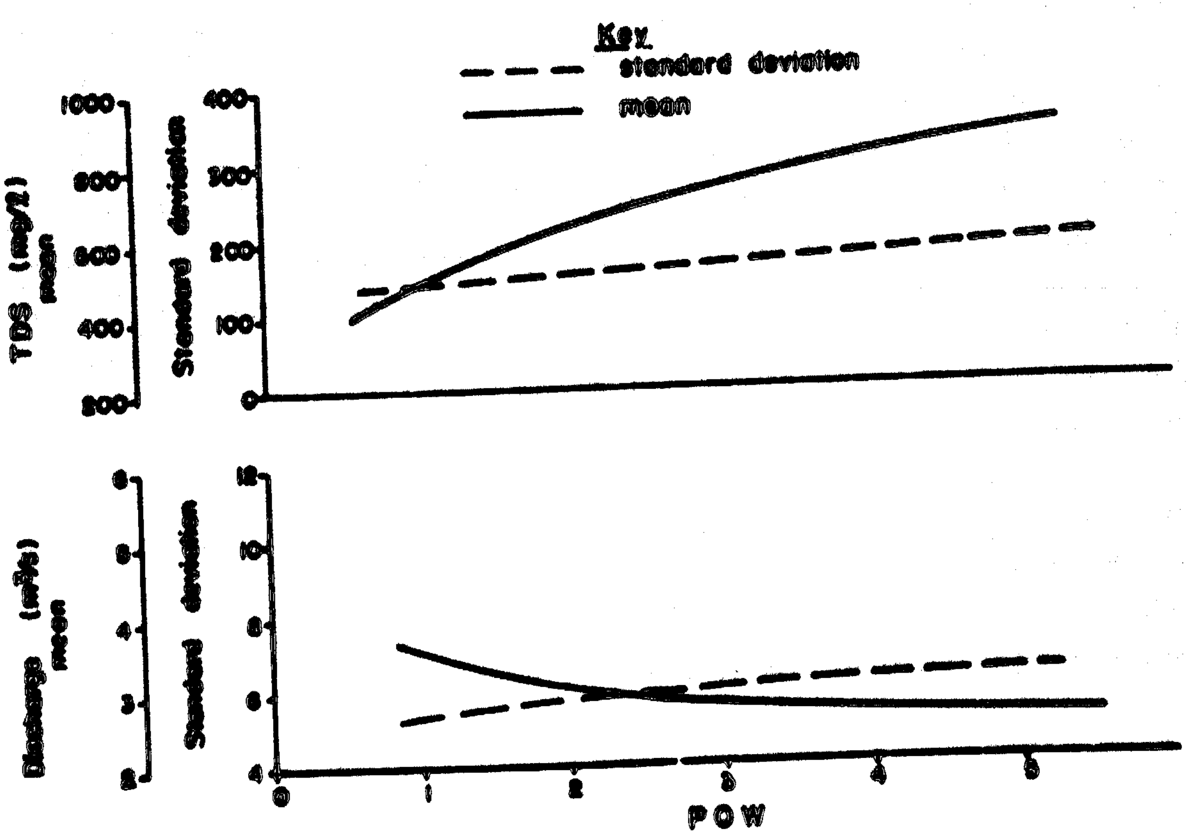

Fig. 4.2: Sensitivity of modelled means and standard deviations to changes in POW

b) <u>SL</u> : A comparison of Figs. 4.3 and 4.4 with Figs. 4.1 and 4.2 reveals that increasing SL has a similar effect on modelled discharges and salinities to that obtained by increasing POW. It is in fact possible, by suitably adjusting POW and FT, to mimic very closely the effect of changing SL.* In view of this apparent redundancy Pitman (1976) advocates setting SL equal to zero in all instances in order to reduce the number of model parameters which need to be calibrated. This approach is perfectly adequate for runoff modelling. In modelling water quality, however, the total soil moisture salt storage is most important as this will control the rate at which soil moisture salinities will change as a result of evaporation, groundwater flow and interflow. Soil moisture salinity changes can therefore be damped out by increasing SL, SE and ST by a constant amount thereby deepening the soil moisture storage without adversely affecting the fit between modelled and observed discharges (slight adjustments would also have to be made to ZMINN and ZMAXN when ST is increased in order to maintain the same balance between soil moisture storage and infiltration rates).

c) <u>SE</u> : From Figs. 4.5 and 4.6 it can be seen that increasing SE has the effect of dramatically increasing both the mean and the standard deviation of daily discharges. The reduced evaporation maintains a high soil moisture storage thereby reducing infiltration rates during storms and also results in greater persistence in the base flows. Increased discharges inevitably lead to reduced salt concentrations as can be seen in Fig. 4.5. The standard deviation of daily salt concentrations is not greatly affected because salt concentrations are decreased for all flow conditions.

---

* The only effect of changing SL which cannot be duplicated is the ability to cause base flows to cease entirely towards the end of the dry season by setting SL > SE thereby allowing evaporation to reduce the soil moisture storage to less than SL. This cannot be exactly duplicated without using the parameter SL because even with high values of POW there will always be very small, geometrically decaying discharges.

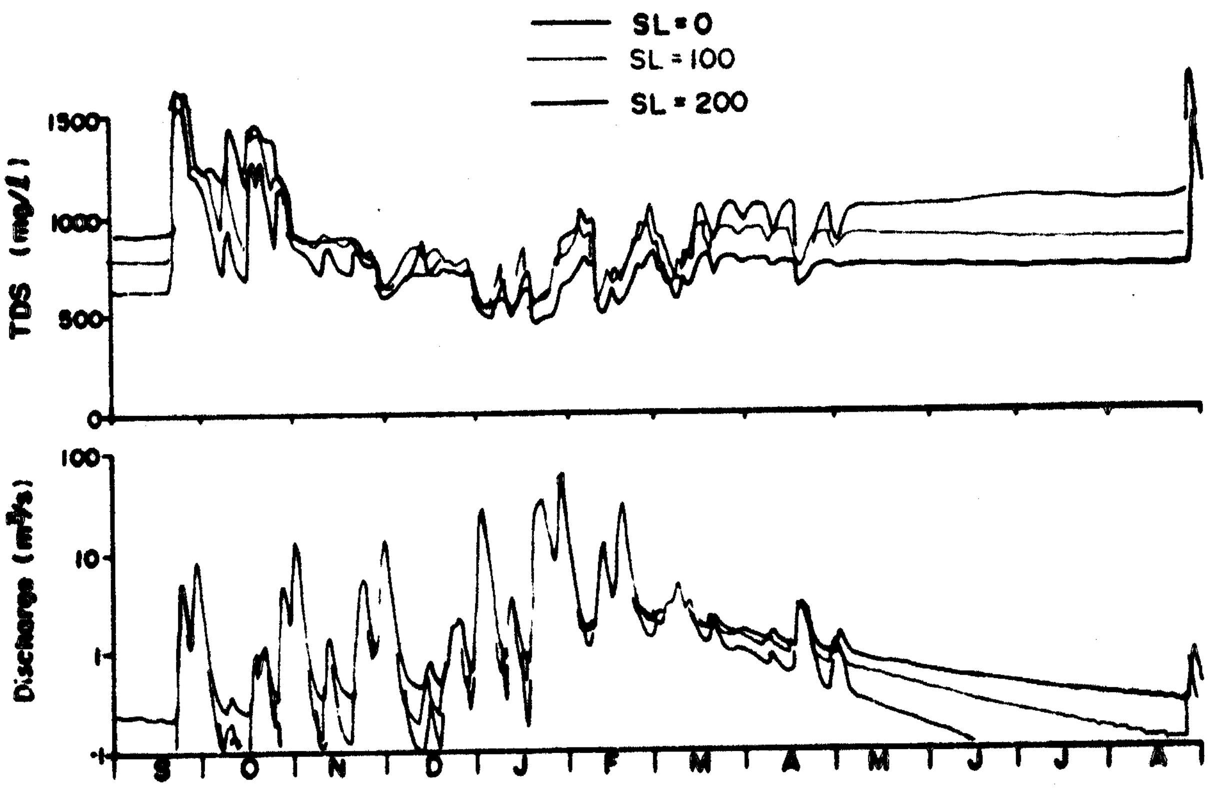

Fig. 4.3: Sensitivity of modelled daily discharges and salt concentrations to changes in SL

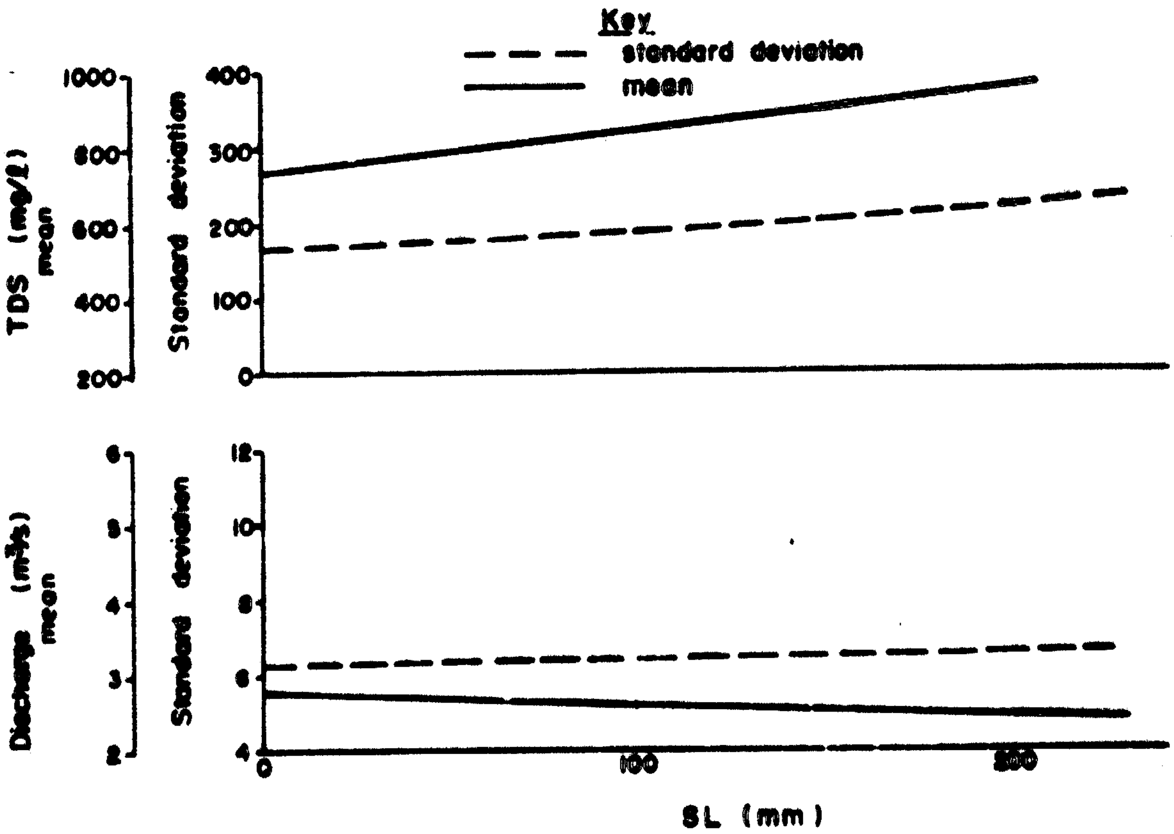

Fig. 4.4: Sensitivity of modelled means and standard deviations to changes in SL.

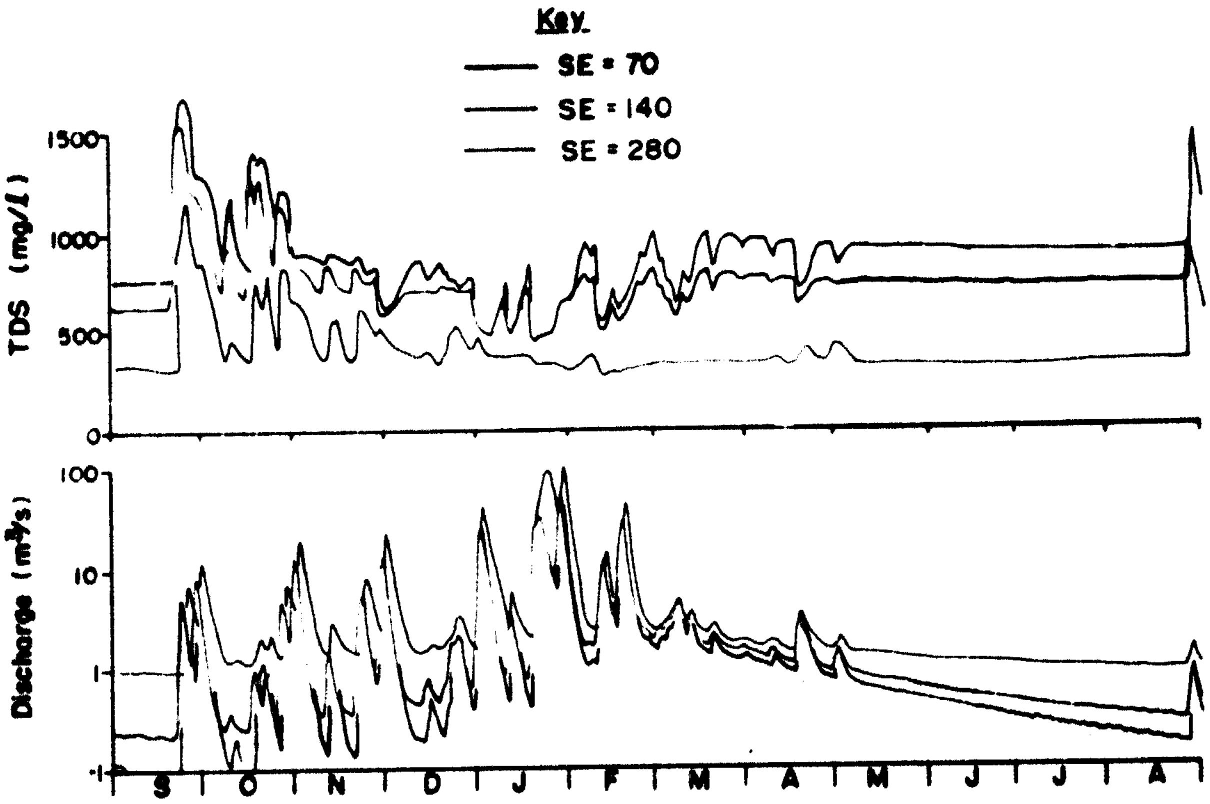

Fig. 4.5: Sensitivity of modelled daily discharges and salt concentrations to changes in SE.

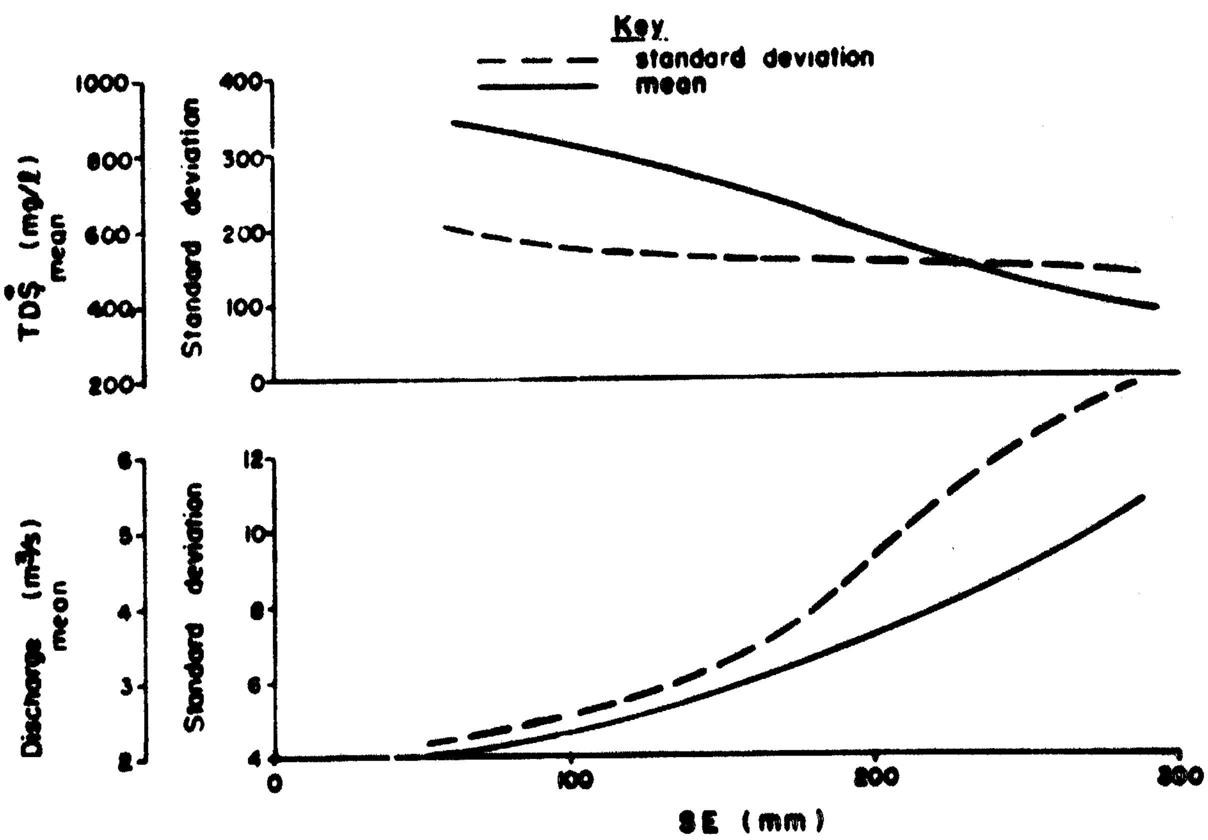

Fig. 4.6: Sensitivity of modelled means and standard deviations to changes in SE.

d) ST : Examination of Figs. 4.5 to 4.8 reveals that increasing ST has an effect on daily discharges and salinities similar to that of decreasing SE. This similarity does not, however, reduce the importance of SE. As was seen in section 4.1.1(b), the flexibility afforded by parameters SL and SE is required in order to maintain the correct long term salt mass balance of the soil moisture.

e) FT : The sensitivity of modelled discharges and salt concentrations to changes in FT is shown in Figs. 4.9 and 4.10. Increases in FT result in higher base flows and lower base flow salt concentrations. The rate at which base flows decay with time, however, is not affected by changes in FT. Mean discharges increase almost linearly with FT, while the standard deviation decreases. At the same time mean salt concentrations decline and the effect on the standard deviation of daily salinities is indeterminate, depending largely upon the balance between water quality parameters.

f) AI : Figs. 4.11 and 4.12 show the effect of changes in the impervious area on modelled discharges and salt concentrations. The main result of increased impervious area is enhanced storm runoff. Reduced infiltration also marginally reduces base flows. If the rate of generation of salts per unit area of impervious catchment surface remains constant (as was assumed in the simulations) then peak salinities during small floods, particularly at the onset of the rainy season, will be increased as AI increases. The enhanced base flow salinities shown in Fig. 4.11 for AI = 0,16 are due to reduced runoff from pervious surfaces and the resulting reduction in interflow (the implicit model assumption is that the catchment under the impervious surfaces remains an integral part of the soil moisture storage. Reduced interflow associated with increased impervious areas therefore results in longer retention times). Catchments of the size for which this model is designed, however, will rarely have as much as 16 percent impervious area (this would represent over 80 percent urbanisation). The effect of smaller impervious areas on base flow salinities is negligible.

Contrary to what might be expected, an increase in AI leads to a decrease in the standard deviation of modelled daily discharges. This is due to the fact that the largest modelled peak discharge at the end of January 1978 actually decreased when AI was increased.

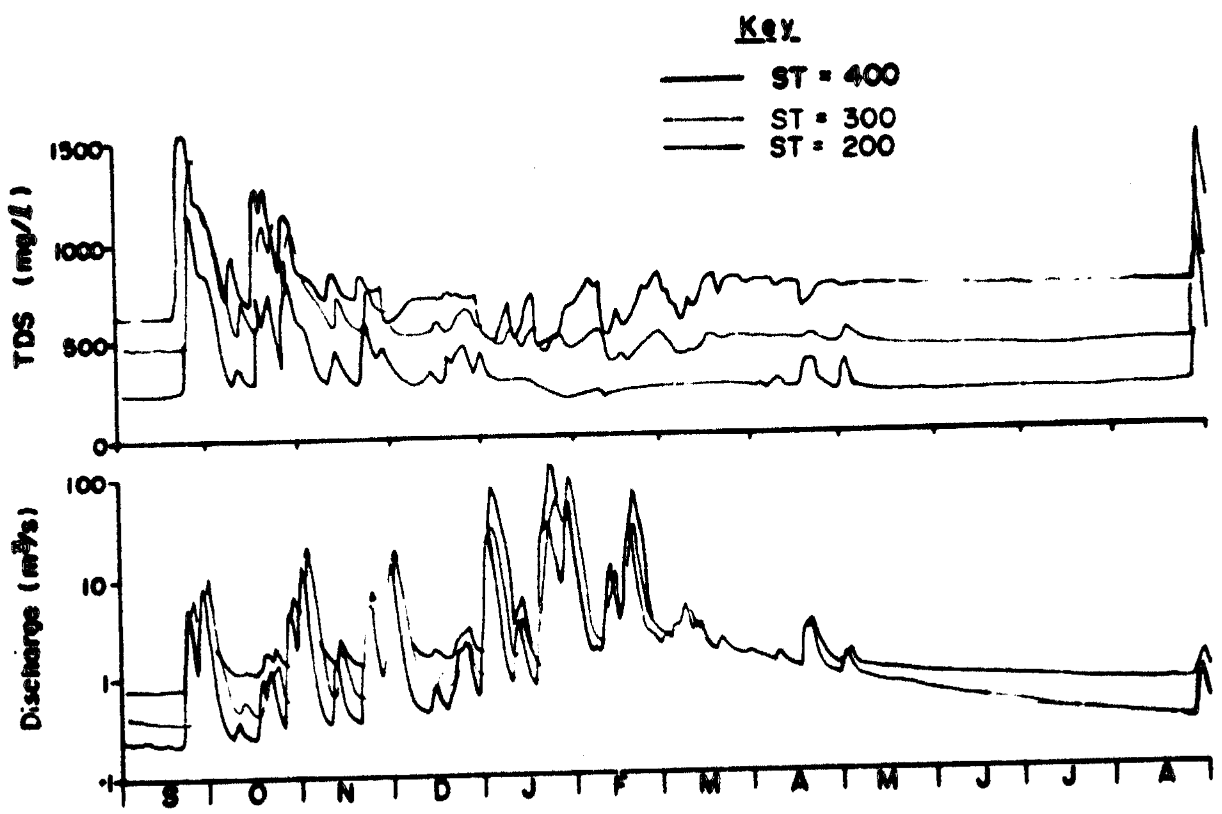

Fig. 4.7: Sensitivity of modelled daily discharges and salt concentrations to changes in ST

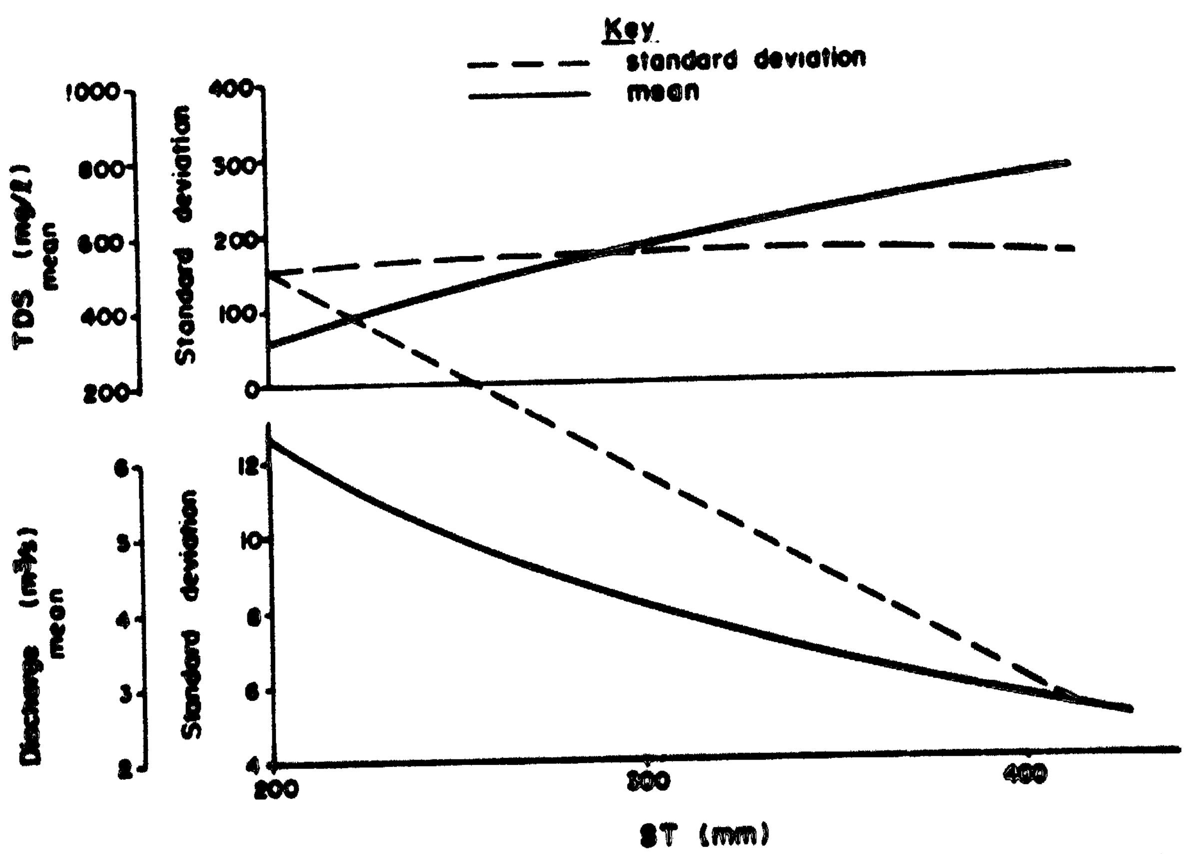

Fig. 4.8: Sensitivity of modelled means and standard deviations to changes in ST

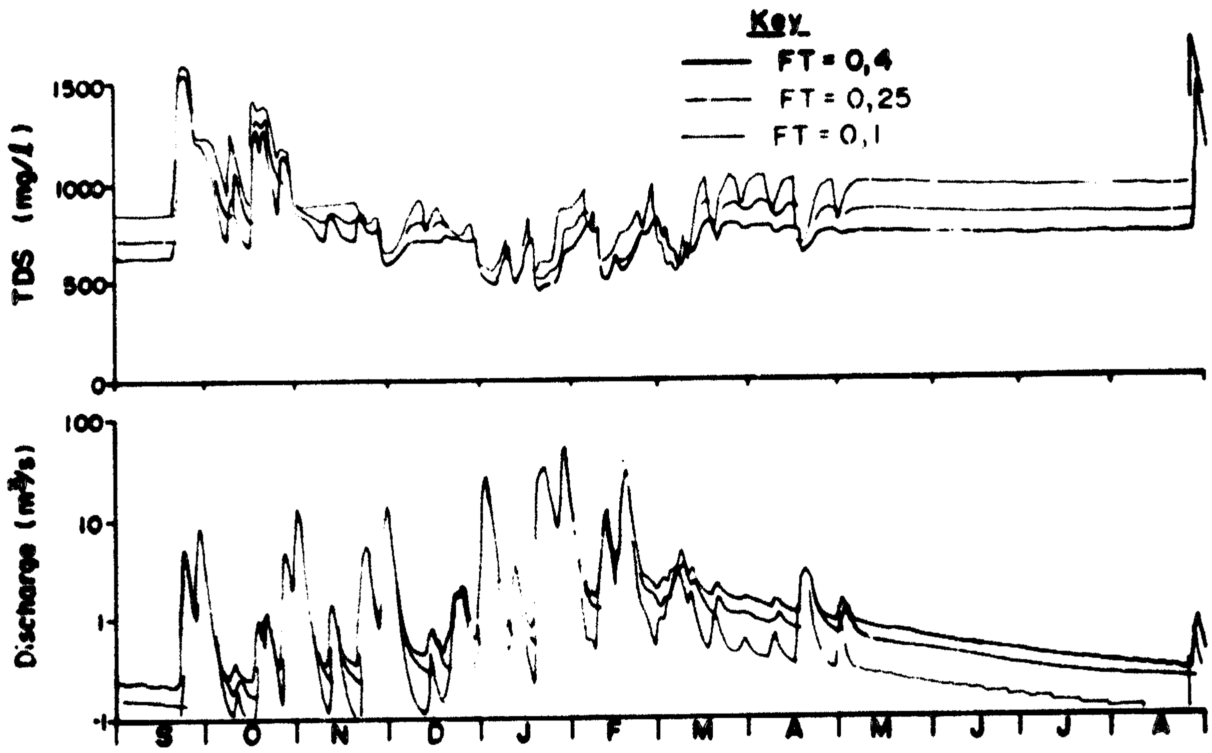

Fig. 4.9: Sensitivity of modelled daily discharges and salt concentrations to changes in FT

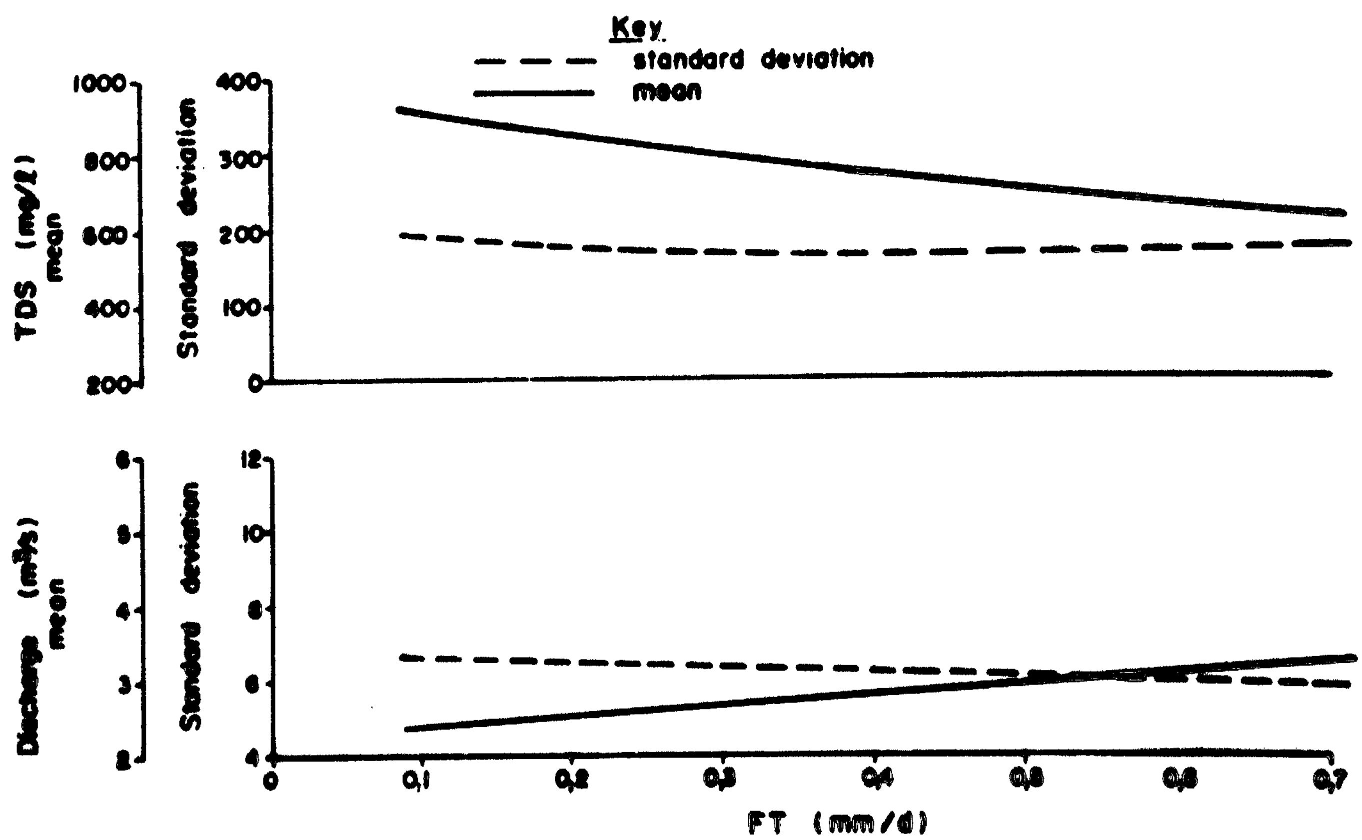

Fig. 4.10: Sensitivity of modelled means and standard deviations to changes in FT

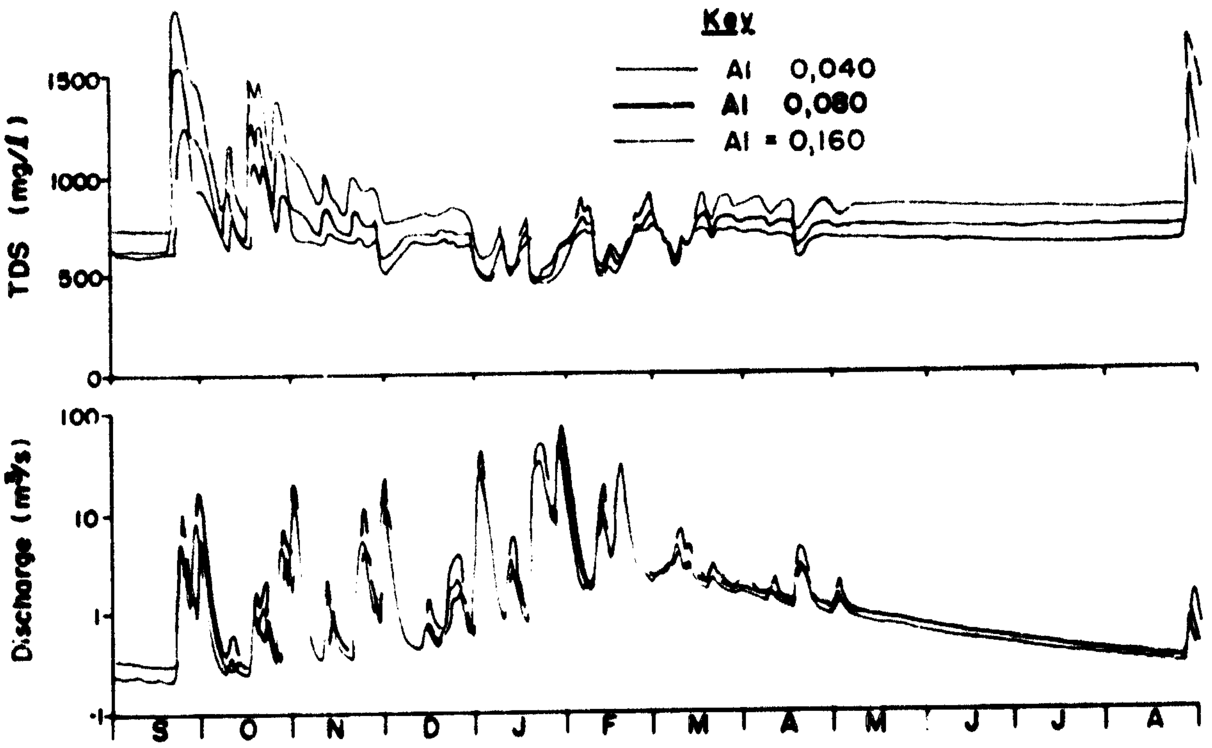

Fig. 4.11: Sensitivity of modelled daily discharges and salt concentrations to changes in AI.

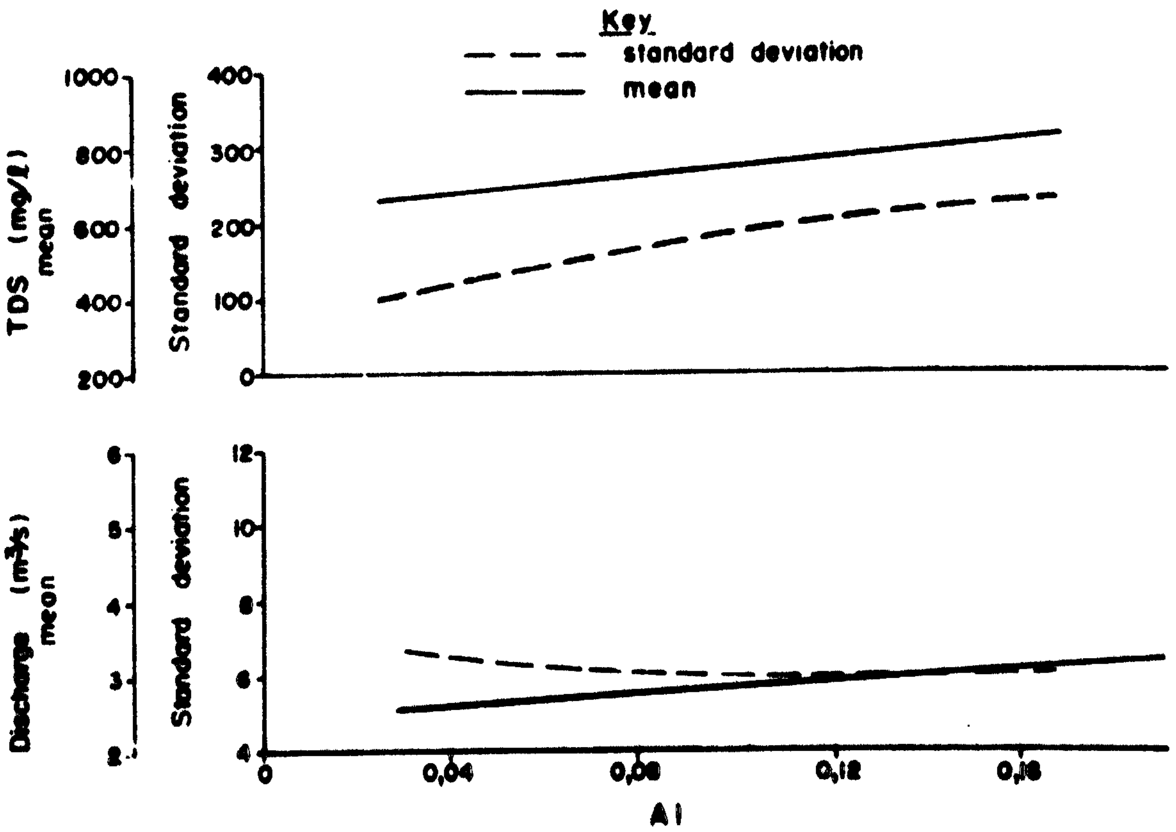

Fig. 4.12: Sensitivity of modelled means and standard deviations to changes in AI.

The peak discharge was lowered because of the reduced infiltration during the storm that caused the preceding flood with the result that there was a lower soil moisture storage at the onset of the smaller storm a week later. The anomaly is therefore another consequence of the assumption that soil moisture storage under impervious surfaces is intimately connected to that under pervious surfaces. The validity of this assumption is dependent upon the lateral permeability of the soils and the average width of the paved portions of the catchment (for example the assumption would be less true for a large paved parking area built on clay than for an equivalent area of narrow road pavement founded on fissured rock).

g) <u>ZMINN</u> : Figs. 4.13 and 4.14 show that an increase in ZMINN reduces the mean discharge but increases the standard deviation. This is because smaller floods are reduced more severely than larger floods which occur later when the soil moisture is nearly saturated. In some instances an increase in the minimum infiltration rate can actually cause flood peaks to increase, as happened with the flood at the end of January 1977 when the enhanced infiltration reduced the preceding flood peak but raised the soil moisture storage state so that the following storm rapidly filled the soil moisture storage, thereby enhancing the runoff efficiency.

The increased infiltration also gives rise to enhanced base flows, although this is not noticeable for the year simulated because the soil moisture storage became saturated at the end of January 1978 even when ZMINN was set to zero.

The salt concentrations during most of the flood peaks increase as ZMINN increases because of predominance of the more saline runoffs from the impervious areas. During the penultimate flood of January 1978, however, the urban salt storage had been largely depleted and the reduced runoff from the pervious surfaces therefore caused a decrease in salt concentrations. The following flood at the end of January, although greater, had a higher salt concentration because of the reduced impact of the diluted runoffs from the impervious surfaces. The effect of changes in ZMINN (and of ZMAXN) on salt concentrations during floods is therefore highly complex and depends upon the balance between the water quality parameters, soil moisture storages and the timing and magnitude of the floods.

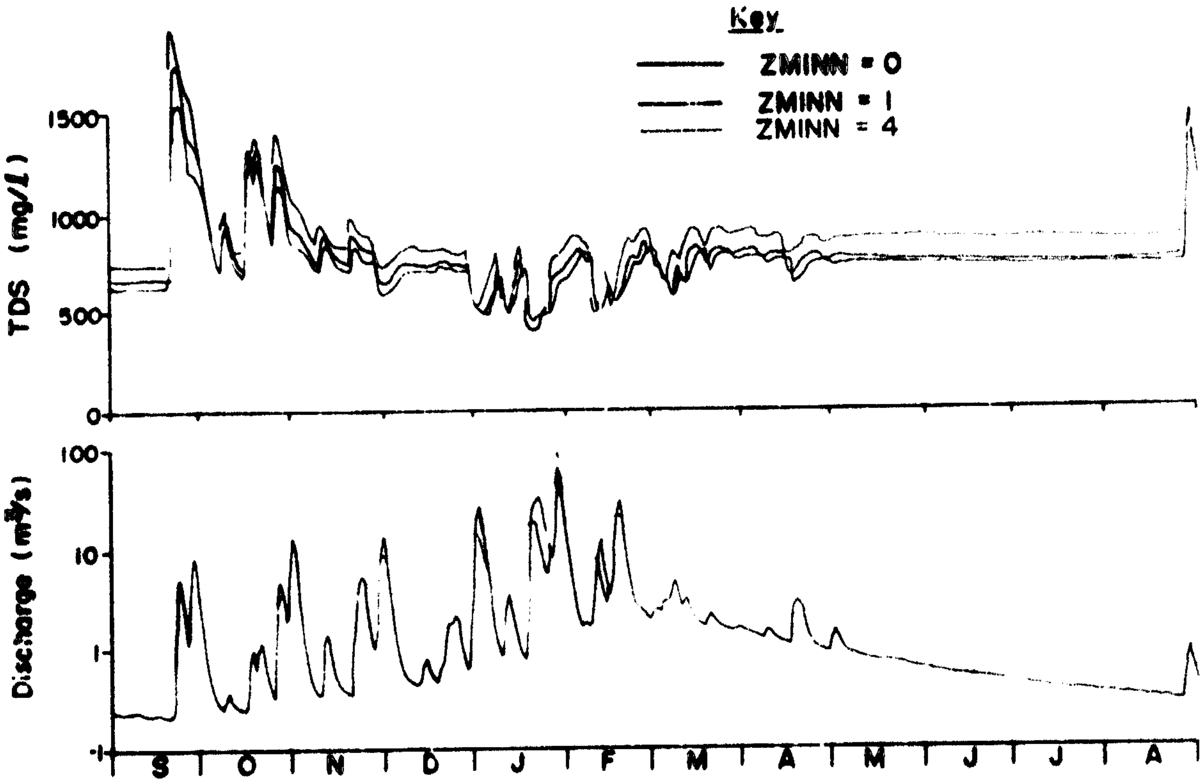

Fig. 4.13: Sensitivity of modelled daily discharges and salt concentrations to changes in ZMINN.

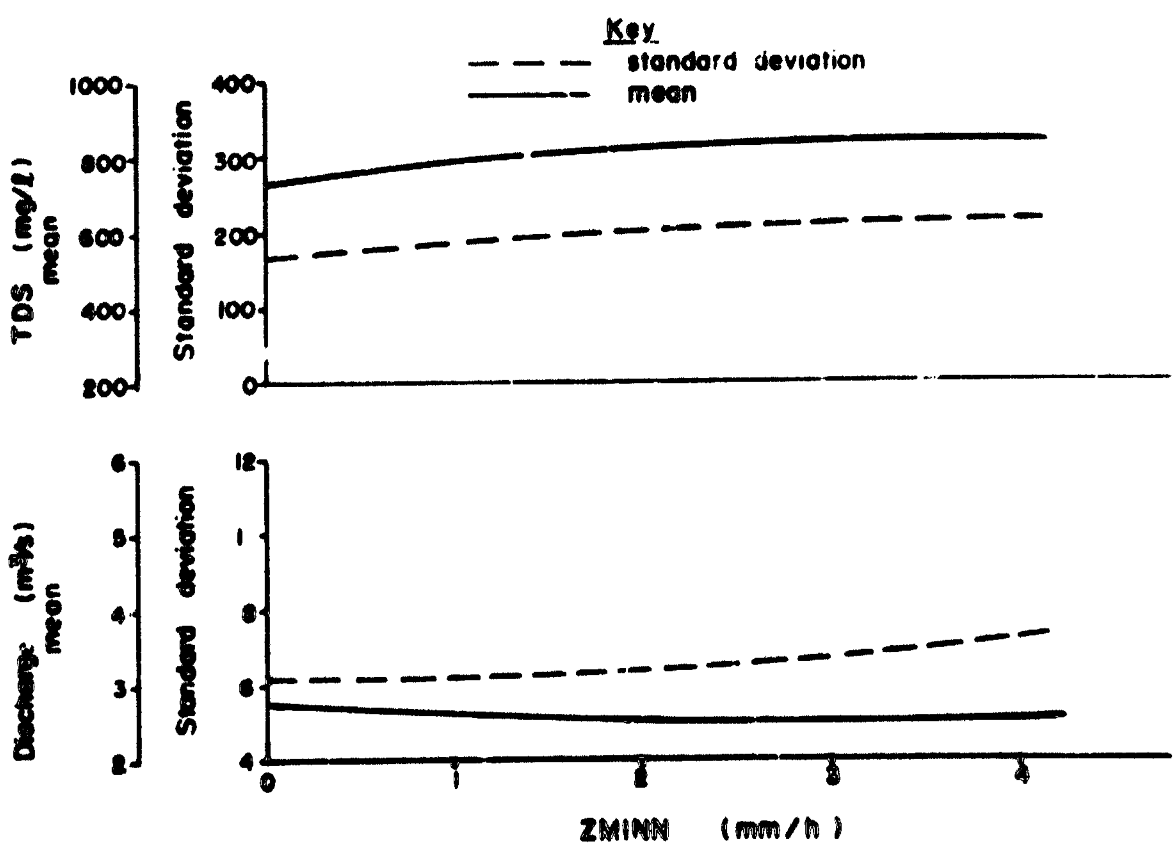

Fig. 4.14: Sensitivity of modelled means and standard deviations to changes in ZMINN

The effect of ZMINN on base flow salt concentrations is more predictable. The increased infiltration carries more salt into the soil moisture with less interflow to flush it out. Concentration due to evaporation therefore ensures that base flow salinities increase as ZMINN (or ZMAXN) is increased.

h) <u>ZMAXN</u> : The effects of increasing ZMAXN upon modelled discharges and salt concentrations are similar to those of increasing ZMINN, except that the relative decrease of larger flood peaks is usually as great, sometimes greater, than that of smaller peaks. As a result the standard deviation of daily discharges tends to decrease as ZMAXN is increased. For larger values of ZMINN, however, the last flood of January 1978 is again increased for the same reasons as discussed in section 4.1.1(g) with an accompanying rise in the standard deviation. Figs. 4.15 and 4.16 show the relationship between ZMAXN and modelled discharges and salt concentrations.

i) <u>PI</u> : The relationship between PI and modelled discharges and salt concentrations is shown in Figs. 4.17 and 4.18. Increasing PI has the effect of reducing all discharges, although base flows are not noticeably affected. The relative reduction of smaller flood peaks is much greater and many are eliminated entirely. Reduced runoffs lead to increased salt concentrations during most floods, although this is dependent upon the relative magnitudes of the runoff from pervious and impervious catchment surfaces. Fig. 4.18 indicates increased base flow salinities as PI is increased. This may not always be the case, however, as much depends upon the relationship between reduced interflow, reduced infiltration of salts and reduced base flows. A smaller value of PINTM, the interflow parameter, might cause the relative reduction of washoff into the soil moisture to predominate and cause the trend of the base flow salinities shown in Fig 4.17 to be reversed.

j) <u>TL</u> : Figs. 4.19 and 4.20 show the effects of changes in the parameter TL. TL, being the storage factor in the Muskingum equation, changes only the shape of the hydrograph without altering the mean discharge. An increase in TL leads to a decrease in the standard deviation of daily discharges. The effect on the mean and standard deviation of daily salt concentrations is small and indeterminate, depending largely upon the balance between water quality parameters.

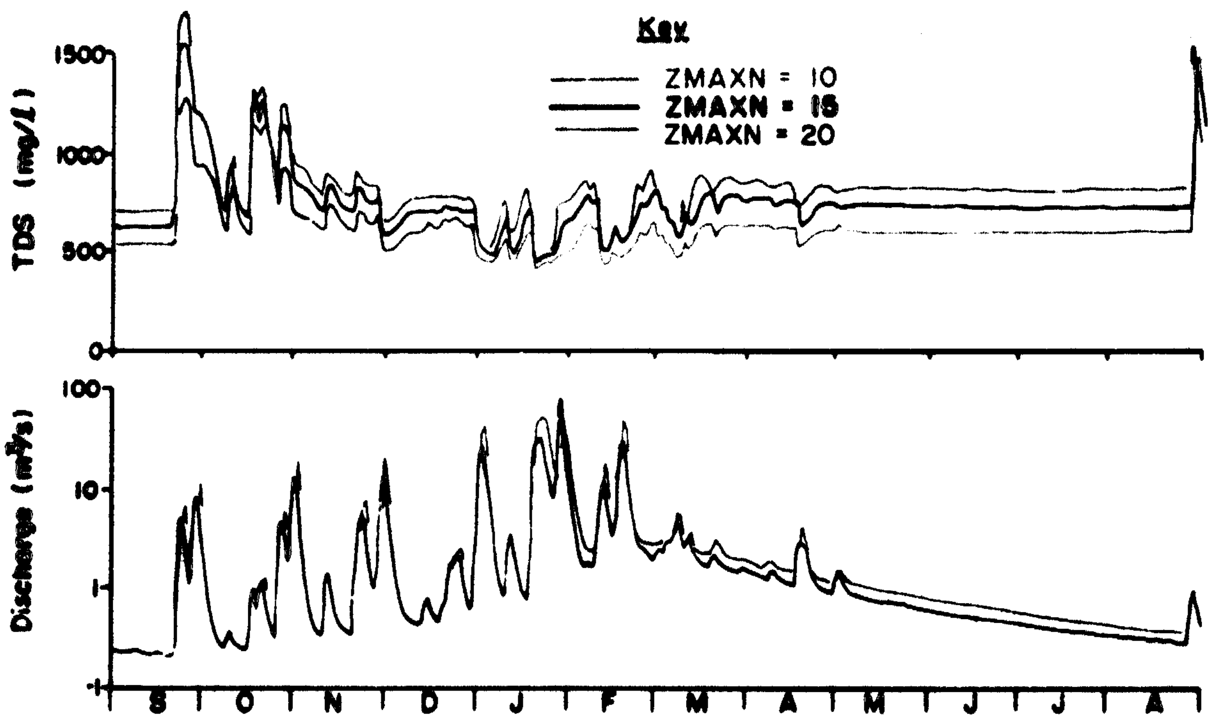

Fig. 4.15: Sensitivity of modelled daily discharges and salt concentrations to changes in ZMAXN.

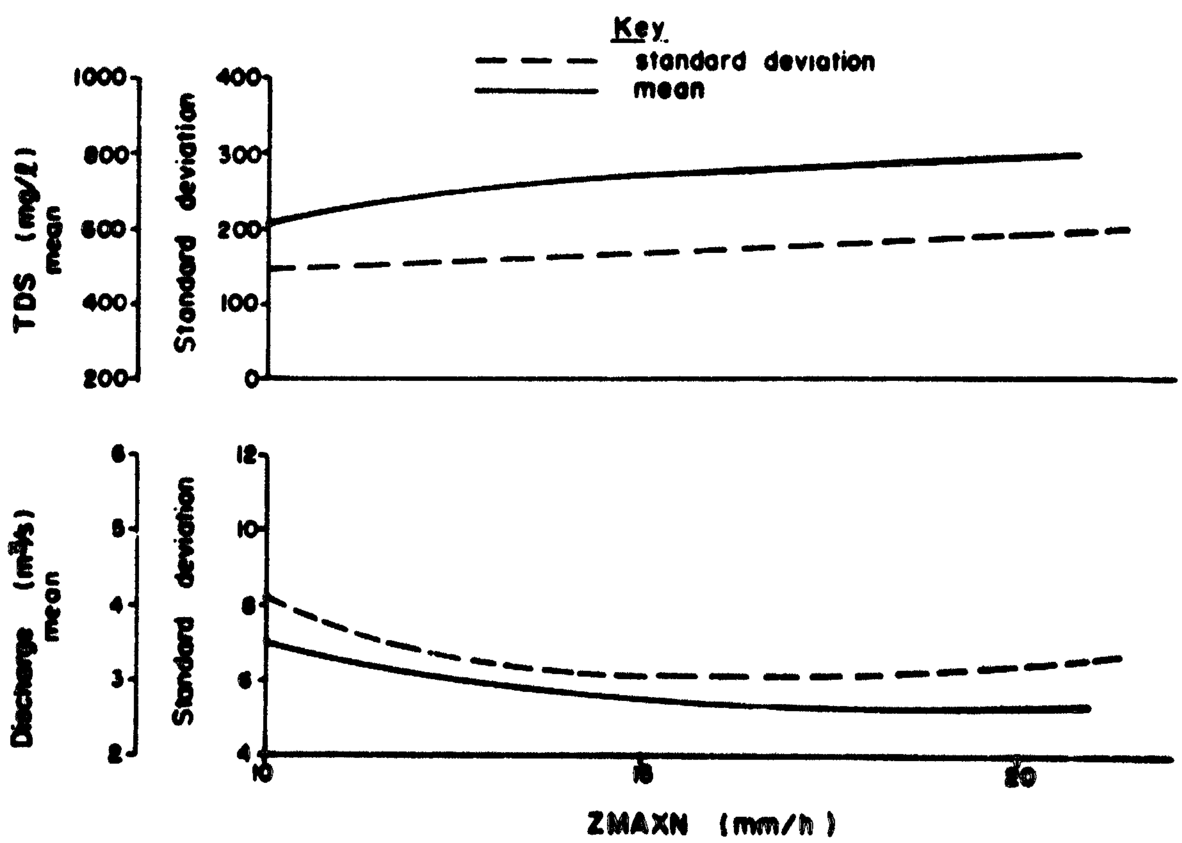

Fig. 4.16: Sensitivity of modelled means and standard deviations to changes in ZMAXN.

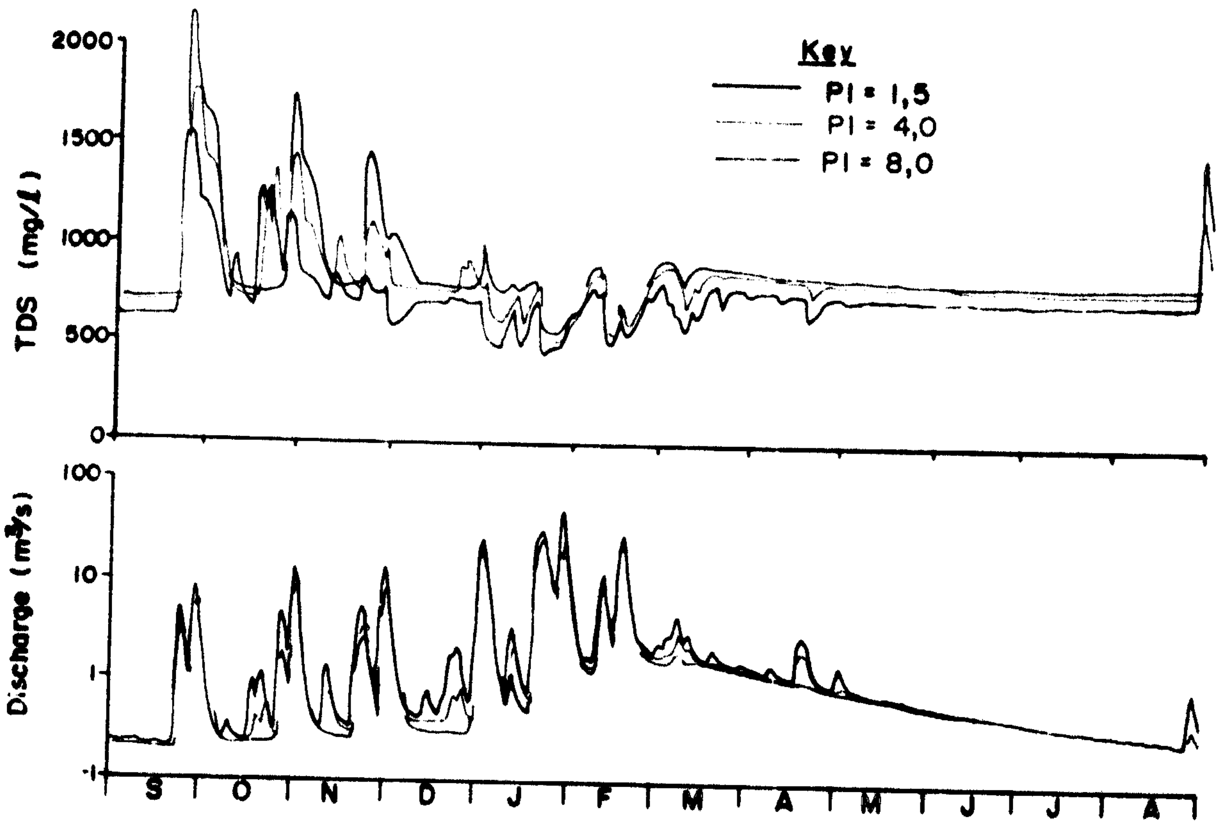

Fig.4.17: Sensitivity of modelled daily discharges and salt concentrations to changes in PI.

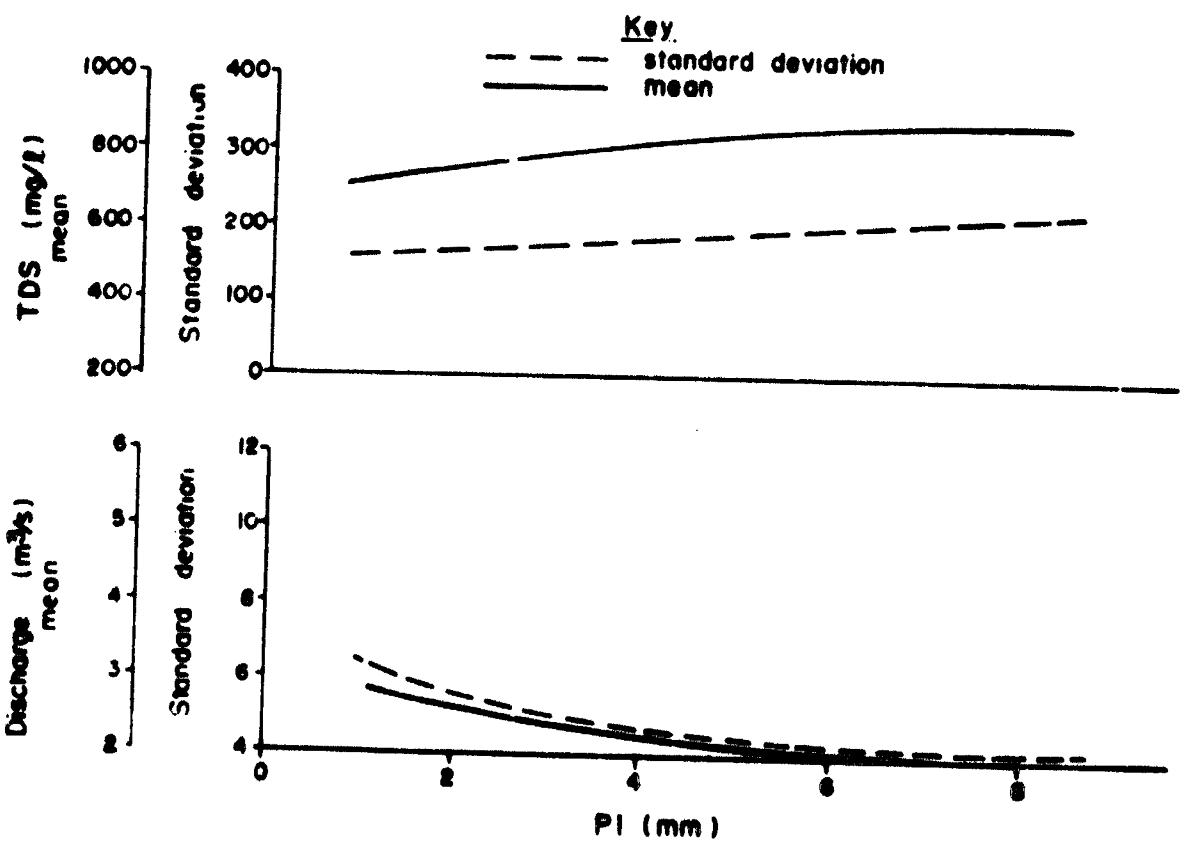

Fig.4.18: Sensitivity of modelled means and standard deviations to changes in PI

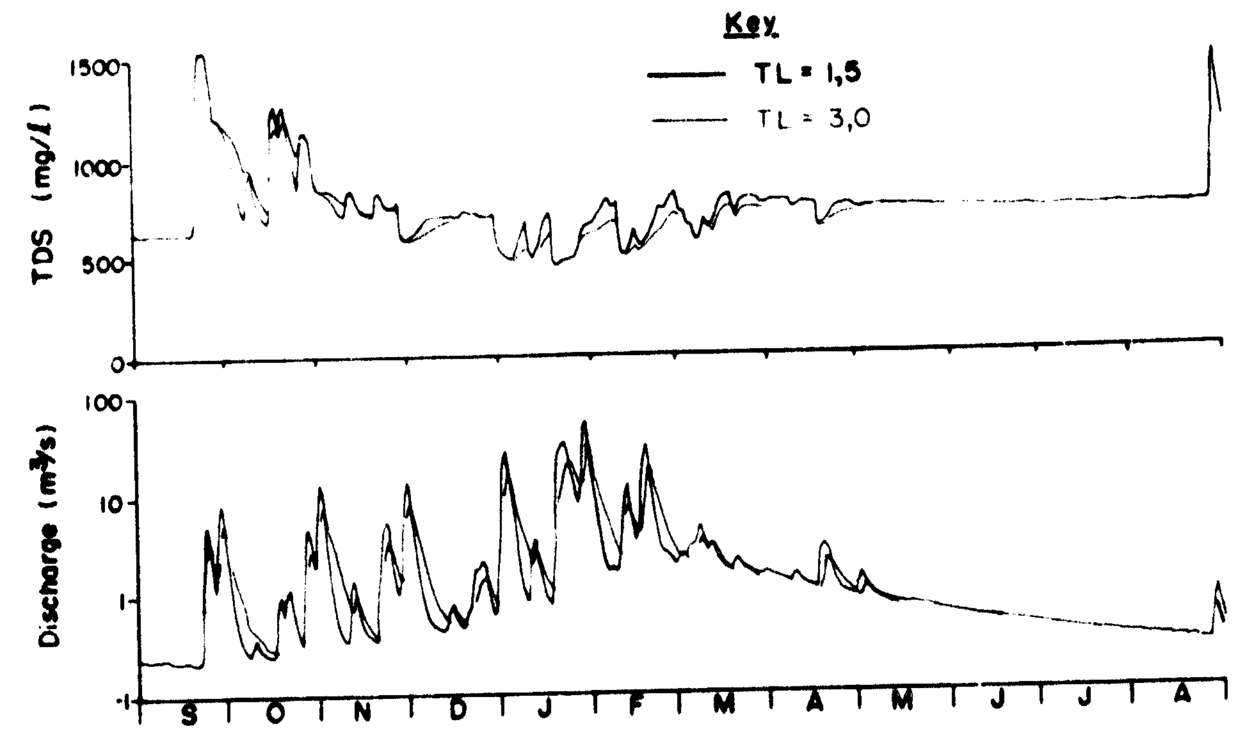

Fig.4.19: Sensitivity of modelled daily discharges and salt concentrations to changes in TL.

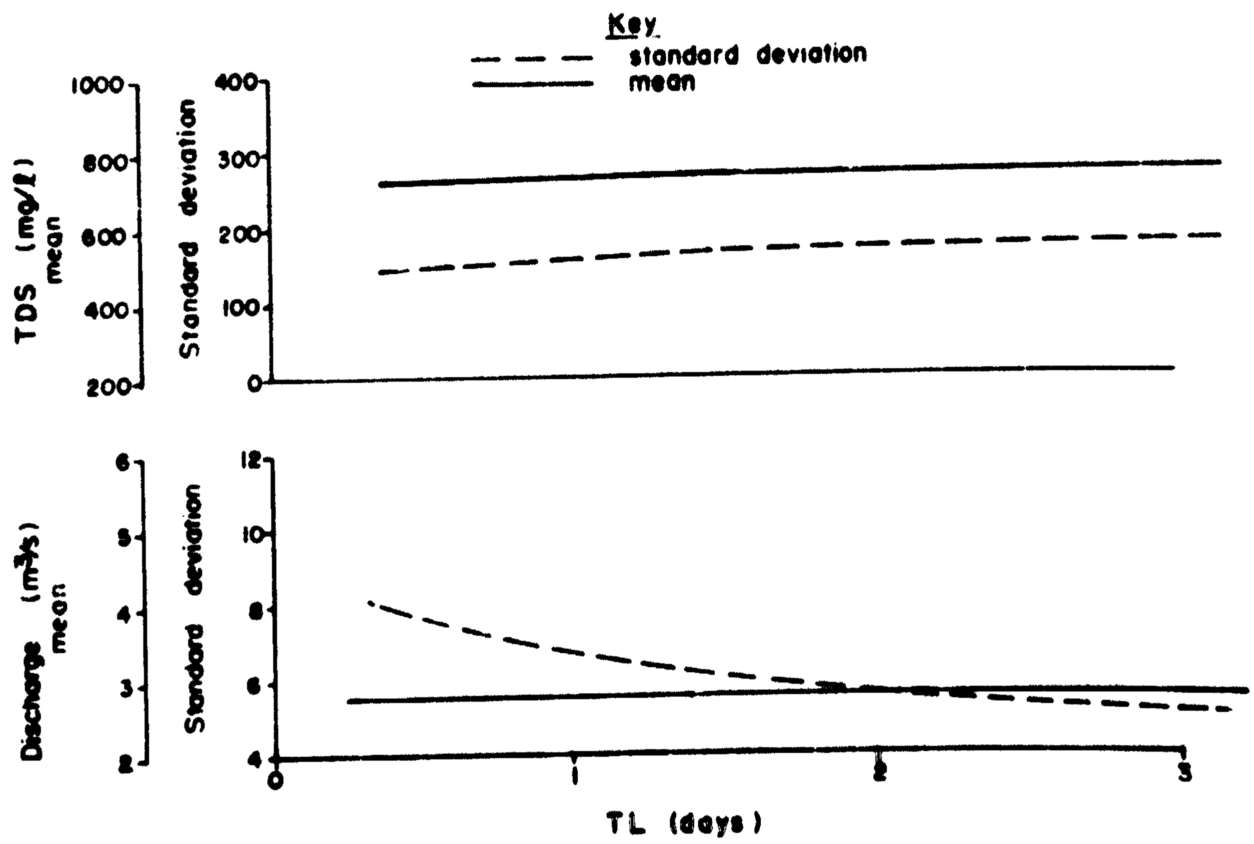

Fig.4.20: Sensitivity of modelled means and standard deviations to changes in TL.

k) LAG : The effect of LAG on modelled values has not been plotted as it results in nothing more than a constant delay of the entire modelled output. This phase shift has no effect upon modelled means and standard deviations.

l) GL : Figs. 4.21 and 4.22 show the effect of GL on modelled discharges and salt concentrations. This parameter controls the release of water from groundwater storage (see section 2.2.1(h)) The unique characteristic of this parameter, as compared with SL, SE and FT which also influence base flows, is the ability to reduce base flows immediately after floods while at the same time increasing base flows later in the dry season. This redistribution of base flows can be seen in Fig. 4.21. Changes in GL furthermore have no effect upon soil moisture storages and therefore do not alter the long term mean discharge because of the assumption that the groundwater storage is free from evaporative losses. This feature also renders any changes to modelled salt concentrations negligible. GL also has little effect upon the standard deviation of daily discharges as the flood peaks, which cause most of the variance, are not affected.

m) QOBS : This is the observed groundwater discharge at the start of the simulation and is used within the model to estimate the initial soil moisture storage. This parameter is not very important, however, as only one or two years are required to run in the model and completely eliminate all memory of the starting conditions. A considerably longer running-in period is in any case required to eliminate the effects of the initial estimate of the soil moisture salt storage (see Fig. 4.42 of section 4.1.2(i)). The effect of QOBS is therefore irrelevant.

n) DGL : The effect of DGL is to remove a constant proportion of the modelled groundwater flow, with its associated salt load, from the modelled output, resulting in reduced base flows but no change in soil moisture and base flow salt concentrations. These effects can be seen in Fig. 4.23. Fig. 4.24 shows that as DGL increases the mean discharge decreases linearly while the standard deviation increases marginally. Salt concentrations are only slightly affected due to small changes in the reduced base flow component immediately after floods. Fig. 4.24 shows a small increase in the standard deviation of modelled daily salt concentrations as DGL increases. This, however, is dependent upon the balance between the water quality parameters.

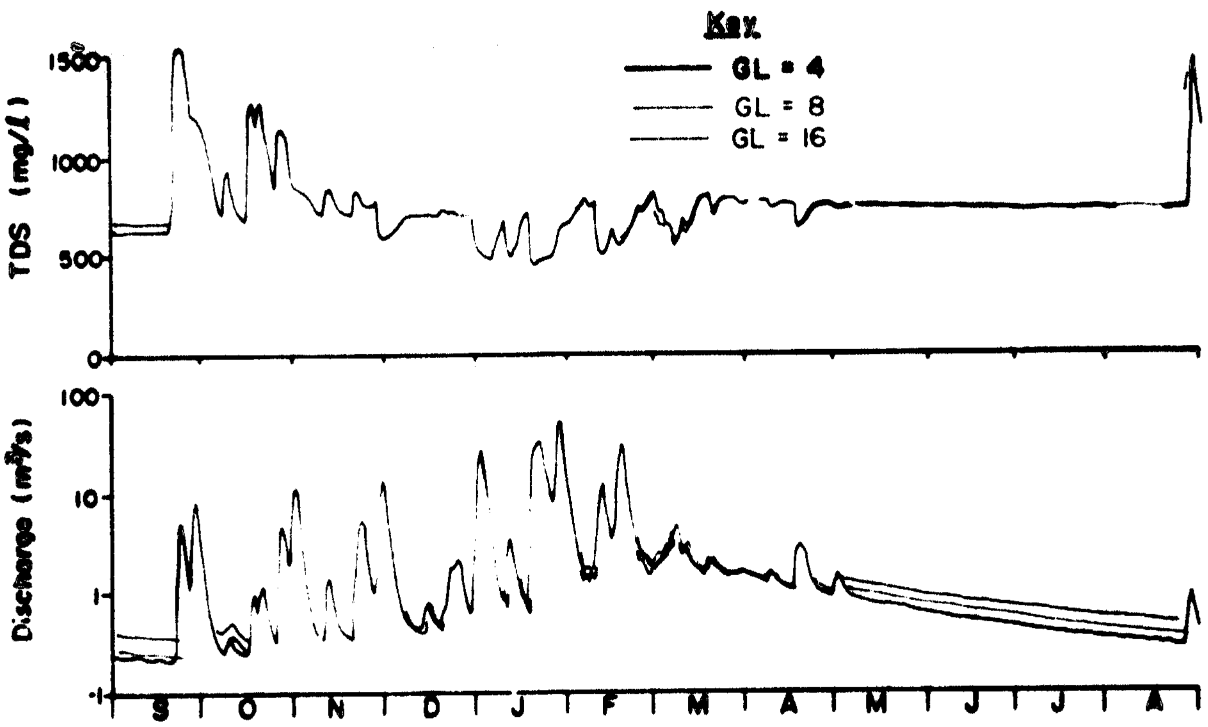

Fig.4.21: Sensitivity of modelled daily discharges and salt concentrations to changes in GL

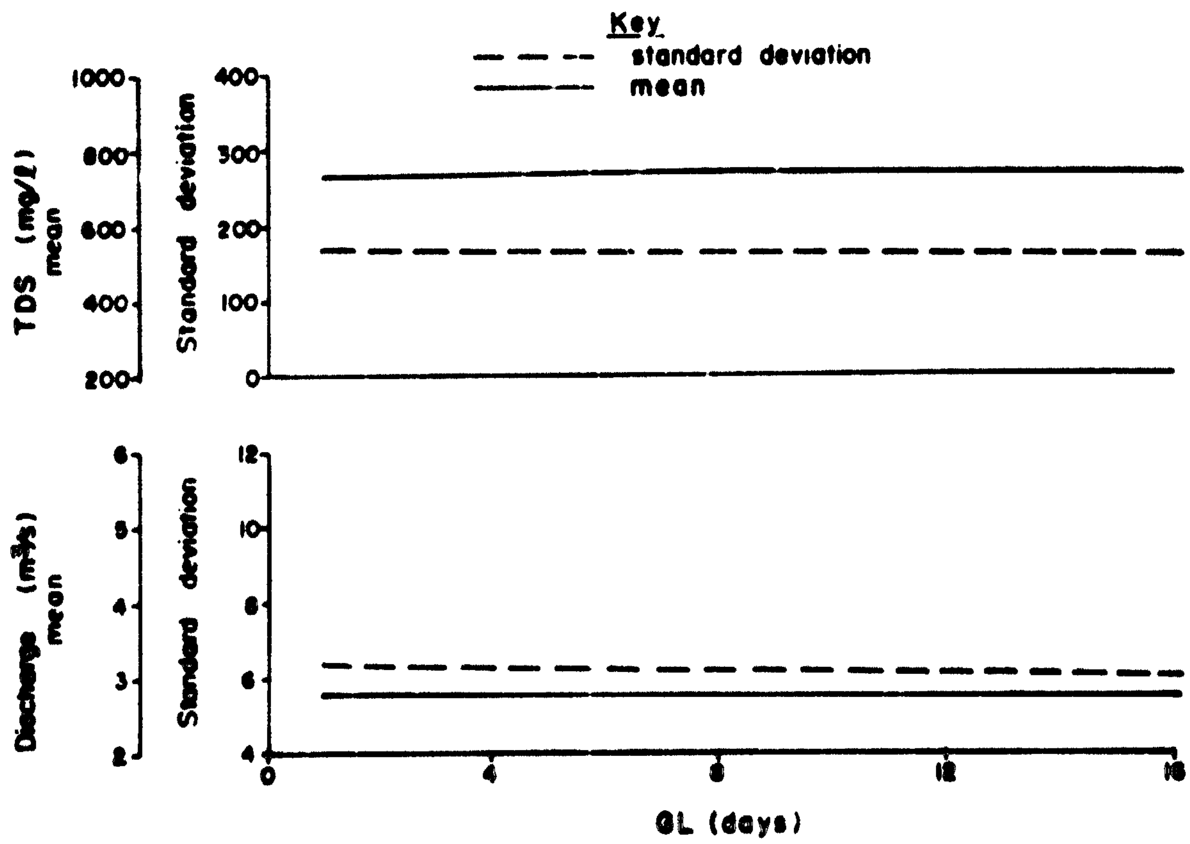

Fig.4.22: Sensitivity of modelled means and standard deviations to changes in GL

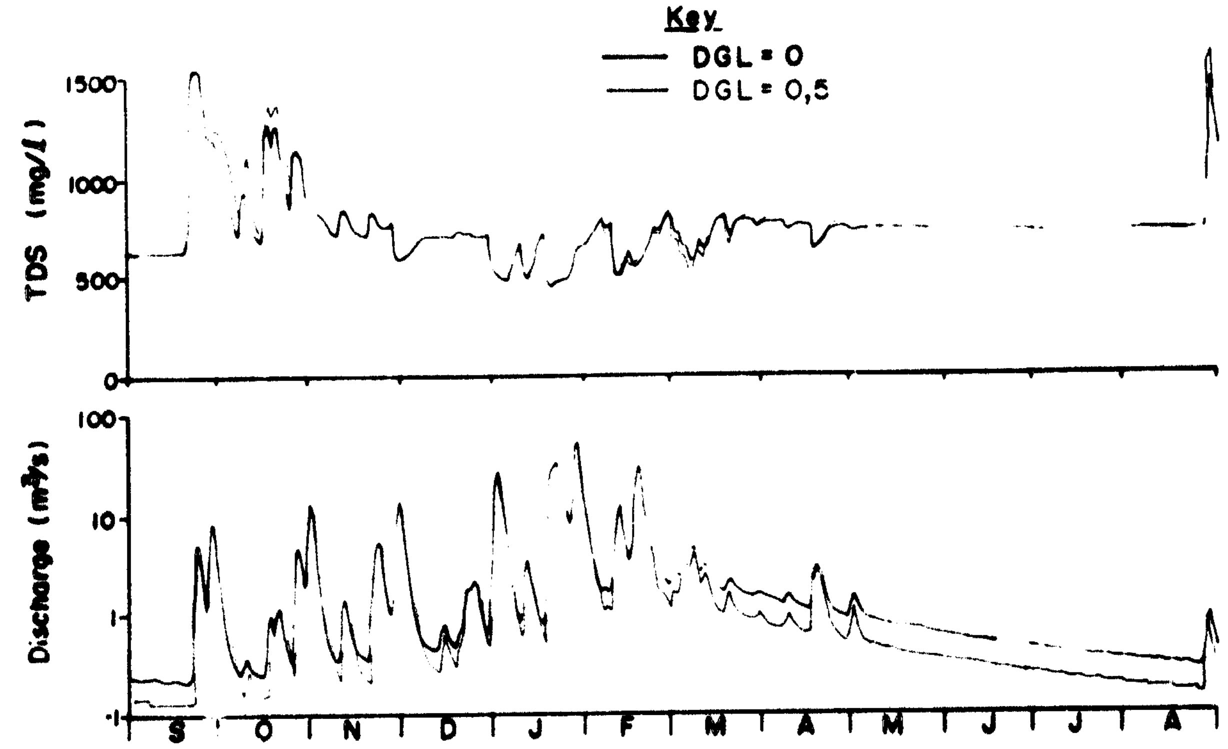

Fig. 4.23: Sensitivity of modelled daily discharges and salt concentrations to changes in DGL.

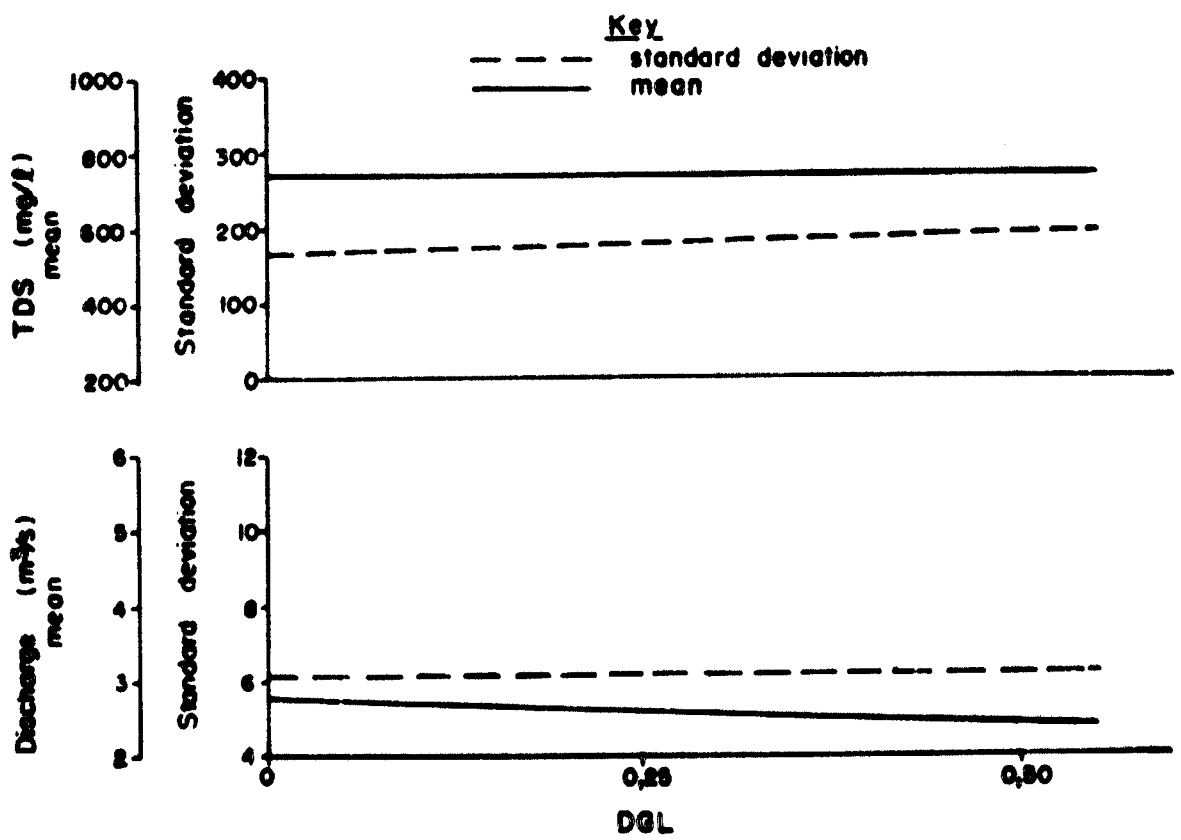

Fig. 4.24: Sensitivity of modelled means and standard deviations to changes in DGL.

4.1.2 Water quality parameters

Base line water quality parameter values are given in Table 4.2.

Table 4.2 : Base line parameter values used in sensitivity analyses of water quality parameters for program NACLØ1

Parameter	Value	Parameter	Value	Parameter	Value
APARR	-0,0008	PDEPS	0,90	SALTR*	97
BPARR	0,1090	CONCBG	10	SALTU*	185
APARU	-0,0100	PINTM	0,90	CONCS*	939
BPARU	1,0000	APARG	0		

* Parameters SALTR, SALTUand CONCS are not really calibration parameters, but initial values. These were adjusted so as to give a reasonable balance between initial and final values.

The sensitivity of modelled salt loads and concentrations to changes in each water quality parameter is discussed below.

a) APARR : Figs. 4.25 and 4.26 show the response of modelled salinities to changes in APARR. It can be seen from Fig. 4.25 that modelled means and standard deviations are highly non-linear functions of APARR. The main effect of reducing APARR is to damp out fluctuations in salt concentrations later in the rainy season when the impervious salt storage has been depleted. The long term mean salt load is not altered, although the annual salt load distribution, being a complex function of the antecedent hydrology, is radically affected. For example, the 1976/77 runoff was somewhat lower than that for 1977/78 (the period plotted in Fig. 4.25). As a result an increase in the value of APARR caused an increase in the mean salt load for the year 1977/78. Had the preceding year produced more runoff relative to that of 1977/78, however, the mean and standard deviation of daily salt loads reflected in Fig. 4.26 would have decreased with increase of APARR.

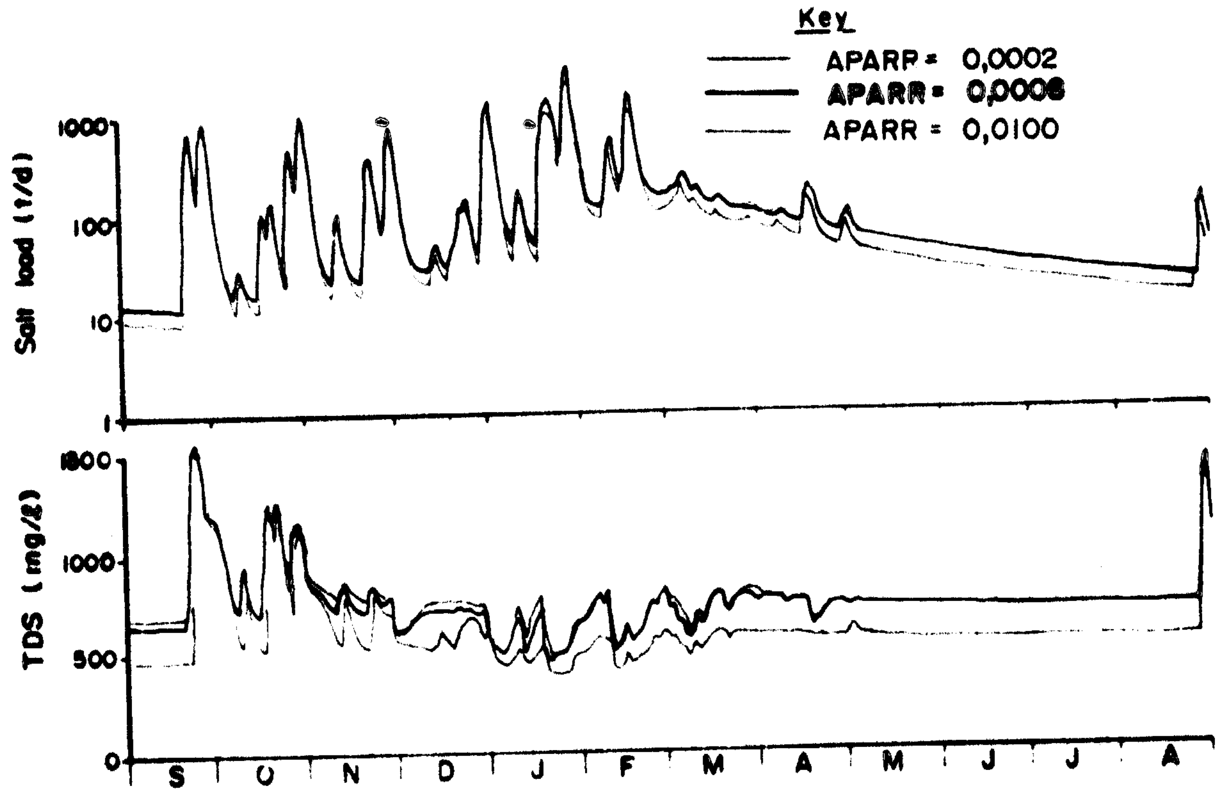

Fig 4.25: **Sensitivity of modelled daily salt concentrations and salt loads to changes in APARR**

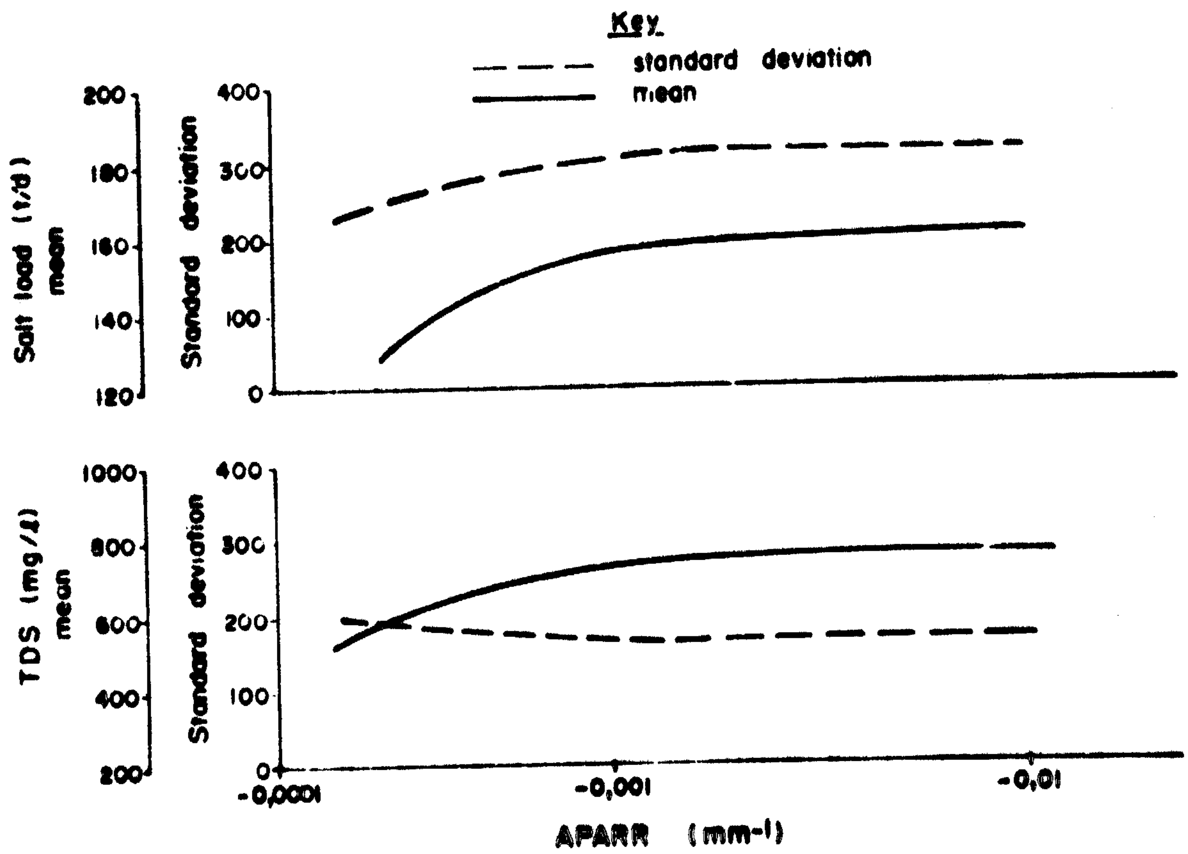

Fig.4.26: **Sensitivity of modelled means and standard deviations to changes in APARR**

A complex relationship also exists among base flow salt concentrations, APARR and the antecedent hydrology. Generally, base flow concentrations can be expected to increase for a year that is preceded by a relatively dry period if APARR is increased. If the preceding hydrology is exceptionally wet, increasing APARR should reduce the base flow salt concentrations.

b) BPARR : The effect of changing BPARR is clearly shown by Figs. 4.27 and 4.28. An increase in BPARR inevitably leads to virtually linear increases in the mean and standard deviation of modelled salt loads and the mean salt concentration. Salt concentrations are increased during both the dry and the wet seasons. Changes in the standard deviation of daily salt concentrations are dependent upon the other water quality parameters and are consequently less predictable. In general, when the salt load contribution from impervious surfaces is large (as in the case reflected in Figs. 4.27 and 4.28), increases in BPARR will cause the standard deviation to decline as base flow salt concentrations rise to match those of the early season floods. On the other hand, if the urban washoff component is small, an increase in BPARR accentuates the difference between the high base flow salinities and the lower salinities during the floods, with a consequent rise in the standard deviation.

c) APARU : The greater washoff efficiencies attributed to paved surfaces means that APARU, unlike APARR, has little effect upon the annual distribution of salt loads. APARU does, however, have a profound effect upon the distribution of salt loads within the rainy season of any given year. This is clearly shown in Fig. 4.29 where it can be seen that an increase in the magnitude of APARU shifts more of the salt load towards the onset of the wet season at the expense of the later months. From Fig. 4.30 it can be seen that APARU has no effect upon mean salt loads, even within a given year. An increase in the magnitude of APARU causes a sharp rise in the standard deviation of modelled daily salt concentrations while the mean also increases, but at a slower rate (this is because the sharp rises in TDS at the start of the wet season are partially balanced by smaller salt concentration decreases during later floods). In the range of values approaching sero an

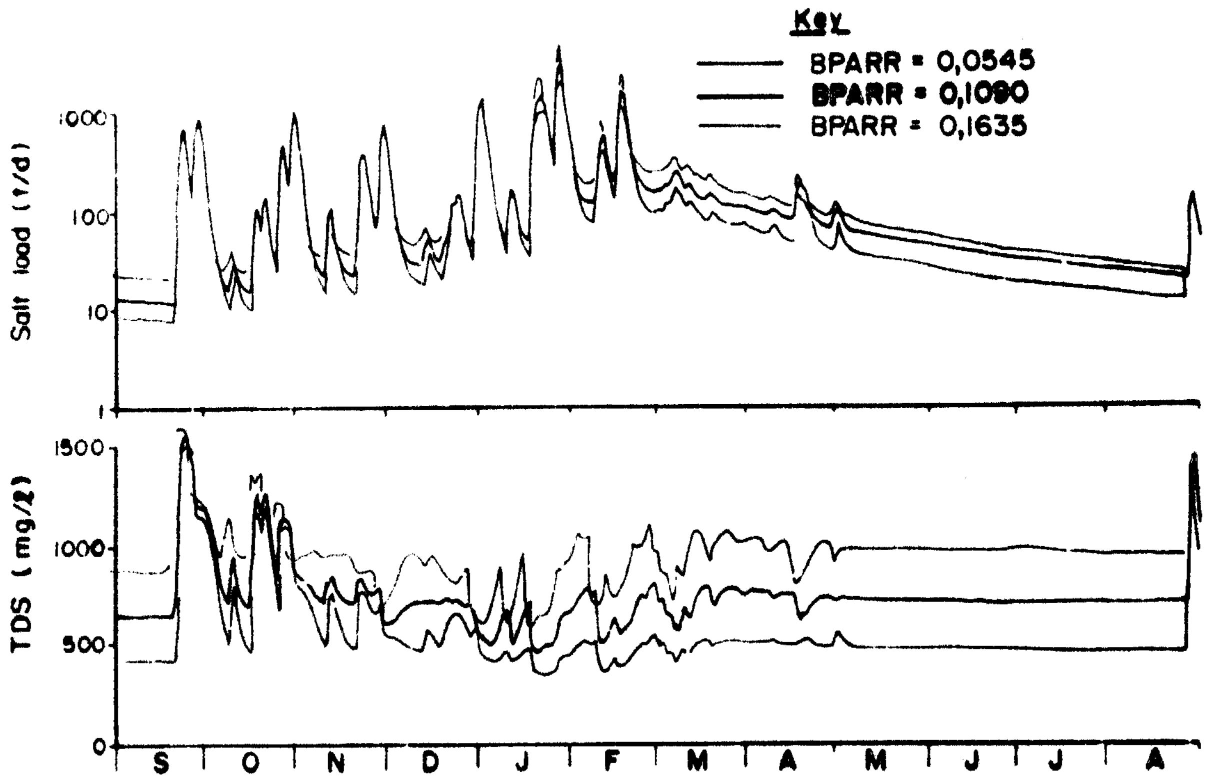

Fig 4.27 : Sensitivity of modelled daily salt concentrations and salt loads to changes in BPARR.

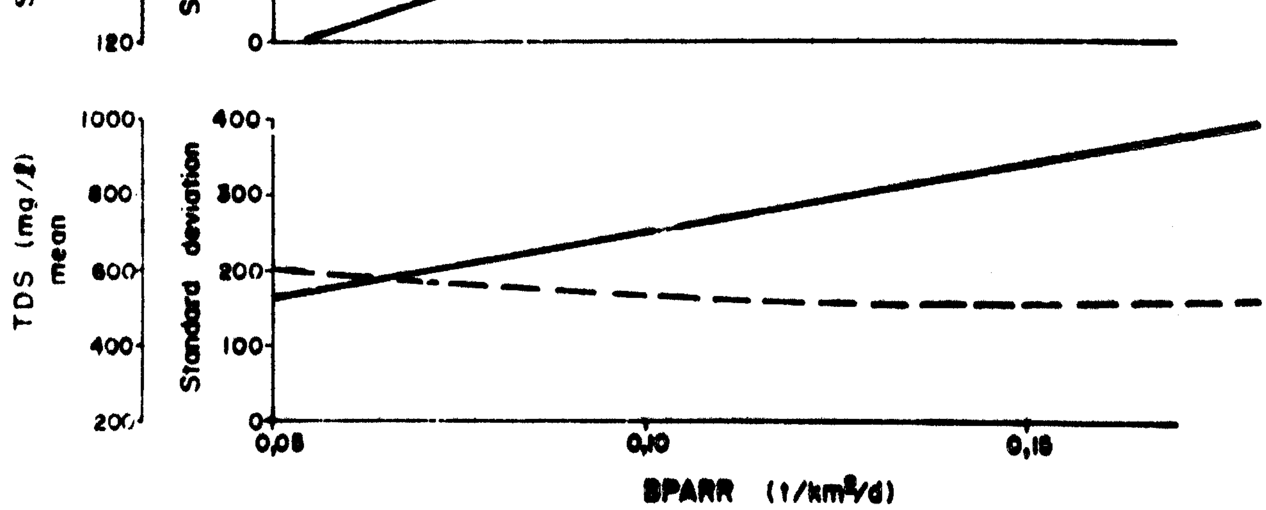

Fig 4.28 Sensitivity of modelled means and standard deviations to changes in BPARR

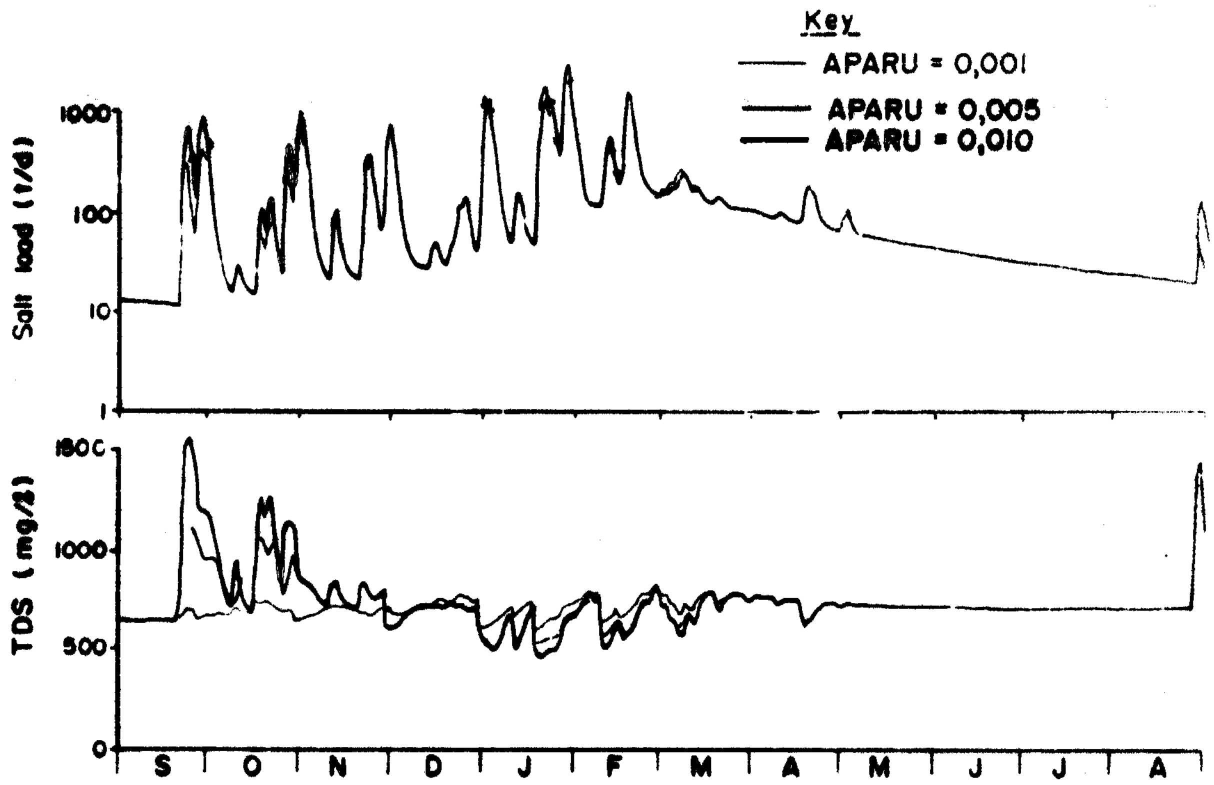

Fig 4.29: Sensitivity of modelled daily salt concentrations and salt loads to changes in APARU

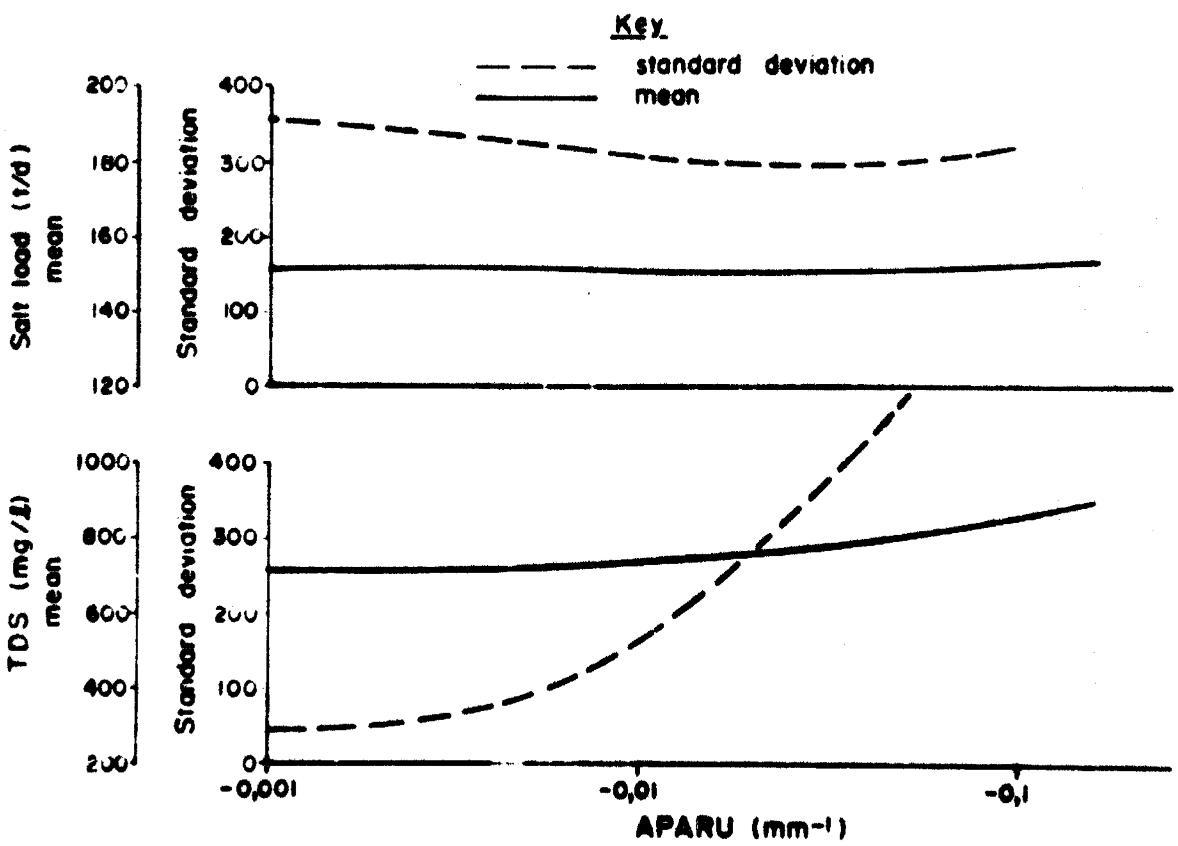

Fig.4.30: Sensitivity of modelled means and standard deviations to changes in APARU

increase in APARU causes a decline in the standard deviation of modelled daily salt loads due to the reduction in the peak loads during the major January floods. Further increases in APARU, however, have little further effect upon the January peak loads but continue to increase the peaks at the start of the rainy season with a resulting rise in the standard deviation.

d) BPARU : Figs. 4.31 and 4.32 show that an increase in BPARU increases the mean and standard deviations of modelled daily salt loads and salt concentrations. From Fig. 4.31 it can be seen that the influence of BPARU is most marked during the early floods of the wet season when larger salt generation rates cause a sharp rise in salt loads and concentrations.

e) PDEPS : Figs. 4.33 and 4.34 show the effects of changes in PDEPS on modelled salt loads and concentrations. PDEPS controls the rate at which base flow salt concentrations rise as a result of evaporation from the soil moisture. An increase in the proportion of salt deposited in the soil moisture therefore results in a decline in average salt concentrations. The influence on the standard deviation of salt concentrations is, however, dependent upon the balance between BPARR and BPARU. Larger values of PDEPS also increase the standard deviation of modelled daily salt loads due to the reduced base flow loads and enhanced peak loads during floods when interflow flushes out part of the deposited salt. The rise in mean salt loads with increasing values of PDEPS reflected in Fig. 4.34 is, however, misleading as PDEPS cannot alter the long term mean. The change in the salt load washed out of the soil in any given year depends upon the antecedent hydrology.

f) CONCBG : The effect of the background TDS (attributed to precipitation) upon modelled salinities is shown in Figs. 4.35 and 4.36. An increase in CONCBG causes an increase in mean concentrations and salt loads. If the interflow component is high (i.e. for high values of PINTM), as in the cases simulated, then an increase in CONCBG results in an increased standard deviation of daily salt loads. This is because much of the extra salt load derived from precipitation, most of which enters soil moisture storage, is ultimately flushed out via interflow during floods. If PINTM is small, however, then most of the salt derived from precipitation

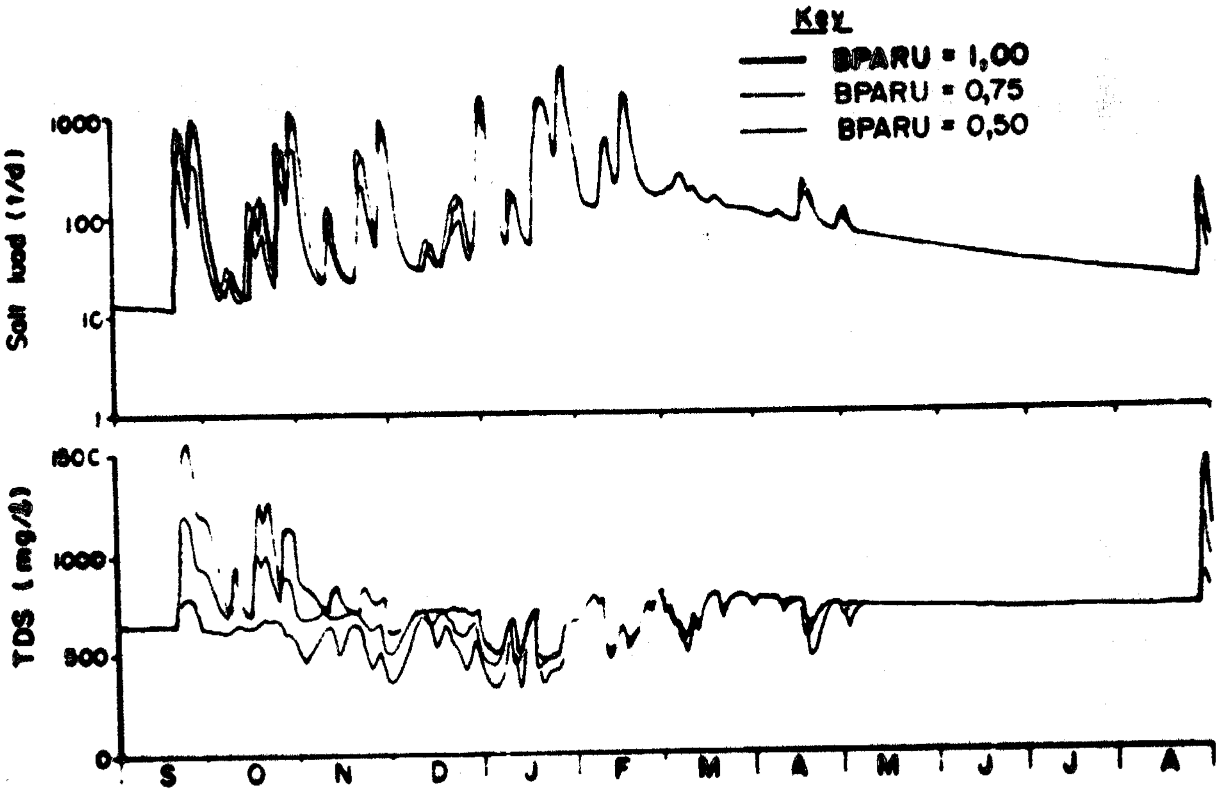

Fig 4.31: Sensitivity of modelled daily salt concentrations and salt loads to changes in BPARU

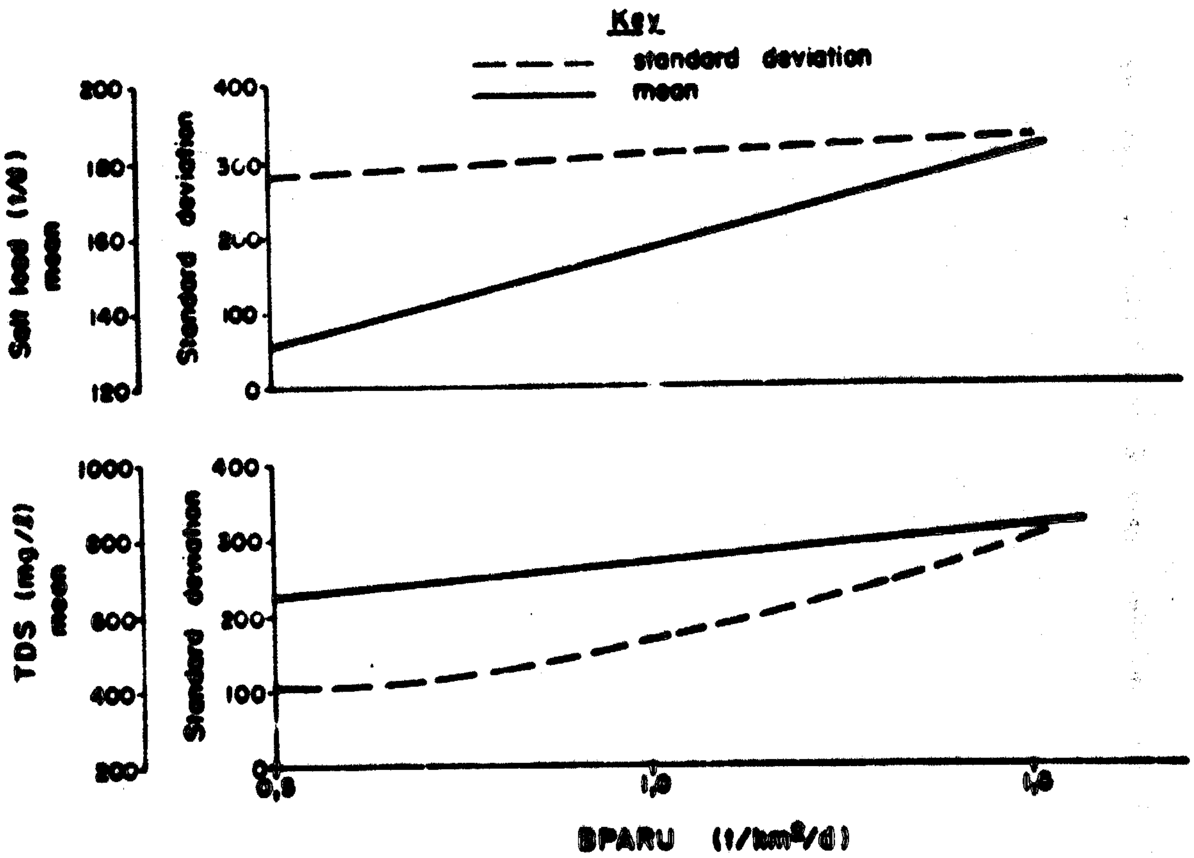

Fig. 4.32: Sensitivity of modelled means and standard deviations to changes in BPARU

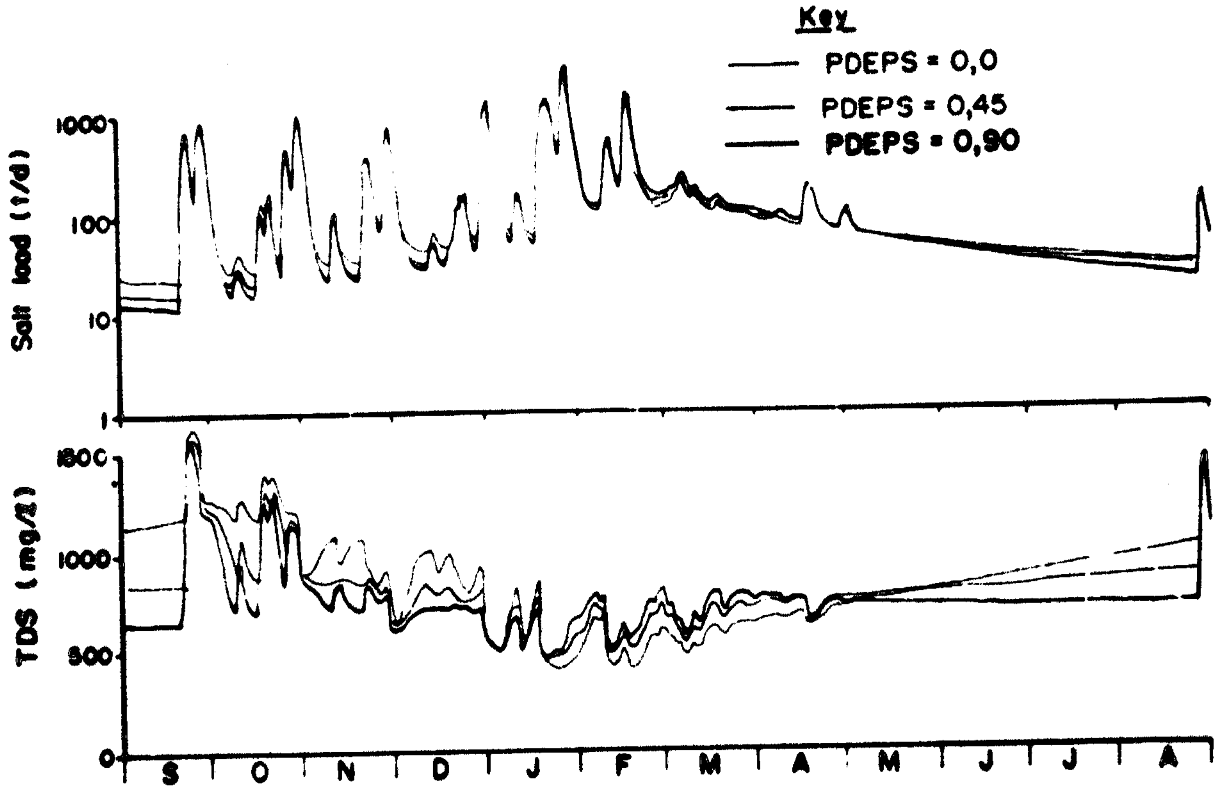

Fig.4.33: Sensitivity of modelled daily salt concentrations and salt loads to changes in PDEPS

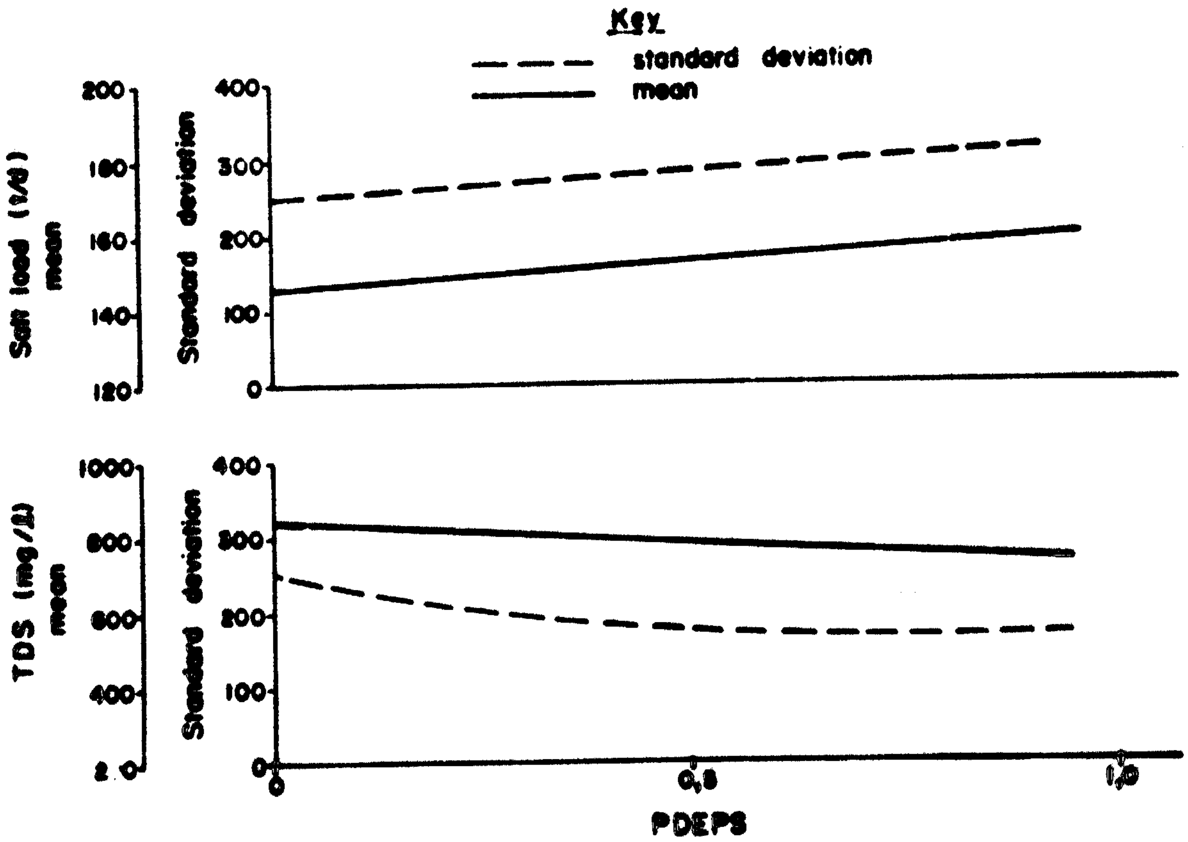

Fig.4.34: Sensitivity of modelled means and standard deviations to changes in PDEPS

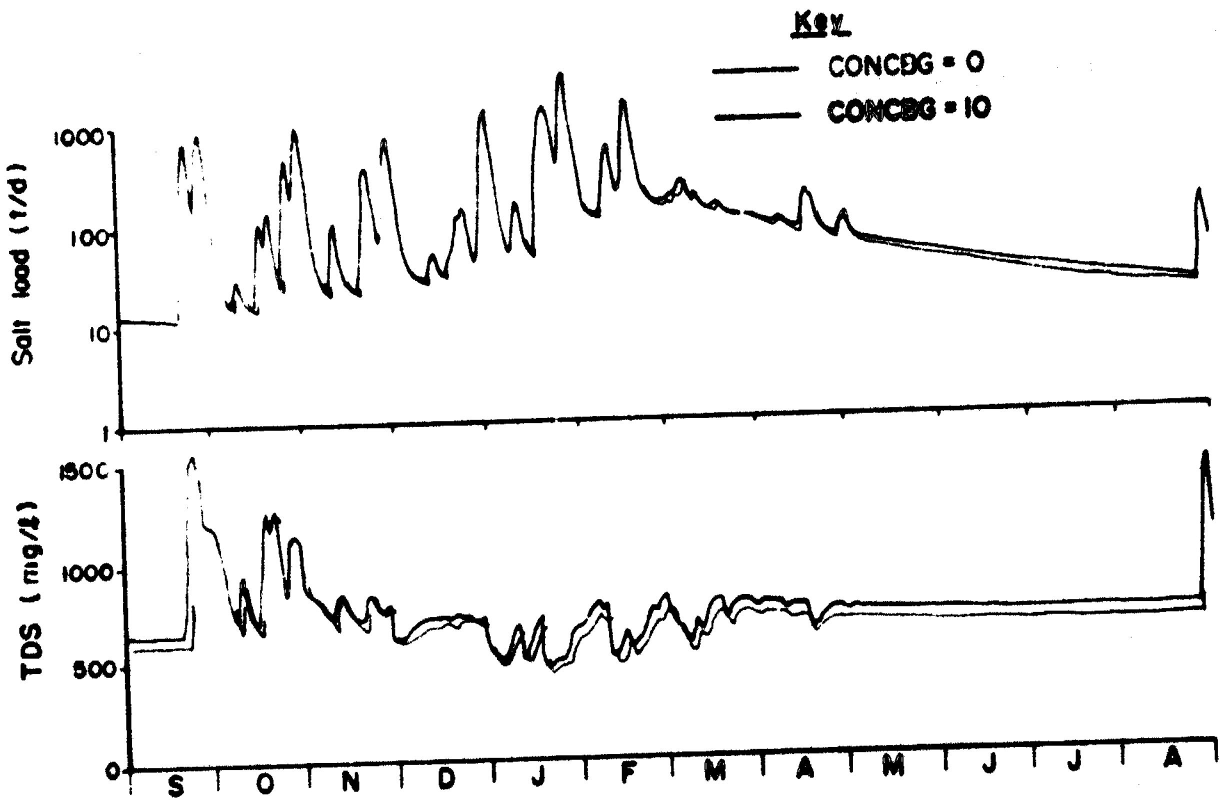

Fig 4.35: Sensitivity of modelled daily salt concentrations and salt loads to changes in CONCBG.

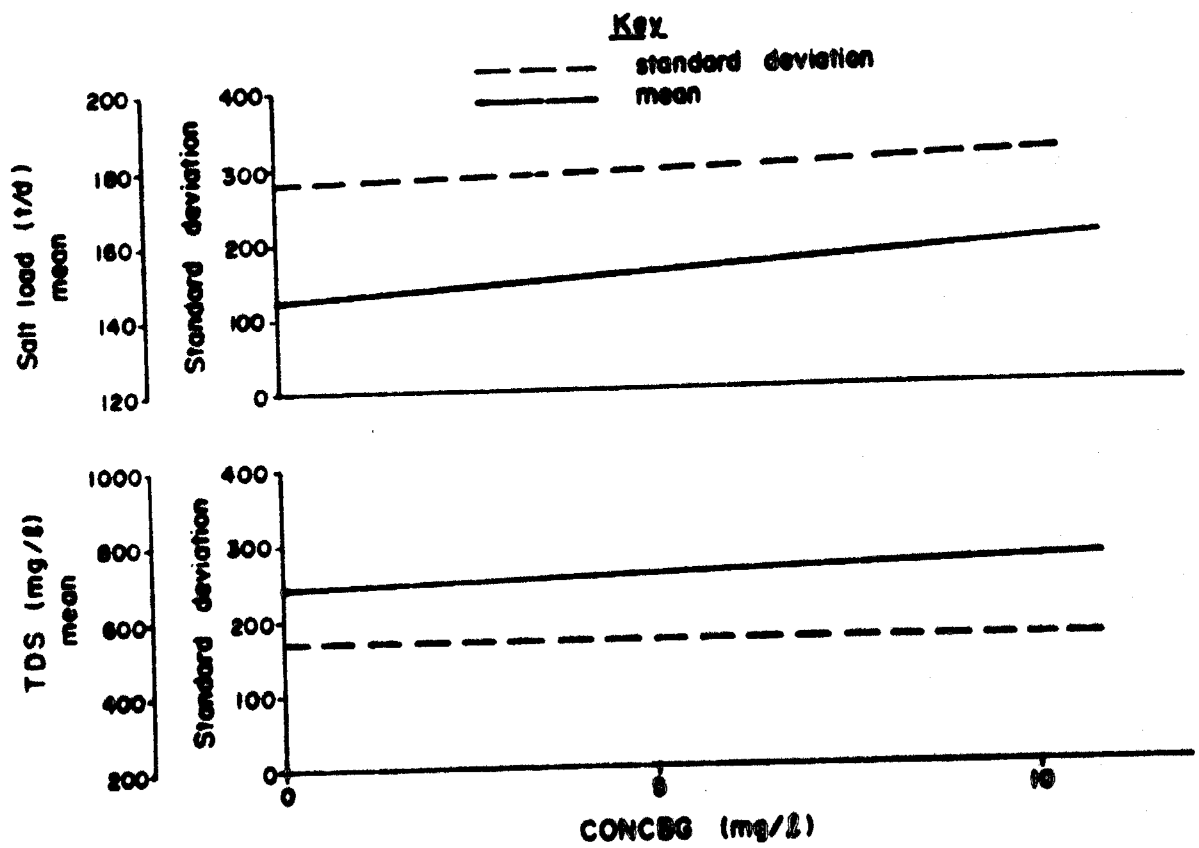

Fig. 4.36: Sensitivity of modelled means and standard deviations to changes in CONCBG

will concentrate in the soil moisture, resulting in a larger relative increase in base flow salt loads with increasing values of CONCBG. This would lead to a reduction in the standard deviation.

The effect of CONCBG on the standard deviation of daily salt concentrations is negligible.

g) <u>PINTM</u> : An increase in the interflow component of surface runoff can be seen from Figs. 4.37 and 4.38 to have the effect of reducing base flow salt loads and concentrations and increasing these values during floods, with the result that the mean and standard deviation of modelled daily salt loads are increased. If a reasonable value of APARR has been adopted (such as that used in Table 4.2) then increases in PINTM will cause the mean and standard deviation of modelled salt concentrations to decline, as indicated in Fig. 4.38.

h) <u>ALEACH</u> : Figs. 4.39 and 4.40 show that an increase in ALEACH leads to increased means for daily salt loads and salt concentrations. In Fig. 4.40 it can be seen that increasing ALEACH results in an increased standard deviation of daily salt loads. This is due to the high value of PINTM which ensured that the increase in peak salt loads would be large relative to the increase in base flow loads. If PINTM had been small enough, the standard deviation would have declined with increasing leaching. The relationship between ALEACH and the standard deviation of daily salt concentrations and other water quality parameters is very complex and is also dependent upon antecedent conditions.

i) <u>Initial parameter values</u> : Fig. 4.41 shows the number of years that have to be simulated in order to eliminate errors resulting from the initial estimates of SALTR and SALTU which are approximately three times too high. What have been plotted are the final total surface salt storages at the end of August 1978 with various simulation starting dates. It can be seen that errors due to inaccuracies in SALTU are rapidly eliminated, while those for inaccuracies in SALTR persist much longer. This is due to the fact that the washoff efficiencies for impervious surfaces are much greater than those for pervious surfaces.

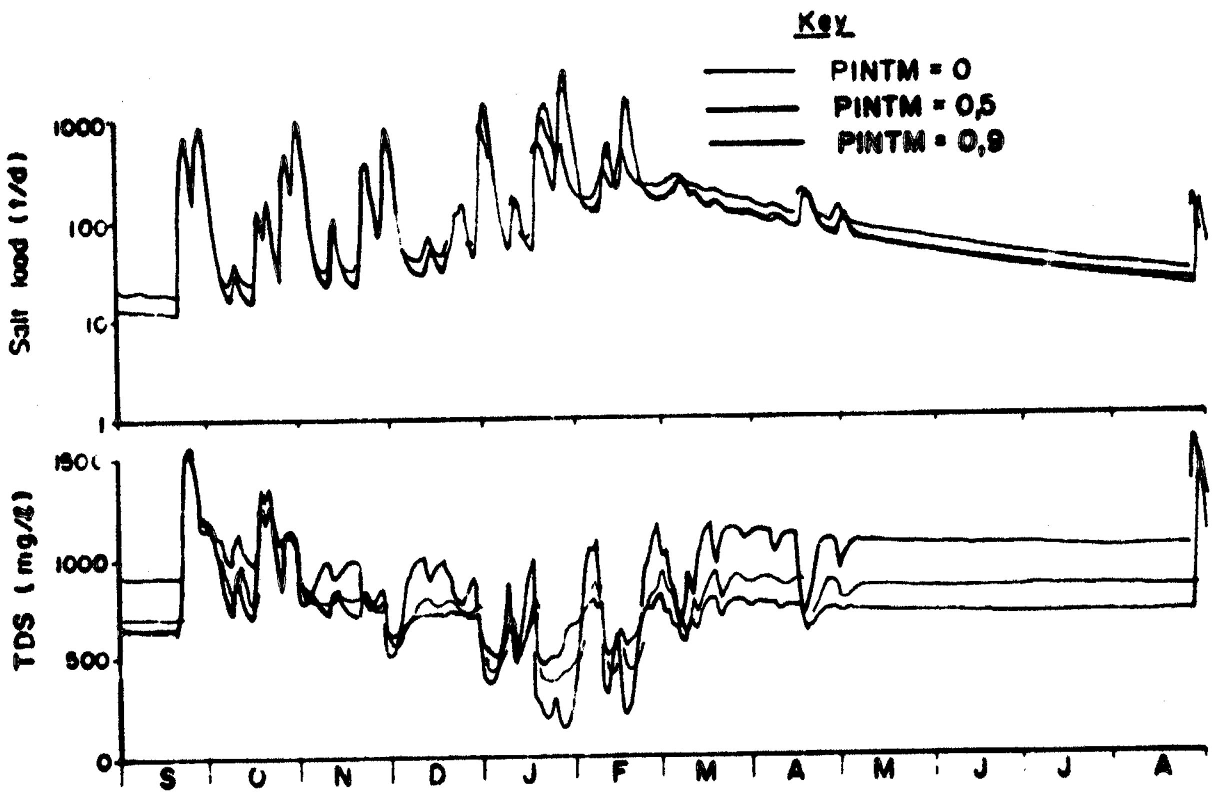

Fig 4.37: Sensitivity of modelled daily salt concentrations and salt loads to changes in PINTM.

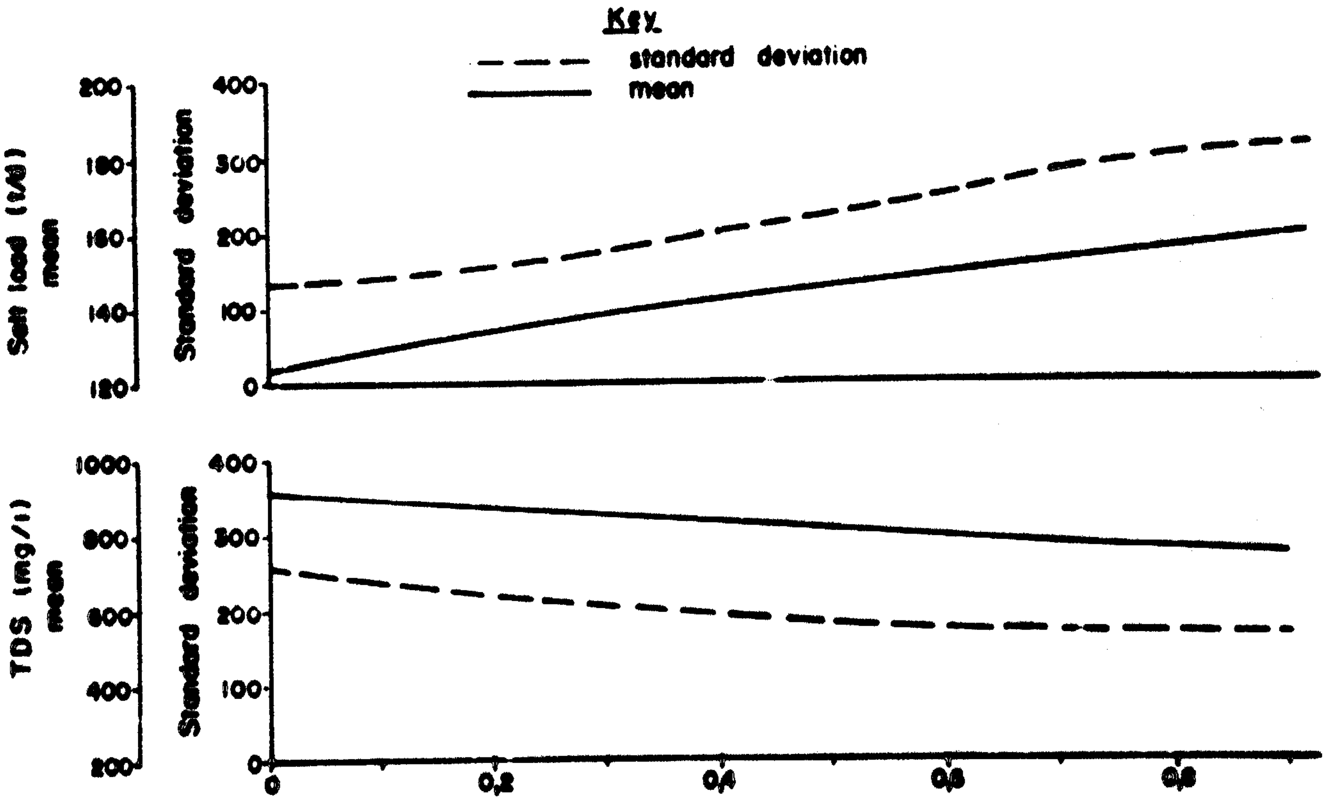

Fig. 4.38: Sensitivity of modelled means and standard deviations to changes in PINTM

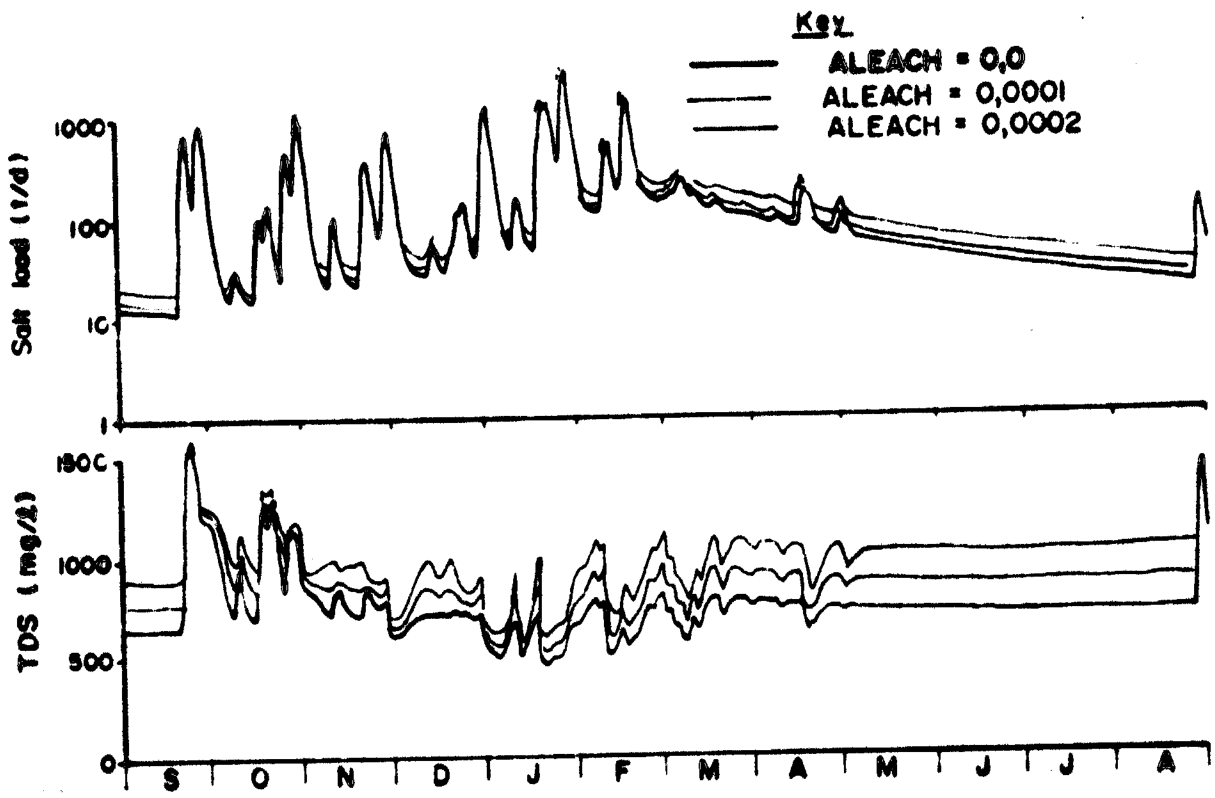

Fig 4.39: Sensitivity of modelled daily salt concentrations and salt loads to changes in ALEACH.

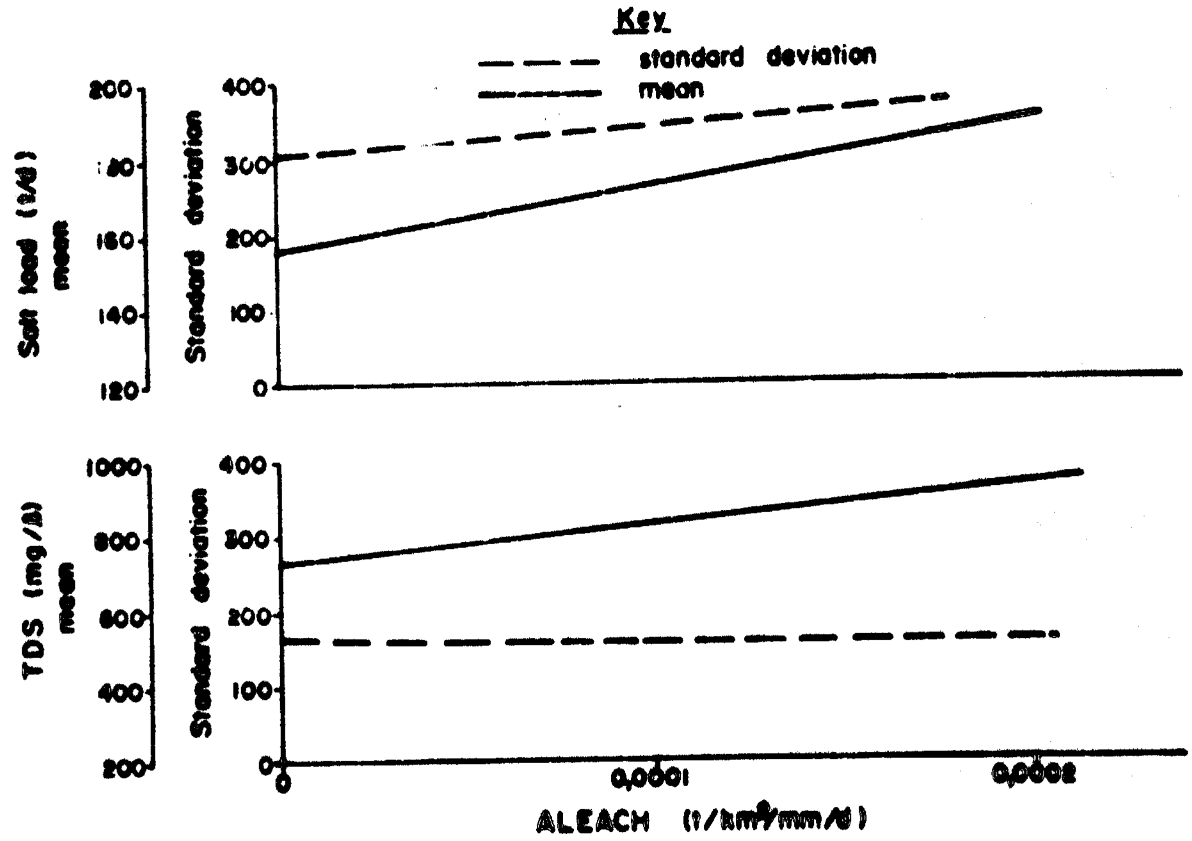

Fig 4.40: Sensitivity of modelled means and standard deviations to changes in ALEACH.

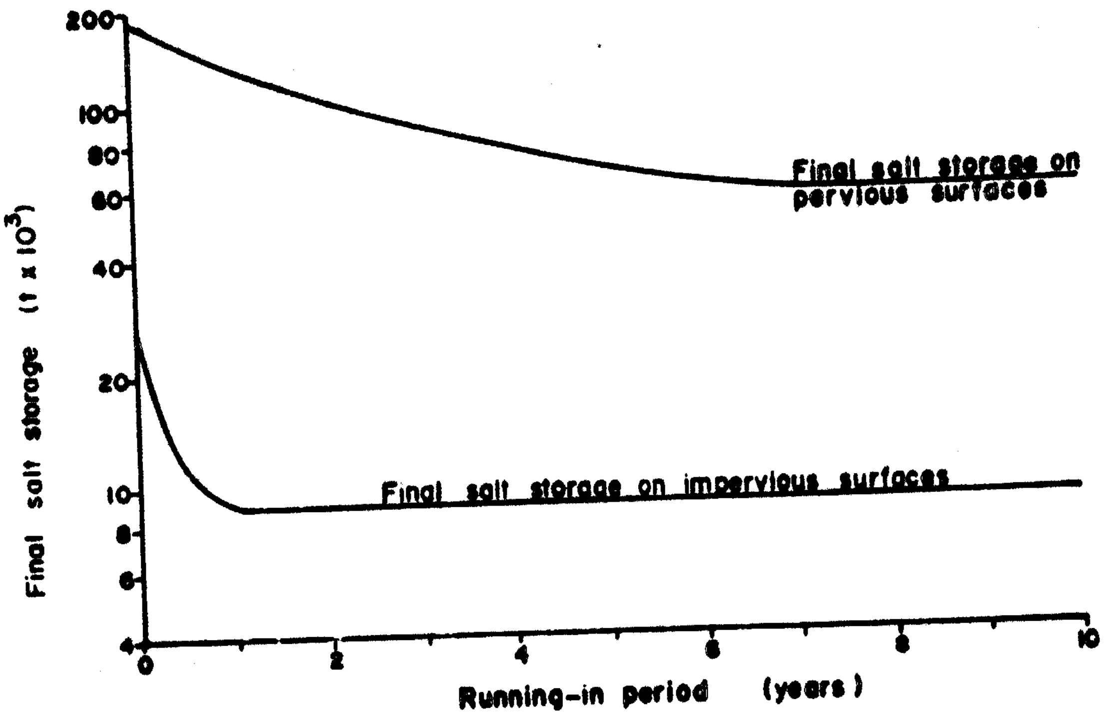

Fig.4.41: Running-in period required to eliminate errors resulting from estimates of SALTR and SALTU.

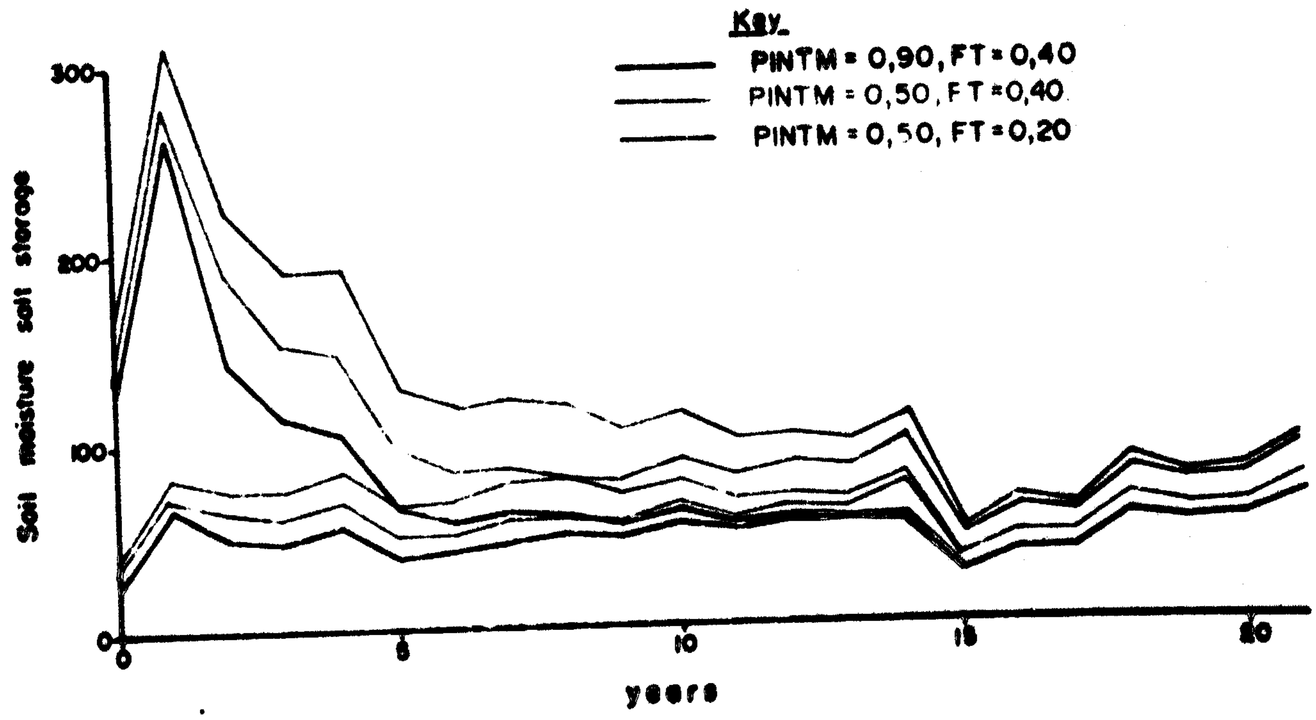

Fig.4.42: Running-in period required to stabilise the soil moisture salt storage.

Fig. 4.42 shows the consequences of specifying initial values of CONCS approximately 50 and 200 percent of the final value in August 1978 for different values of PINTM and FT. It can be seen that in all cases the convergence is extremely slow because of the long soil moisture storage retention times. It is clear therefore that a long running-in period is required in order to reduce errors due to initial estimates of CONCS. When calibrating the model it is also desirable to adjust CONCS in such a way as to ensure that the initial and final soil moisture salt storages are mutually compatible (i.e. if a zero growth rate is specified for salt recharge rates, then the initial and final values should be reasonably close to one another).

It follows from Fig. 4.42 that the memory of the soil moisture storage is reduced when interflow and groundwater discharge are increased. The irregularity of the plotted soil moisture salt storages also indicates that the hydrology also has an influence on the running-in period required.

4.2 Program NACLØ2

Output from program NACLØ2 for the period 1977.08 to 1978.08 for the model parameters given in Tables 4.1 and 4.2 were used as input to program NACLØ2. A one month running-in period was allowed, to warm up the channel routing model, and the period 1977.09 to 1978.08 was then used to test the sensitivity of modelled daily discharges and salinities from a single reach to changes in model calibration parameters and channel characteristics.

Fig. 4.43 shows the assumed channel cross-section.

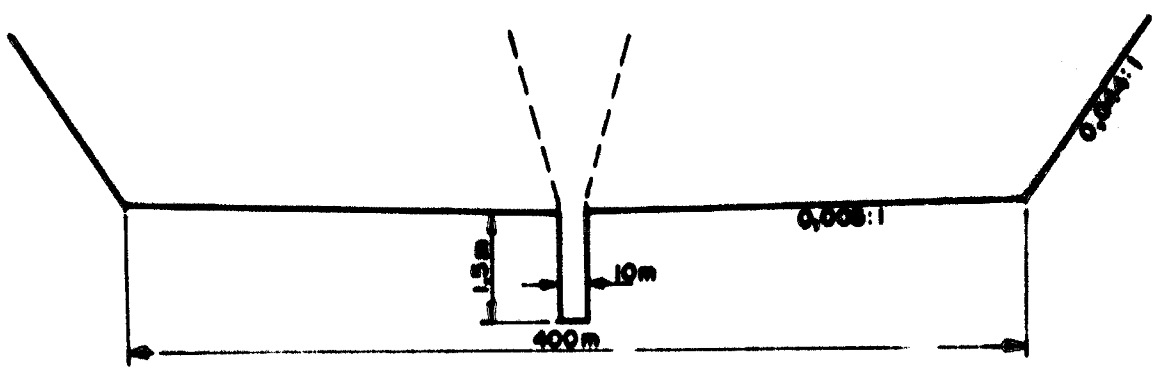

Fig.4.43: Assumed channel cross-section

The sensitivity of the modelled output from program NACLØ2 to changes in parameters controlling the computational accuracy is described in section 4.2.1 while sensitivity to changes in channel characteristics and model calibration parameters is discussed in section 4.2.2.

4.2.1 Parameters controlling computational accuracy

The parameters controlling computational accuracy are given in Table 4.3. These values were varied each in turn, while all remaining parameters were kept constant. Channel characteristics and calibration parameters were maintained constant at the values given in Tables 4.4 and 4.5 of section 4.2.2.

Table 4.3 : Computational accuracy parameters

Parameter	NQMAX	ERROR	NSTEP	NMAX	NMIX
Value	10	0,001	3	10	5

The sensitivity of modelled output to changes in each parameter is discussed below.

a) NQMAX : Fig. 4.44 shows the relationship among NQMAX, the mean and standard deviation of modelled discharges and computation time required to simulate one year using an IBM 370 computer. NQMAX is the maximum number of iterations allowed for convergence of the water balance equations (see section 2.3.1(i)). If the error does not reduce to less than ERROR within NQMAX iterations, the time step is halved and the computation for the day repeated until convergence occurs. From Fig. 4.44 it can be seen that reducing NQMAX from 10 to 4 has virtually no effect. This is because the Newton-Rhapson solution procedure is extremely efficient and usually converges within 4 iterations. When NQMAX becomes smaller, however, the computational time step has to be drastically reduced in order to satisfy the convergence criteria and as a result the computation time rises sharply. An NQMAX value greater than 5 is therefore recommended.

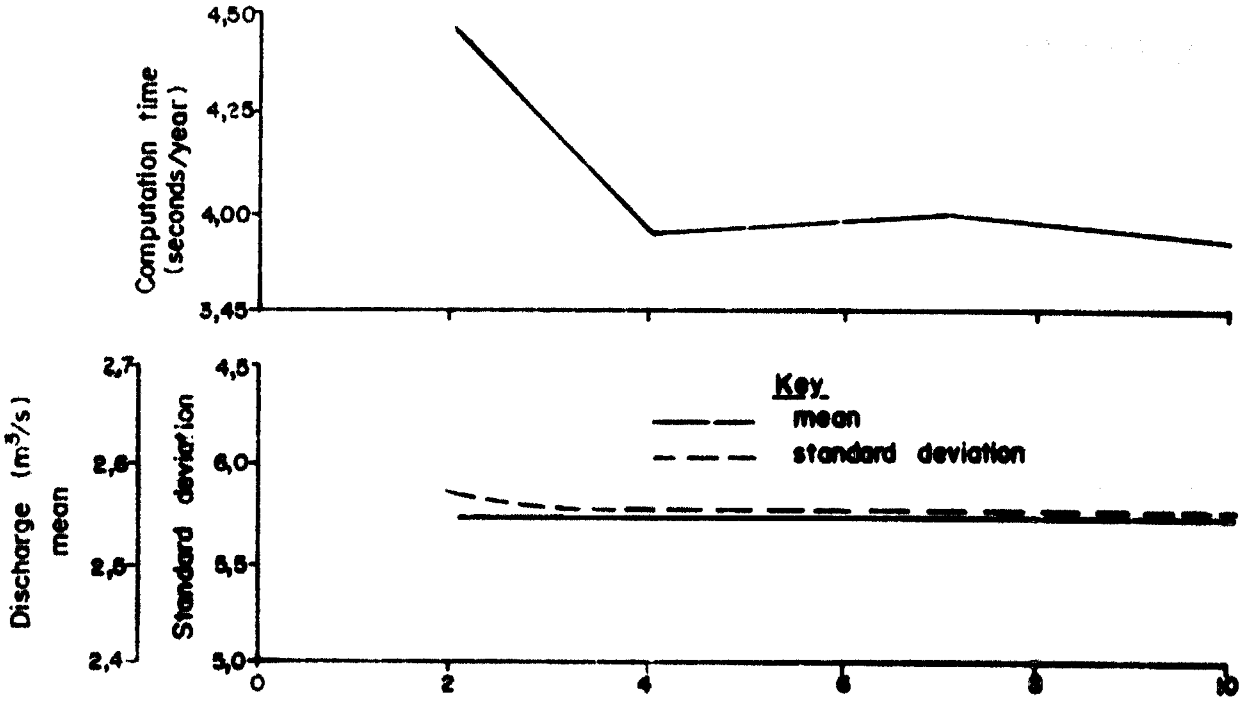

Fig.4.44: Sensitivity of modelled means and standard deviations to changes NQMAX

b) ERROR : Fig. 4.45 shows the effect of the allowable computational error on modelled discharges and computation time. As can be seen varying the allowable error by two orders of magnitude (between 0,0001 and 0,01 metres) has little effect upon computation times. This is because of the very rapid second order convergence associated with the Newton-Rhapson procedure. Larger errors cause a sharp drop in computation time but also lead to reduced accuracies, as can be seen by the change in the standard deviation of modelled daily discharges. The mean discharge is little affected by ERROR, however, because of the check calculations described in section 2.3.1(i) which are made to rectify errors in the water balance.

Because ERROR is the allowable modelled error in stage, it is recommended that it be set at a value slightly smaller than the measurement accuracy of the stage recorder used to measure discharges. A value smaller than one centimetre should therefore be adequate.

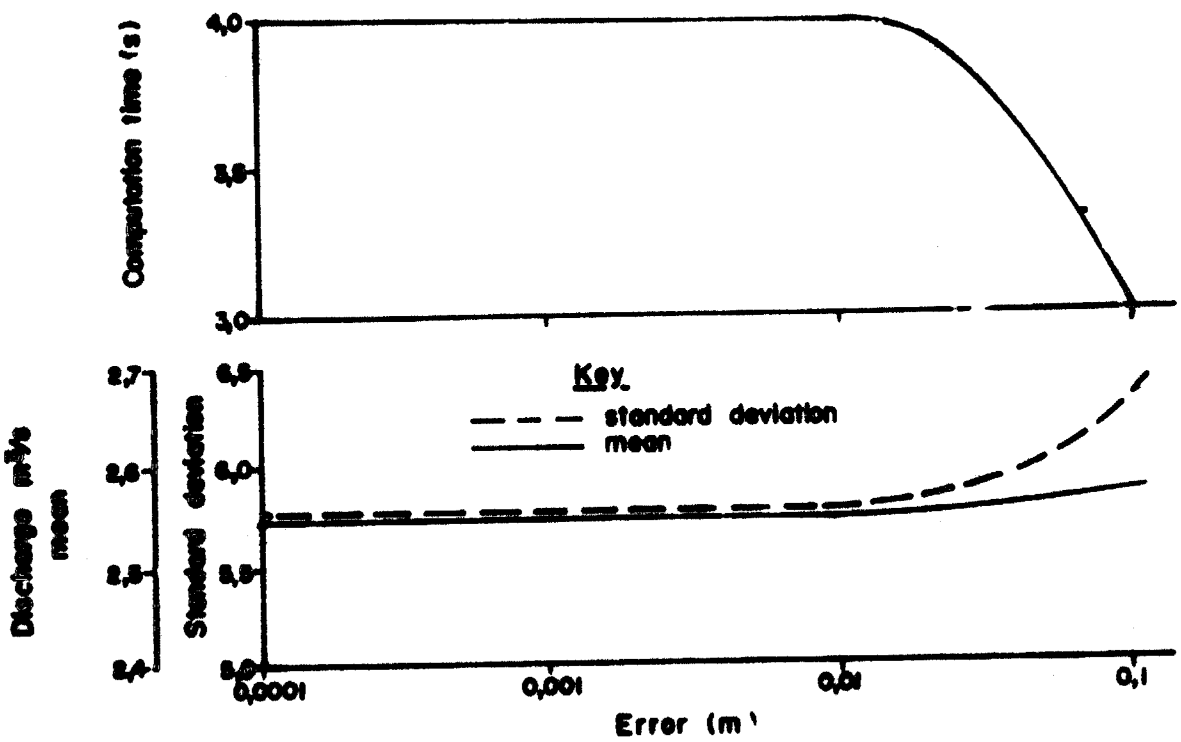

Fig.4.45: Sensitivity of modelled means and standard deviations to changes in ERROR.

c) NSTEP : The number of computational time steps within a day required to ensure adequate accuracy for total daily discharges can be seen from Fig. 4.46 to be not very great. Three steps is quite sufficient under most circumstances. It should be noted, however, that under certain conditions stability requirements may necessitate larger values of NSTEP. A sharply falling recession limb after a large flood on the input hydrograph may, for example, demand a larger NSTEP value in order to prevent the reach from being emptied during a single time step.

The computation time increases linearly with the number of time steps per day.

d) NMAX : Varying NMAX between 3 and 10 had no effect upon computation times, nor on the mean and standard deviation of modelled daily salt loads and concentrations. An NMAX value of 3 is in fact equivalent to a two-cell model because when the number of cells reaches NMAX, the first two cells are automatically mixed.

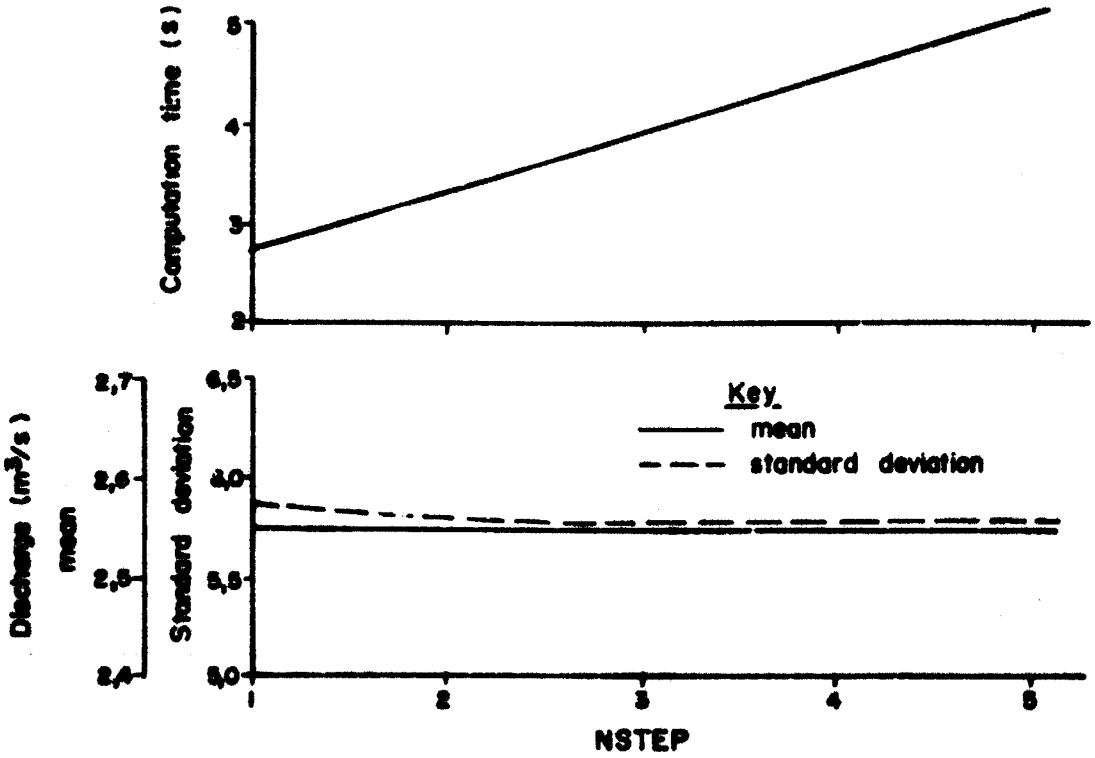

Fig 4.46: Sensitivity of modelled means and standard deviations to changes of NSTEP

e) NMIX : As might be expected from the insensitivity of modelled salinities to the maximum number of cells, the number of cells mixed when NMAX is exceeded also has little effect. Varying NMIX between 2 and 8 produced no effect upon modelled salt loads and concentrations. Computation times were also unaffected.

Part of the reason why changes in NMAX and NMIX have so little effect upon computational time is that under most flow conditions the number of cells seldom exceeded three because the discharges involved are large relative to the reach storage.

The sensitivity of modelled output to changes in NMAX and NMIX is dependent upon reach geometry, lateral inflows relative to upstream discharges and reach storage relative to upstream inflows. A large reach storage, for example, combined with relatively small upstream inflows would require a larger number of cells for adequate water quality modelling. The relationship between discharges in the central channel and in the flood plain is also an important consideration.

In view of the above considerations a larger NMAX value (say 10) together with a small NMIX value (say 2) is recommended. Such a choice should have little effect upon running costs when discharges are large relative to reach storage because then the number of cells will be kept small by advection through the reach. When through flows are small, the number of cells will increase with resultant increase in running costs, but under such conditions the allowable number of cells cannot be reduced without affecting modelling accuracy.

4.2.2 River reach characteristics and calibration parameters

Tables 4.4 and 4.5 give channel characteristics and calibration parameter values for the single channel reach simulated.

Table 4.4 : Parameters used in program NACLØ2

Parameter	Value	Parameter	Value	Parameter	Value
AVLEI*	10,0	FLEACH	0,50	CONSL+	800
AIRRIG*	5,0	PLAT*	0,20	GLOSS	0
CHAIN*	20,0	PUP*	0,80	SLOPE*	0,001
RETURN	0,2	HSTART+	1,50	AMANC	0,04
FIX	0,7	CONSU+	800	AMANF	0,15

* These are not calibration parameters as such as they can be measured directly.

\+ These are really starting values. Very short running-in periods are required because of the short memory of the channel routing model.

Table 4.5 : Parameters used in program NACLØ2

Parameter	Month											
	S	O	N	D	J	F	M	A	M	J	J	A
FEVAP	0,3	0,3	0,3	0,3	0,3	0,3	0,3	0,3	0,3	0,3	0,3	0,3
FIRRIG	1,0	1,0	1,0	1,0	1,0	1,0	1,0	1,0	1,0	1,0	1,0	1,0
FTRANS	0,30	0,40	0,47	0,50	0,47	0,40	0,30	0,20	0,13	0,10	0,13	0,20

The sensitivity of modelled output to changes in model parameters is discussed below.

a) AVLEI : Although AVLEI is not a calibration parameter, the effect of changes in vlei area is still of interest. Figs. 4.47 and 4.48 show the effects of changes in AVLEI. The discontinuities in the plotted salt concentrations for September and August occur because the modelled discharges cease during these periods (in fact when discharges fall below 0,005.$10^6 m^3/d$, salt concentrations are ignored by the model and are not taken into consideration when computing the statistical properties of modelled salt concentrations; this avoids misleading results).

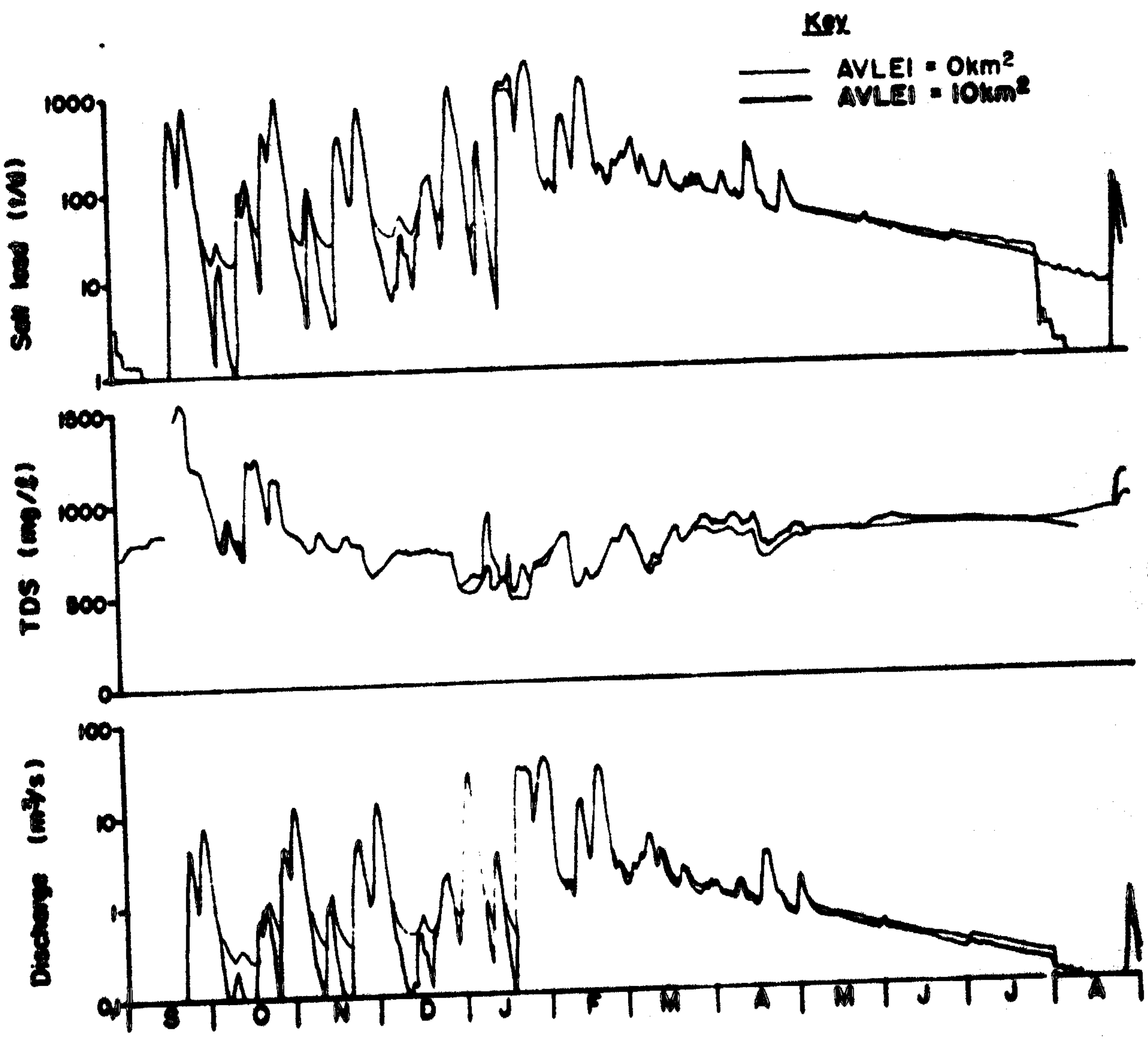

Fig.4.47 : Sensitivity of modelled daily discharges, salt concentrations and salt loads to changes in AVLEI.

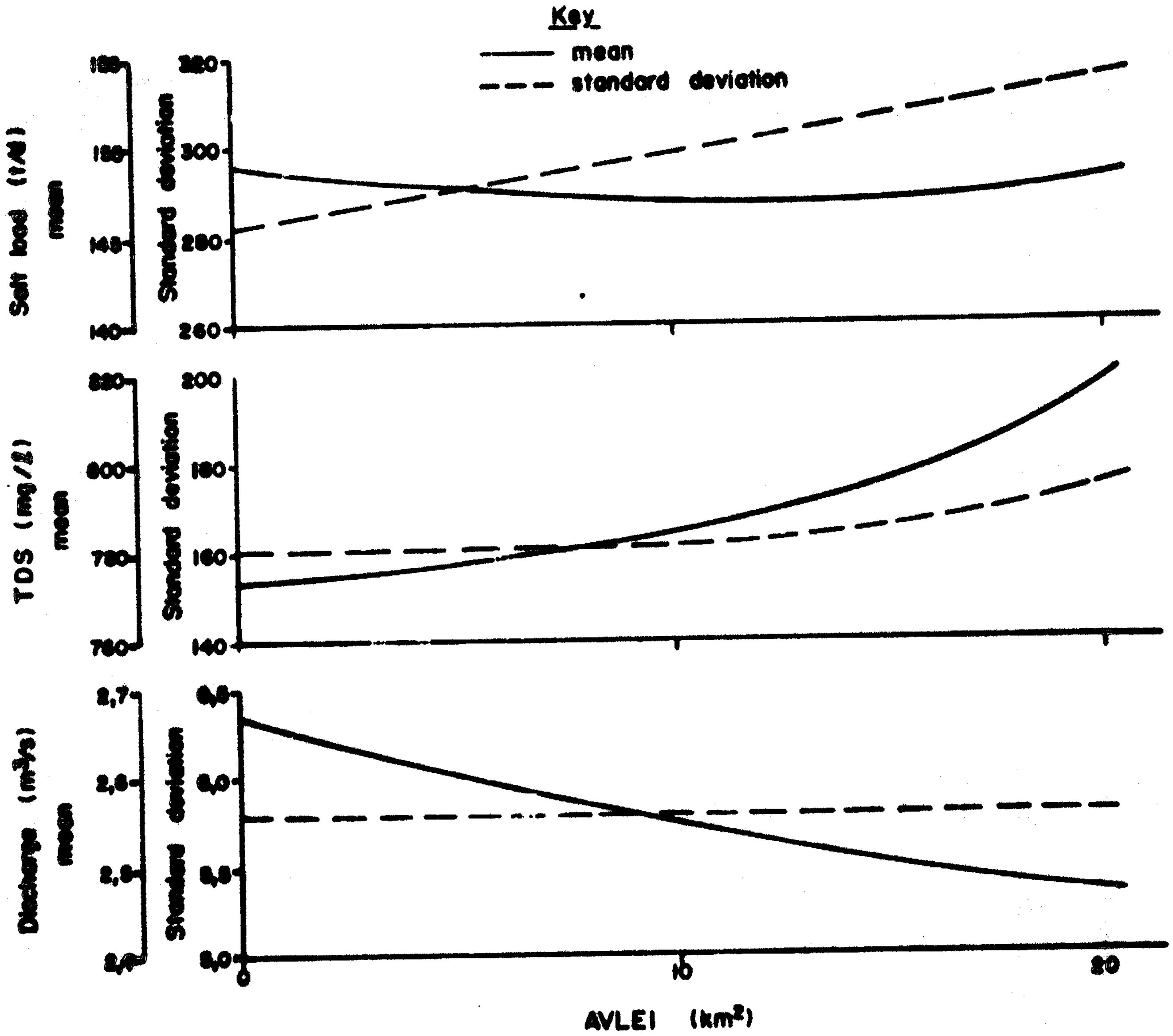

Fig.4.48: Sensitivity of modelled means and standard deviations to changes in AVLEI.

From Figs. 4.47 and 4.48 it can be seen that an increase in vlei area leads to a reduction of discharges during low flow conditions with a resultant decrease in the mean and rise in the standard deviation. The mean and standard deviation of modelled daily salt concentrations also increase due to the increased transpiration losses, as does the standard deviation of daily salt loads. The long term mean salt load remains constant, although it may vary during any given year depending upon antecedent conditions. Of particular note is the rise in salt concentrations in January and the accompanying increase in peak salt loads, resulting from an increase in AVLEI. This is due to the increased salt load accumulated in the vlei sponge as a result of transpiration. This salt is then leached out during the January floods.

b) <u>FTRANS and FEVAP</u> : Figs. 4.49 and 4.50 show the effect upon model results of two alternative assumptions concerning FTRANS and FEVAP. In the first instance FTRANS is assumed to vary seasonally in a sinusoidal pattern as shown in Table 4.5 and FEVAP is assumed to remain constant at 0,3. The annual average total gross evaporation is thus assumed to be 60 percent of the gross lake evaporation (as suggested by Rijks (1969) for an established reed bed). The second assumption is that FTRANS is zero and FEVAP remains constant at 1,0. This would be equivalent to removing all the vegetation. Finally, FEVAP was assumed to remain constant at 1,0 with FTRANS as per Table 4.5, yielding a total gross evaporation 1,3 times that

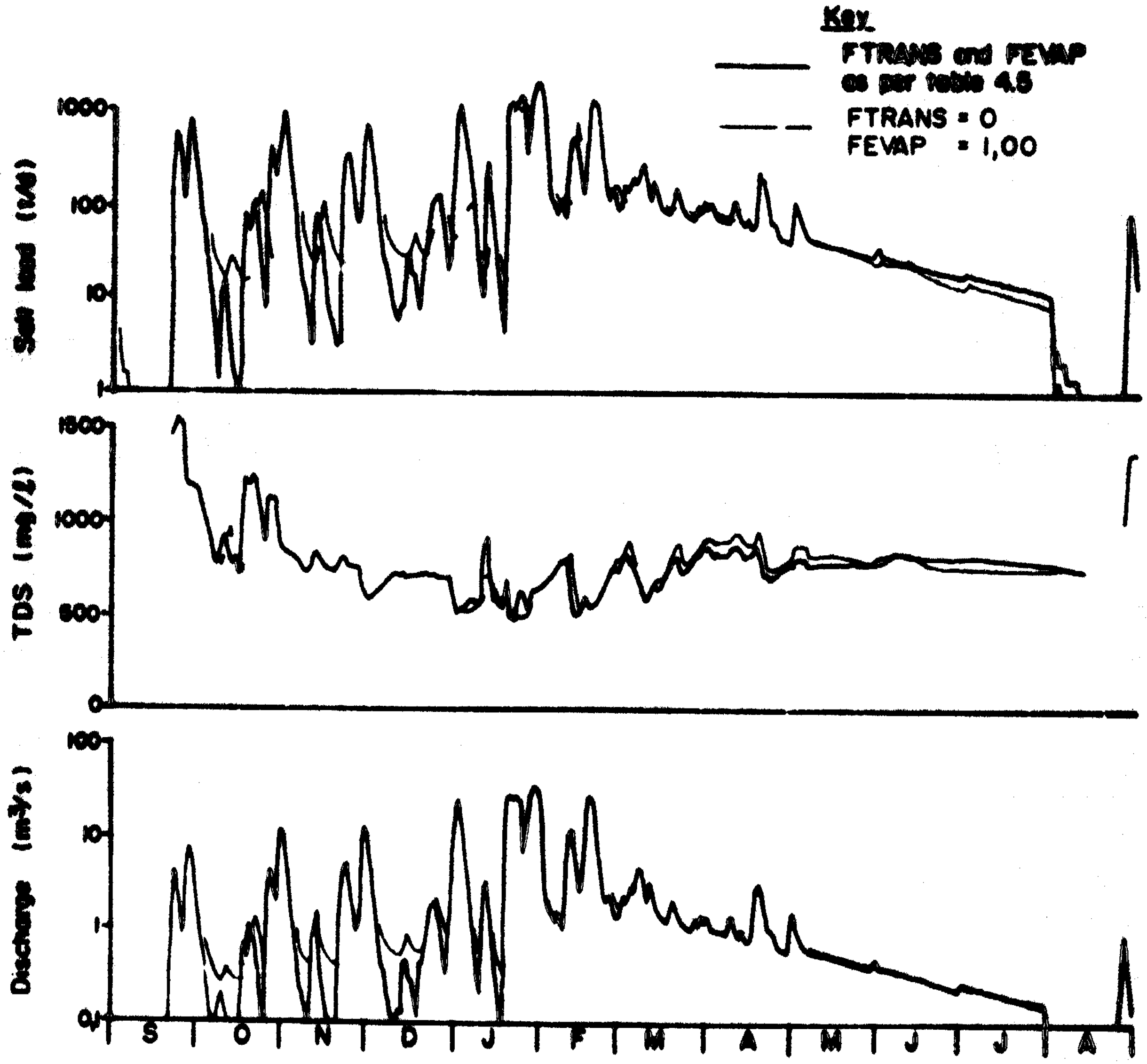

Fig.4.49 : Sensitivity of modelled daily discharges, salt concentrations and salt loads to changes in vlei evapotranspiration factors

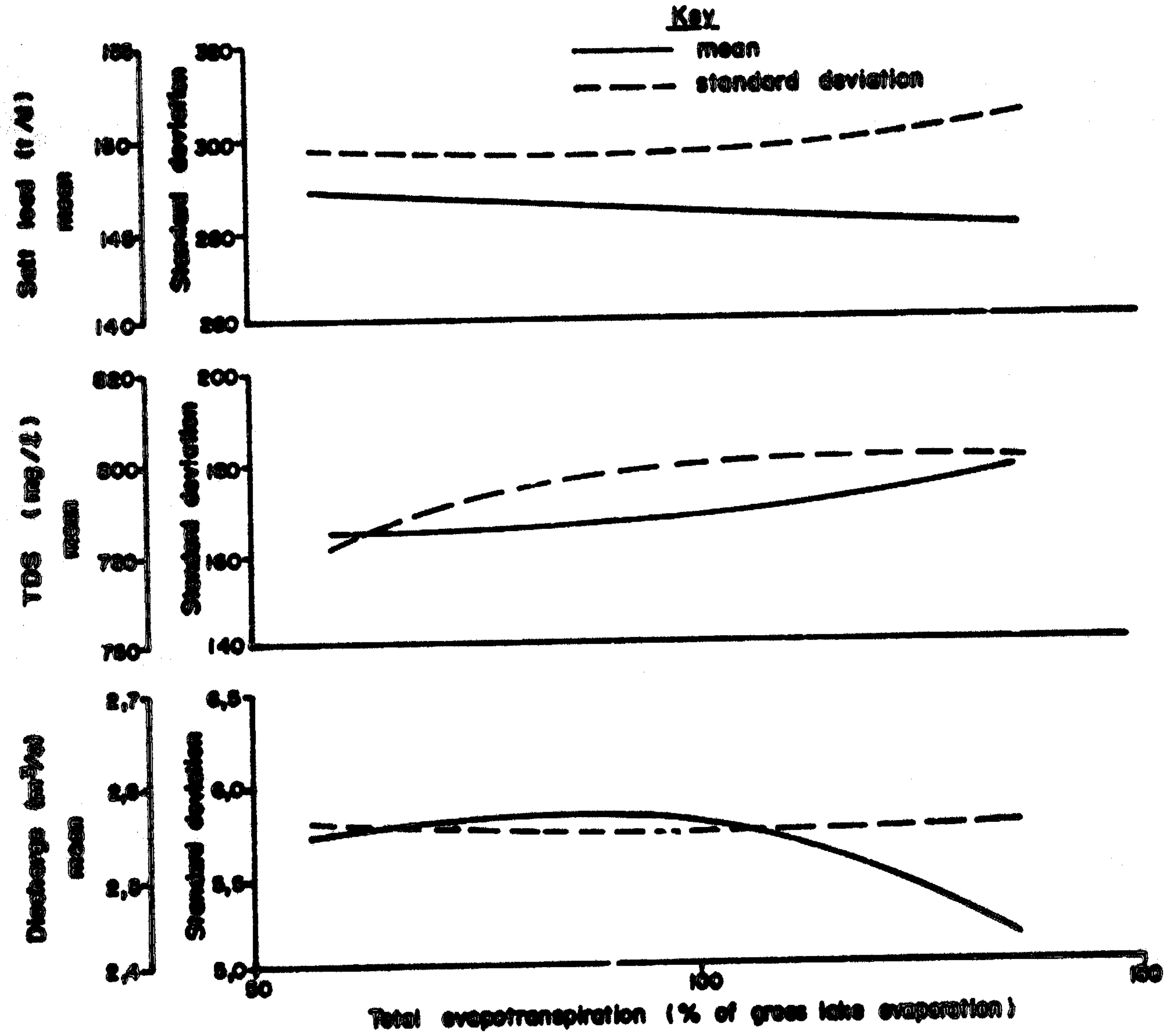

Fig. 4.50: Sensitivity of modelled means and standard deviations to changes in vlei evapotranspiration factors.

from an equivalent lake. This is equivalent to assuming that the shading effect of aquatic growth has no effect on evaporation rates. Only the first two cases are plotted in Fig. 4.49. It can be seen from Fig. 4.49 that the effect of the vlei is to reduce low flow discharges during the summer months. Under such conditions when the flow is confined to the central channel, the reeds in the vlei continue to transpire, drawing water from the central channel. The assumption that there is reduced evapotranspiration from the vlei during the winter months (see Table 4.5) leads to a small increase in base flows. This is because the transpiration loss from the vlei is outweighed by the reduction in evaporation from the free water surface by virtue of the shading effect of the reeds. During floods, when the flood plain is inundated, the shading effect of the reeds also reduces evaporation. As a result there is very little change in the mean discharge. Removal of the vlei would also remove the effect discussed in section 4.2.2(b) whereby salts that had accumulated in the vlei would be flushed out during floods. In the third case the increased evaporation reduces mean discharges and increases mean salt concentrations. At the same time the standard deviations of daily discharges and salt loads are also increased.

Changes in FTRANS and FEVAP have no effect upon the long term mean salt load, whereas the effect upon the standard deviation of daily salt concentrations depends upon the input pollutograph.

c) <u>FLEACH</u> : Figs. 4.51 and 4.52 show the effect upon modelled salinities of changes in FLEACH. The effect on the mean and standard deviation of modelled salt concentrations is dependent upon the input pollutograph. Mean salt loads are unaltered, but the standard deviation increases as FLEACH increases as this has the effect of liberating salts stored in the vlei sponge during the flood peaks, rather than a gradual release during the flood recession.

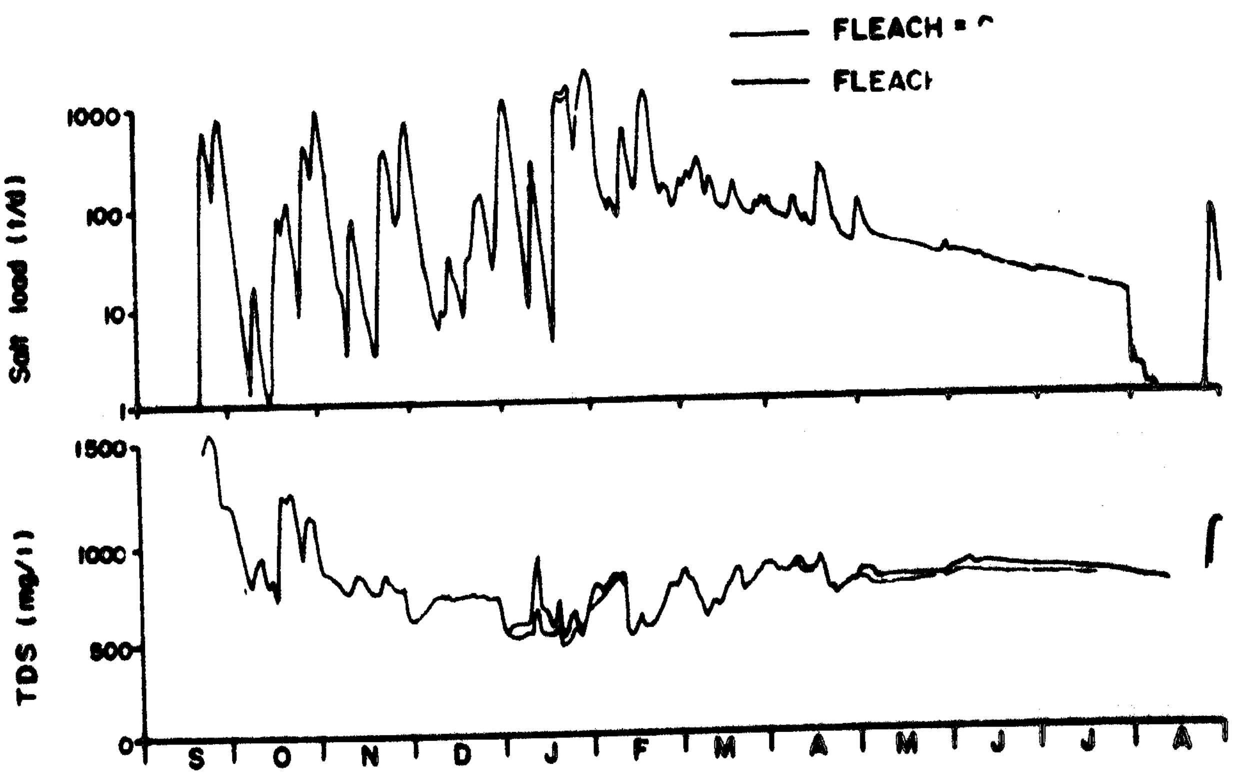

Fig 4.51: Sensitivity of modelled daily salt concentrations and salt loads to changes in FLEACH.

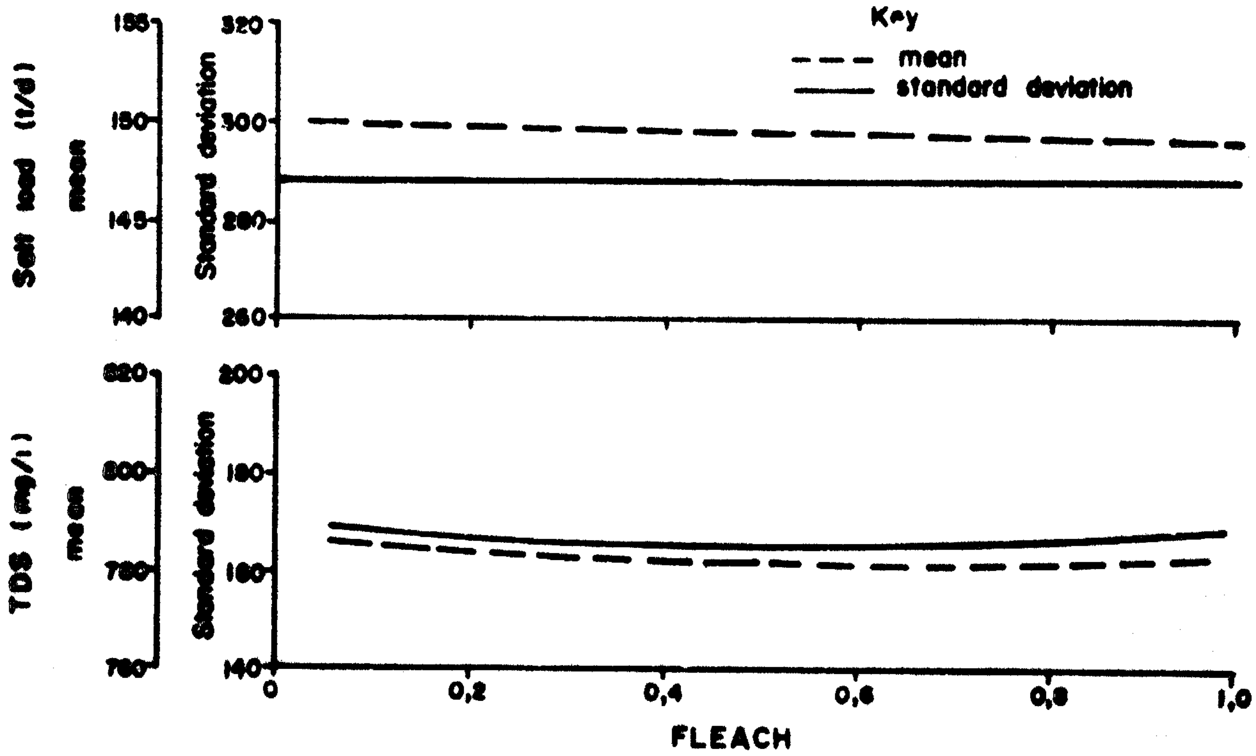

Fig.4.52: Sensitivity of modelled means and standard deviations to changes in FLEACH.

d) **SLOPE** : Figs. 4.53 and 4.54 show the effect of inaccuracies in the measurement of the channel slope. Increasing the slope has no effect upon the long term mean discharges and salt loads, but does increase the corresponding standard deviations. The diminished flood attenuation has the effect of reducing the mixing. As the larger floods are usually diluted, this means that the reduced mixing has the effect of increasing salt concentrations if the base flows are fairly saline (as in the cases reflected in Figs. 4.53 and 4.54).

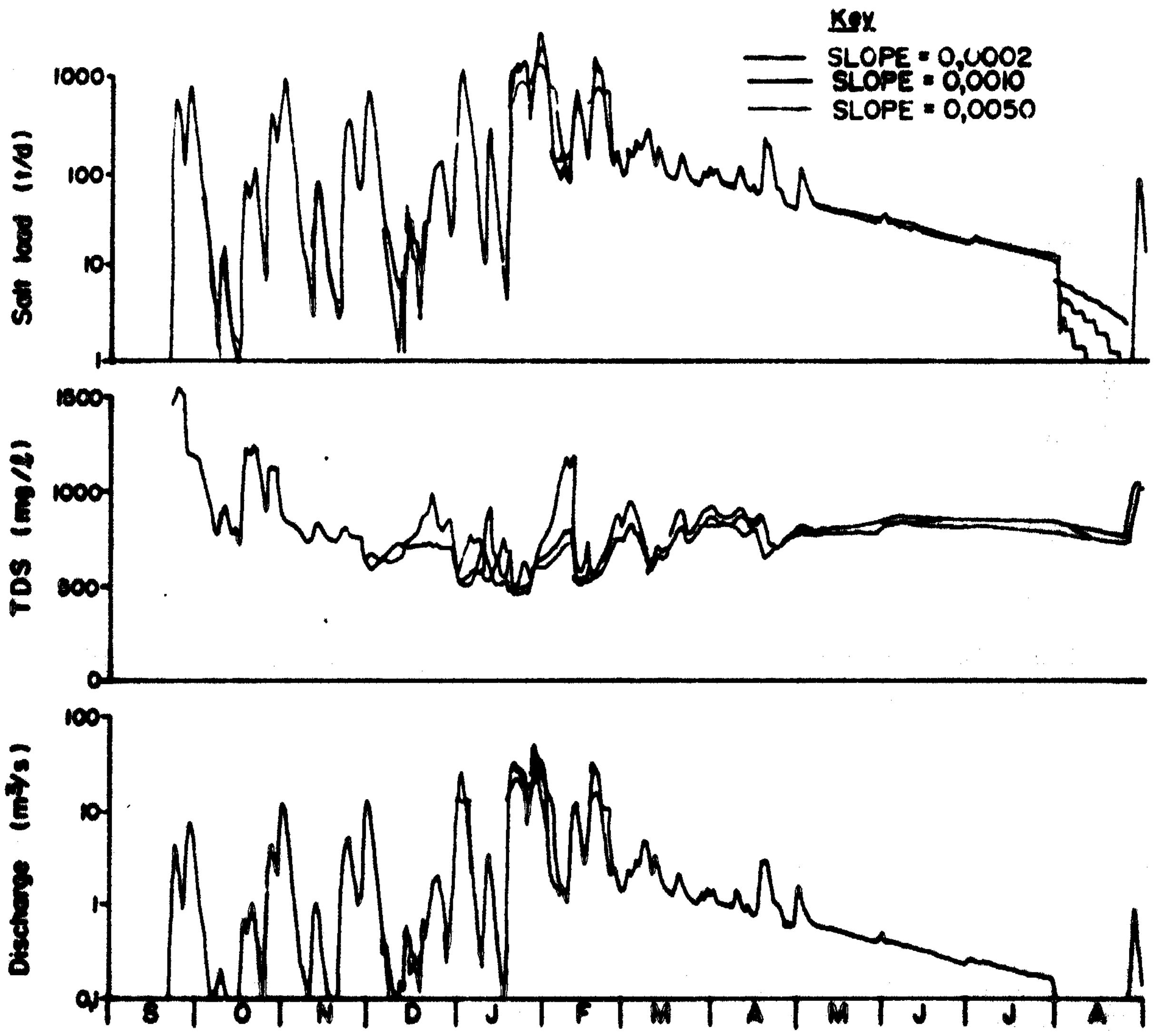

Fig.4.53 : Sensitivity of modelled daily discharges, salt concentrations and salt loads to changes in SLOPE.

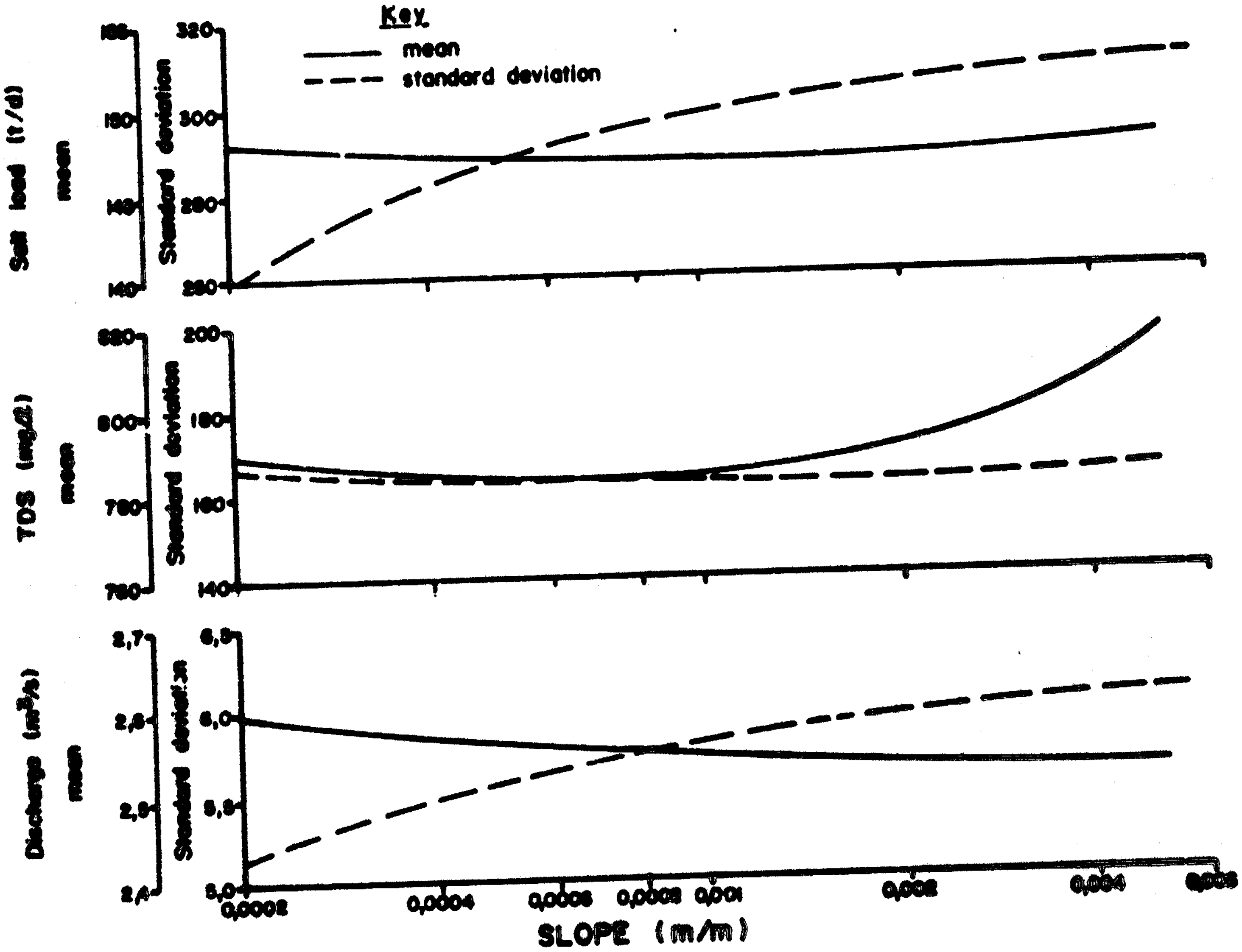

Fig. 4.54: Sensitivity of modelled means and standard deviations to changes in SLOPE.

e) AMANC : Figs. 4.55 and 4.56 show the sensitivity of modelled output to changes in the Manning's n value for the central channel. Increasing AMANC attenuates peak discharges and salt loads. The corresponding standard deviations therefore decline. Raised water levels also increase the evaporation loss during the dry season with a consequent rise in base flow salt concentrations. Increased salt concentrations in turn increase the salt load deposited in the vlei sponge and lost to irrigation, hence the decrease in base flow salt loads. Increased inundation during smaller floods in the first part of the rainy season results in an early release of salts stored in the vlei sponge. This is reflected in the plots of daily salt concentrations in Fig. 4.55.

AMANC has little effect upon the mean discharge and causes a small decline in the long term mean salt load due to an increased irrigation loss caused by higher base flow salt concentrations. The effect upon the mean salt load during any given year varies according to the antecedent hydrology. The mean salt concentration generally rises, but the effect upon the standard deviation can vary.

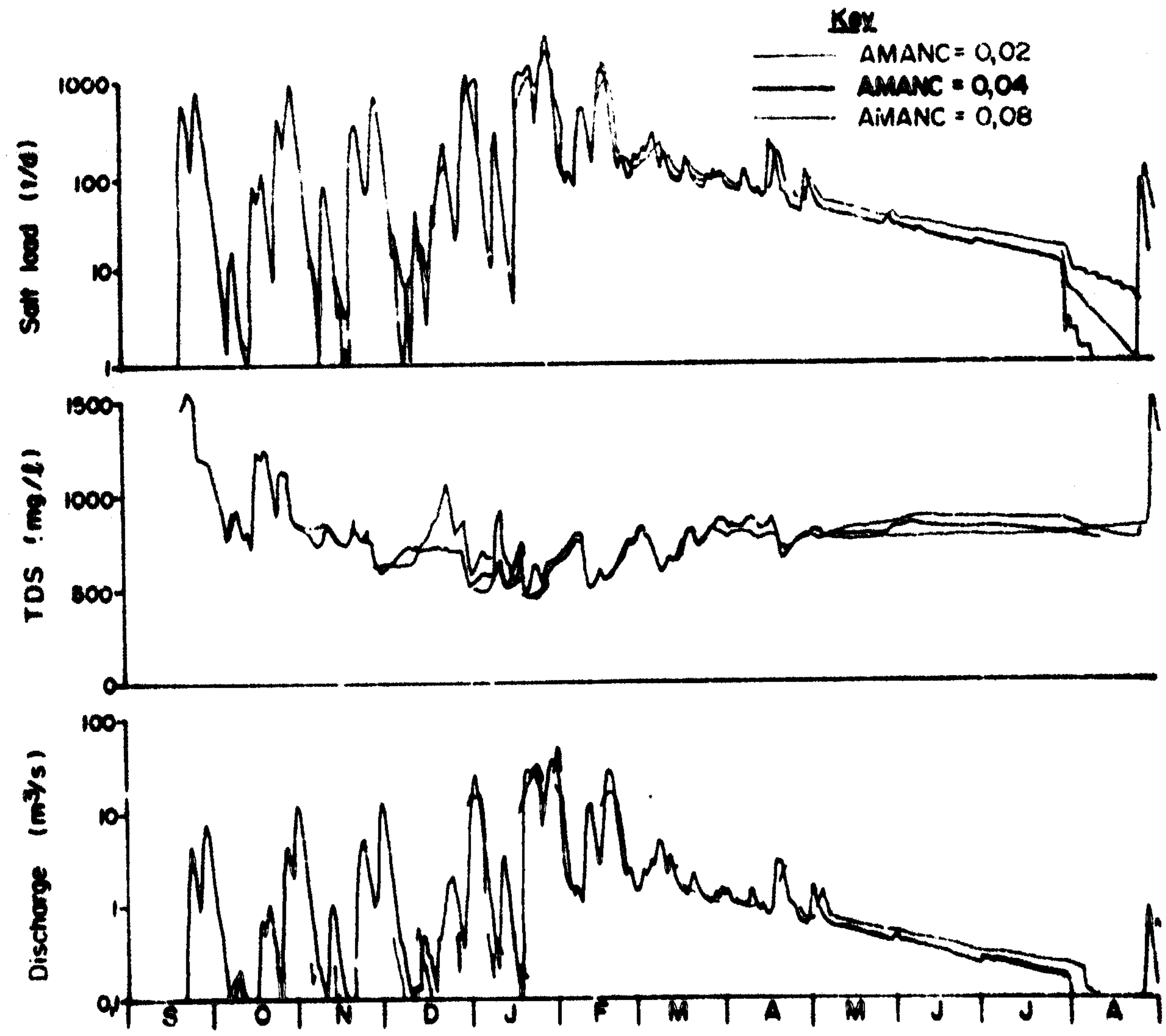

Fig.4.56: Sensitivity of modelled daily discharges, salt concentrations and salt loads to changes in AMANC

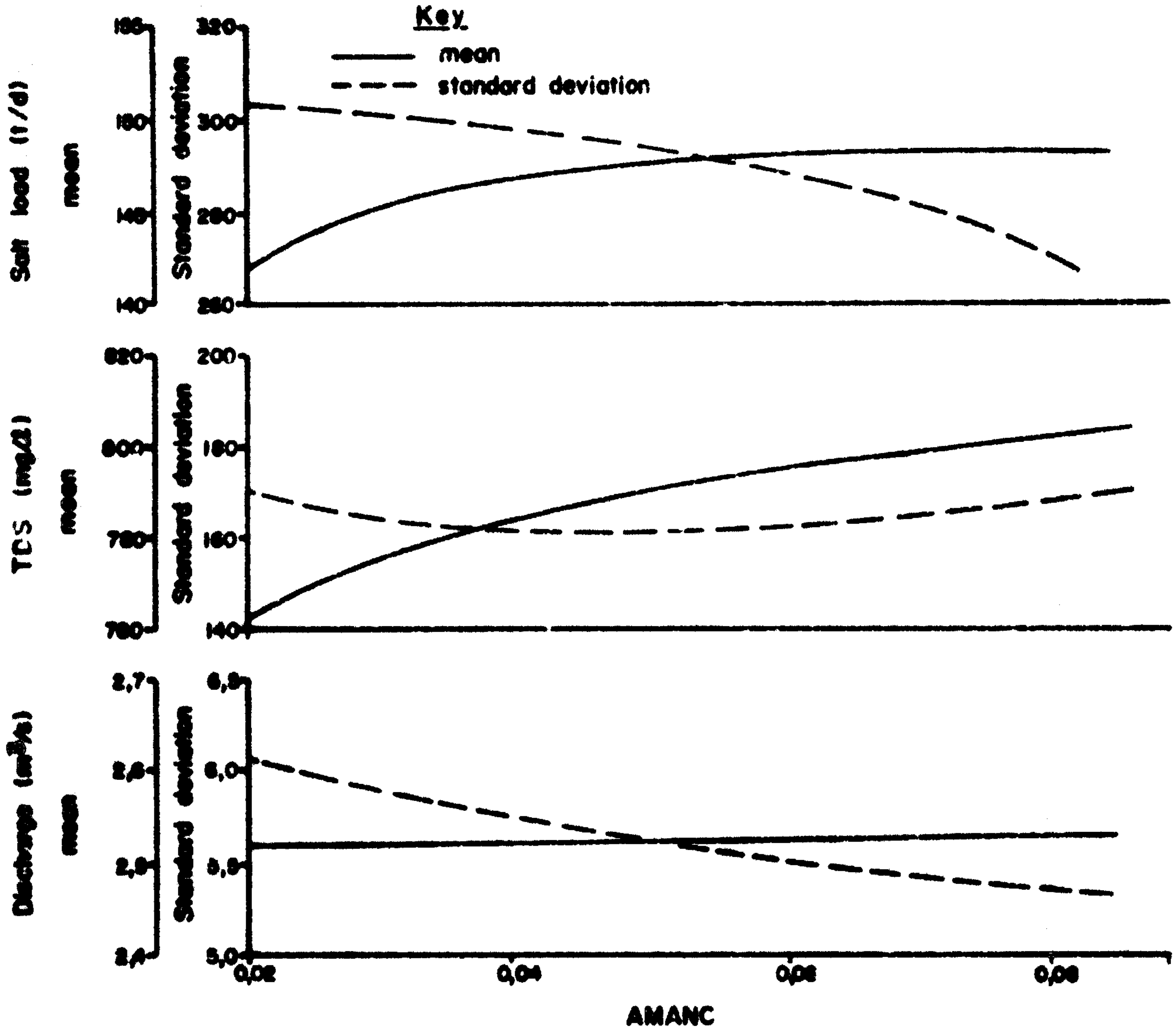

Fig. 4.56: Sensitivity of modelled means and standard deviations to changes in AMANC.

f) AMANF : The effects of changes in AMANF upon modelled discharges and salinities are similar in all respects to those changes in AMANC, but much less pronounced, and were therefore not plotted. The influence of AMANF is most marked during the larger floods. The effect of AMANF during the lower discharges is very small as most of the flow is confined to the incised channel.

g) Channel geometry : The sensitivity of the model output to changes in the geometry of the central channel is shown in Figs. 4.57 and 4.58. Channel geometry is not really a calibration parameter but in many of the examples of Chapter 3 channel cross-sections had to be assumed due to the paucity of data. The effects of inaccuracies in these ass'.mptions are therefore of some interest.

A reduction in the size of the central channel can be seen to reduce the standard deviation of modelled daily discharges and salt loads, while the mean salt concentration increases. The long term mean salt load should decline as a consequence of the higher salt con- centrations, with the associated higher irrigation loss. An unex- pected feature of Fig. 4.58 is the decline of the mean discharge as the channel area is increased, despite the increased base flows. This anomaly is due to the increased surface areas during the heavier rain storms which result in a net gain of water during the year simulated. It should be noted, however, that this feature is a peculiarity of the 1977/78 hydrology and will not always be the case.

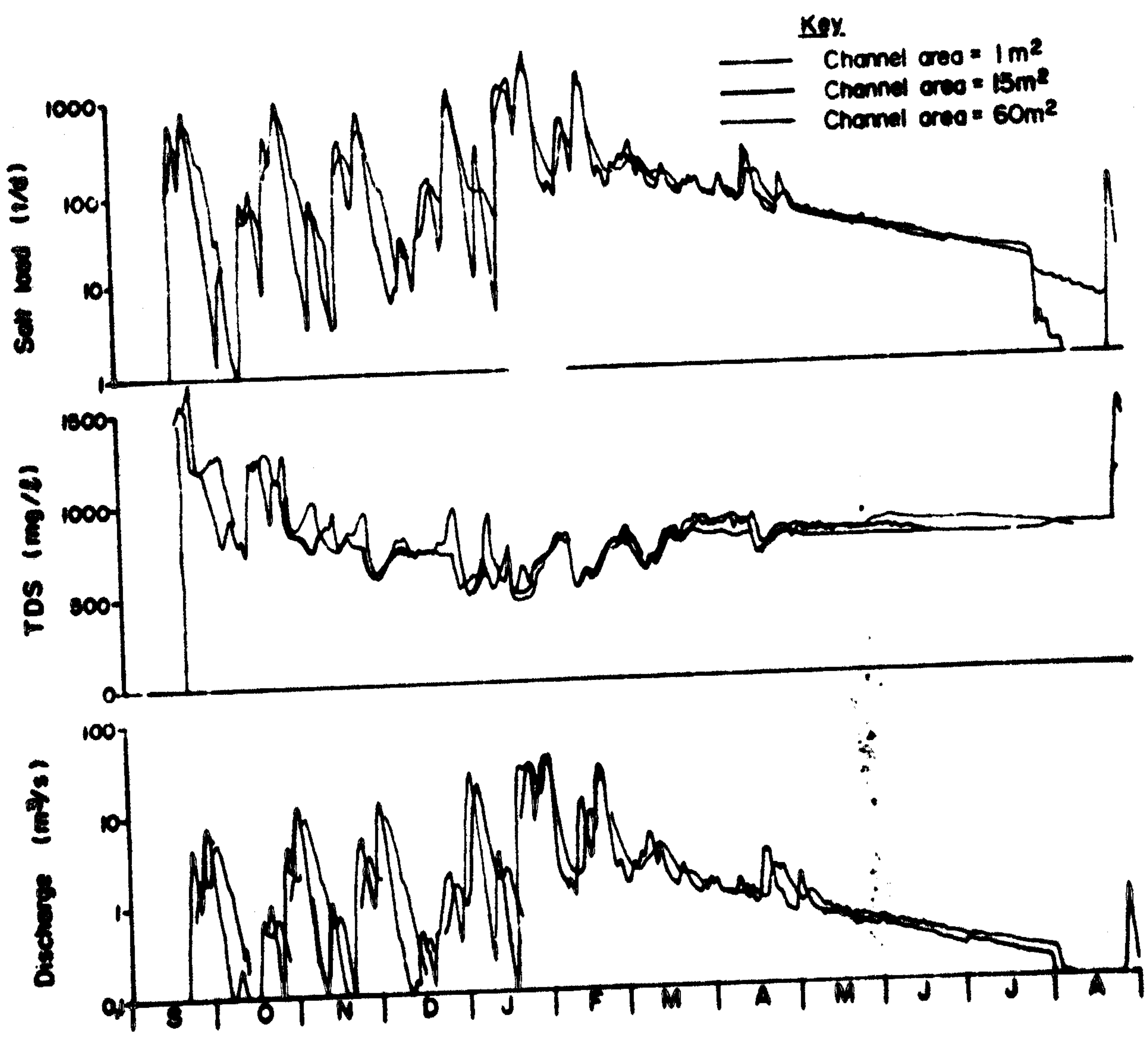

Fig.4.57: Sensitivity of modelled daily discharges, salt concentrations and salt loads to changes in channel geometry.

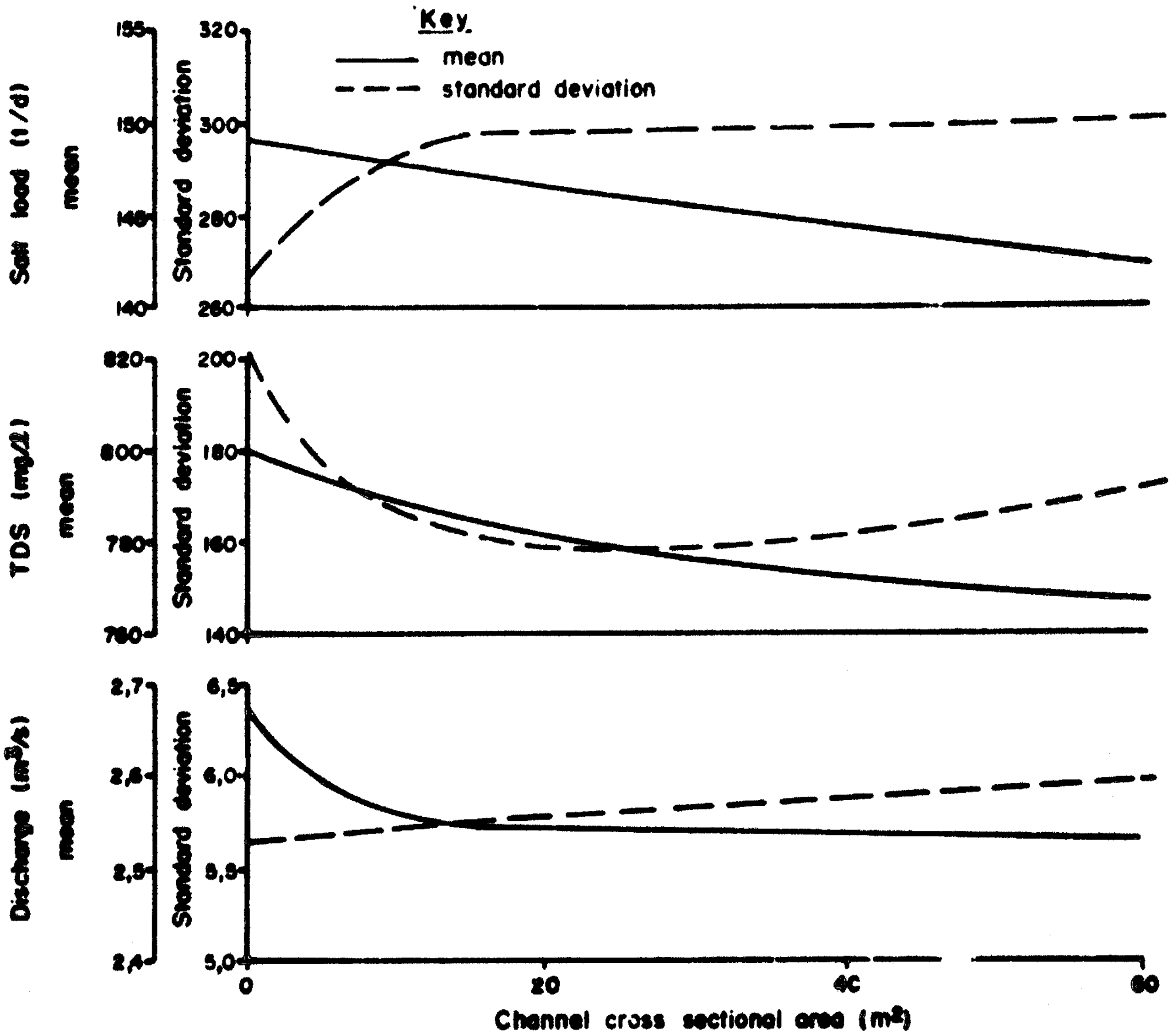

Fig. 4.58: Sensitivity of modelled means and standard deviations to changes in channel geometry.

A decrease in the size of the central channel affects the release of salts from the vlei sponge in a manner similar to that of increasing AMANC (see section 4.2.2(e)). The relationship between channel geometry and the standard deviation of daily salt concentrations is dependent upon the input pollutograph.